



OSLO METROPOLITAN UNIVERSITY
STORBYUNIVERSITETET

GRUPPE NR. 24

TILGJENGELIGHET
Åpen

Telefon: 67 23 50 00
www.oslomet.no

Institutt for Bygg- og energiteknikk - Bygg

Postadresse: Postboks 4 St. Olavs plass,
0130 Oslo
Besøksadresse: Pilestredet 35, Oslo

BACHELOROPPGAVE

Analytical study of long floating pontoon bridges subject to tidal variations	Dato 26.05.2021
	Antall sider/Antall vedlegg 88/1
Forfattere Emil Ingvar Lindersson Tord Rønning Per Henrik Ellefsen	Veileder Jian Dai
Utført i samarbeid med OsloMet	Kontaktperson Jian Dai

Sammendrag

Analytical comparison of two bridge designs using Matlab. 4 km long floating pontoon bridge subject to tidal variations. Moment distribution and deflection controls with validation through SAP2000. Two main issues facing long floating bridges are investigated; deflection and outlier moments from restraint forces. Proposed solutions are long first spans and changing the reference tidal height.

3 Stikkord

Floating bridge

Tidal variations

Pontoon bridge

Preface

This thesis has been written as the final part of a three-year bachelor level program in construction engineering at OsloMet - Oslo Metropolitan University, during the spring semester of 2021. The thesis constituted 20 credits.

The issue and scope of the thesis was elaborated and given by Oslomet.

Exploring the highly relevant floating bridge solutions and the impact of tidal effects has been both challenging and rewarding, as the three of us share the same interest in structural engineering and bridge design in particular.

The thesis work has provided great learning outcomes. Especially a better understanding of structural engineering and use of the softwares - Matlab and SAP2000. Furthermore, it helped us develop a greater knowledge of how scientific research is conducted and presented - resources that will benefit us in our future studies and work.


The target audience of this thesis are students who have the same pre knowledge of the topics that we had before starting this project. Some understanding of structural engineering and mechanics is advantageous in order to get the full benefit out of this thesis.

We would like to extend our deepest gratitude to our mentor Associate Professor Jian Dai, for his engaging support and guidance throughout the entirety of the project. We would also like to thank everyone that provided much appreciated feedback.

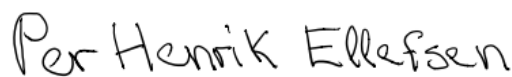
Oslo, 26.05.2021



Emil Ingvar Lindersson



Tord Rønning



Per Henrik Ellefsen

Abstract

The Norwegian Public Roads Administration is developing a ferry free connection between Kristiansand and Trondheim. One of the more challenging fjord crossings is the Bjørnafjord. Four different bridge designs have been proposed for the crossing, three curved and one straight [\[44\]](#). In this thesis two different bridge designs are compared using Matlab (MathWorks, R2020b), with the main focus being on moment distributions and deflection induced by tidal variations. A third simpler generic bridge is examined to validate the results against a SAP2000 (Computers & Structures, 2021) model.

Constructing floating pontoon bridges is an effective way to cross deep water bodies with poor seabed conditions. However, unlike conventional bridge designs, a floating bridge is far more subject to tidal loads as it is not vertically restrained.

Complete calculation and design of a floating bridge is extremely complex. Dynamic loads, support conditions, self weight and eigenfrequency analysis, all have to be considered in order to numerically calculate the optimal bridge design. Advanced programs, based on mathematical models, are utilized to make these calculations. These models have to be further developed to meet the demands of longer floating bridges according to the Norwegian Public Roads Administration [\[1\]](#).

This thesis presents an analytical approach, using trigonometric trial functions. This has the advantage of computational efficiency in evaluating the forces and deformations of various floating pontoon bridge designs subject to tidal variations.

It is found that long floating pontoon bridges are less subject to tidal variations than shorter bridges. The outermost pontoons have increased restraint forces and deflections. The results show that by changing the reference tidal height it is possible to reduce the outlier maximum moment by a significant amount without compromising on serviceability.

Sammendrag

Statens vegvesen jobber med å bygge en ferjefri forbindelse mellom Kristiansand og Trondheim. En av de mest utfordrende fjordkryssingene er Bjørnafjorden. Fire forskjellige løsninger har blitt presentert; tre buede- og en rett bro. I denne oppgaven sammenlignes to forskjellige brodesign ved hjelp av Matlab, med hovedfokus på momentfordelinger og nedbøyninger under tidevannsvariasjoner. En tredje, enkel generisk bro, undersøkes for å validere resultatene mot en SAP2000-modell.

Flytende pontongbroer er en effektiv måte å krysse områder med dyp havbunn og dårlige grunnforhold. Imidlertid, i motsetning til konvensjonell brodesign, er en flytebro i større grad utsatt for belastning fra tidevann, fordi de ikke er forankret vertikalt.

Fullstendige beregninger og design av en flytebro er ekstremt kompleks. Dynamiske belastninger, opplagerbetingelser, egenvekt og egenfrekvens analyse, må vurderes for å beregne det optimale brodesignet numerisk. Avanserte programmer basert på matematiske modeller blir benyttet til å utføre disse beregningene. Disse modellene må videreutvikles for å imøtekomme kravene til lengre flytebroer, ifølge Statens vegvesen.

Denne oppgaven benytter en analytisk tilnærming, ved hjelp av trigonometriske funksjoner. Dette kutter ned ressursene som kreves ved beregning av krefter og deformasjoner i forskjellige brodesign som er påkjent tidevannsvariasjoner.

Det er funnet at lange flytende pontongbroer er mindre utsatt for tidevannsvariasjoner enn korte. De ytterste pontongene får større tvangskrefter og nedbøyninger. Resultatene viser at ved å endre referanse på tidevannshøyden, kan det maksimale momentet reduseres betydelig, uten å gå på bekostning av brukervennligheten.

Table of contents

Preface	III
Abstract	III
Sammendrag	V
Table of contents	VI
Glossary	VIII
Chapter 1 Introduction	1
1.1 Background	1
1.2 Literature review	2
1.3 Research gaps and motivation	5
1.4 Objective	5
1.5 Scope and limitations	5
1.6 Organisation of thesis	10
Chapter 2 Methods and models	11
Problem definition	11
2.1 Overview of viable research methods	11
2.1.1 Quantitative and qualitative methods	11
2.1.2 Case study and research by design	11
2.2 Methodology	12
2.2.1 Numerical implementation	12
2.2.2 Numerical verification	13
2.3 Models and formula	14
2.4 Parameters, assumptions and idealization	17
Chapter 3 Simple curved floating bridge	18
3.1 Introduction	18
3.2 SAP2000 simple bridge models	
3.2.1 Finite element method	20
3.2.2 Coordinates	20
3.2.3 Frame and support modeling	21
3.3 Homogenous simple bridge with convergence study	25
3.3.1 Results and discussion	26
3.4 Inhomogeneous simple bridges	29
3.4.1 Convergence and discontinuities	29
3.4.2 Inhomogeneous symmetric	29
3.4.3 Inhomogeneous non-symmetric	32
3.5 Tidal variations	35
3.5.1 Method	36
	VI

3.5.2 Tidal variation results	37
3.6 Simple bridge concluding remarks	41
Chapter 4 Bjørnafjorden curved floating bridge	43
4.1 Background Bjørnafjorden curved and straight bridge	43
4.2 Organization of chapter	44
4.3 Introduction	44
4.4 SAP2000 and initial draft	47
4.5 Tidal variations including a simple convergence study	49
4.5.1 Tidal variation results	51
4.6 Parametric study	56
4.6.1 Parametric study results	59
4.7 Alternative tide design	62
4.7.1 Alternative tide design conclusions	64
4.8 Bjørnafjorden curved bridge concluding remarks	65
Chapter 5 Bjørnafjorden straight bridge	67
5.1 Introduction	67
5.2 Parameters	69
5.3 Method	70
5.4 Tidal variation results	70
5.5 Parametric study	74
5.5.1 Parametric study results	75
5.6 Bjørnafjorden straight bridge concluding remarks	78
5.7 Bjørnafjorden curved and straight comparison	80
5.7.1 Curved and straight comparison conclusions	80
Chapter 6 Discussion and conclusions	81
6.1 Discussion	82
6.1.1 Calibrations	82
6.1.2 Generalizability	82
6.2 Conclusions	83
6.3 Recommendations for future work	85
References	86
Appendix	A

Glossary

AADT - Annual Average Daily Traffic, total volume of traffic annually divided by 365

Abutment - Substructure at the end of the bridge

Analytical calculation - Calculating an exact solution

Arch action - The strength of an arch where vertical forces are converted to compression in the arch without creating large tension under the elements

Ballast - Material used to weigh down floating elements, usually wet sand or water

Buoyancy - Uplift created due to displacement of liquid

Conventional bridge design - Cable stayed bridge or suspension bridge built on solid rock

Convergence - In mathematics and engineering, convergence relates to the approaching of a finite limit as variables of a function are increasing or decreasing

Crossbeam - A beam that is placed transversely between two structure parts, commonly to provide out-of-plane stiffness

Degrees of freedom - In structural analysis, degrees of freedom refers to the six possible movements for a particular point and whether they are restrained or free to move

Discontinuity - In mathematics, a function has a discontinuity if its not continuous at any given point

Draft - Vertical distance from waterline to the bottom of the hull

Environmental loads - Loads caused by wind, waves, snow and other environmental forces

FEM - Finite element method, numerical solving method used in various engineering fields

Initial draft - Draft created by the permanent loads of the bridge

I_x - Second moment of inertia about axis x

I_y - Second moment of inertia about axis y

Literature review - A survey and presentation of current knowledge within a particular topic

Matlab - Matrix Laboratory, a programming language widely used for numerical computations

Mesh - A network of points adding up to the total structure. Large mesh size improves the accuracy of the computations

Mode - A pattern of vibration of the structure at a specific frequency

Mooring line - Steel cable connecting floating elements to the seabed

Norwegian Standard - Documents agreed upon and approved for use in Norway.

Used in most fields, voluntary but commonly followed. Gives a baseline goal with concrete requirements.

NTNU - Norwegian University of science and technology

Numerical calculation - Approximation by sufficient amounts of iterations, usually performed by a computer

Poisson ratio - A measure of how much a material tend to expand or contract perpendicular to the direction of the force applied

Pontoon - Large hollow element that displaces water. Usually made of steel or reinforced high strength concrete

Return period - An average time or an estimated average time between the incident environmental events

SAP2000 - Structural analysis software based on the finite element method

SLS - Serviceability limit state, design that ensures the functionality of a structure. Deflections and vibrations are two of the included controls

Structural fatigue - Fatigue caused by repeatedly acting forces upon a structure over time. This could be dynamic wave loads on coastal infrastructure or repeated tidal cycles

The Norwegian Public Road Administration - Government agency responsible for the public roads in Norway

Tidal effects - Forces derived from the daily increase in water level

Torsion - Rotation about the longitudinal axis of an element

Trigonometric trial function - A series of sinusoidal functions that are deemed reasonably close to the exact solution. They are often used in a linear superposition manner to approximate the solution.

Vierendeel beam - A truss structure made of rectangular frames

Chapter 1 Introduction

1.1 Background

Norway's landscape makes it problematic to build efficient routes through the country. One of the challenges are the wide and deep fjords, commonly crossed via ferries, which are time consuming. To simplify this, the Norwegian Public Roads Administration is developing a large project called ferry-free E39^[2]. The project aims to replace the ferries, and thus make travel time shorter for road users. One of the plans is to build a floating bridge over the Bjørnafjorden, from Eldholm on Tysnes to Gulholmane in Os. Due to the large fjord depth, up to 1300 meter in Sognefjord, it is impractical to foundation the columns of the bridge down to the seabed. As such, a floating bridge solution is appropriate and technically feasible. However, the composite load a floating bridge will be subject to under these circumstances makes it very challenging to design.

1.2 Literature review

A floating bridge is a beam-like structure with a series of pontoons along its length. The pontoons displace water, which in turn provides a buoyancy force. Floating bridges used to be famous for their use in war, as a quick way to erect a bridge for crossing rivers. They can be built by connecting boats with chains and boards, and can transport light vehicles and people. The weight of the bridge is balanced with the buoyancy of the pontoons.

A floating bridge uses Archimedes' principle to create a stable structure. Archimedes' principle states[3] that the buoyancy force exerted on a body immersed in a liquid is equal to the weight of liquid it displaces. A modern pontoon bridge uses large empty or partially empty hollow steel or concrete pontoons.

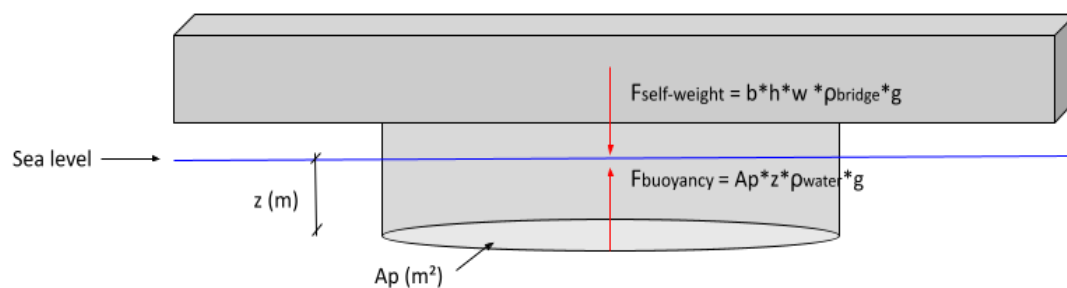


Figure 1.1 Vertical equilibrium established between a bridge and the buoyancy force induced by displaced water. A_p refers to the horizontal cross-section area of the pontoon, parallel to the waterplane. Z is the depth of which the pontoon is submerged below sea level. B , h and w are the bridge dimensions within the given cut. ρ_{water} and ρ_{bridge} are equivalent densities and g is the gravitational acceleration of Earth.

As shown in the [figure 1.1](#) above, the formulas provide a number of variables that may be manipulated. They are all of importance for keeping the equilibrium intact, but can only be handled at various degrees. The bridge girder parameters might be restrained to certain dimensions, while gravity, in addition to the density of water and steel are to be assumed as constant. The variable z is widely referred to as the pontoon draft. The bridges addressed in this thesis are resting upon several pontoons, giving the opportunity to examine the effects induced by individually implemented drafts.

Mooring lines are used to counter the horizontal forces of the waves and wind. Additionally, the bridge can be constructed with curved geometry along the waterplane. This technique allows transversal loads to be transmitted through arch action. By optimizing the curvature, forces induced by waves and wind may be transferred to the abutments as axial forces while reducing moments. This effect could be beneficial when the bridge is exposed to horizontal loads. It could be investigated if constructing curved elements is a more suitable choice in areas with rather homogeneous waves and current conditions across the entire span of the water body.

While they may provide advantages when countering loads along the waterplane, the curved elements are naturally longer than their straight counterparts and therefore increase the total self-weight of the structure.

Historically, floating bridges have been used to temporarily cross rivers during wartime. In China, during the Quin dynasty they found a way to permanently link the pontoons together using chains as “thick as a man's thigh”[\[4\]](#) and moore them to the shore with large steel rods hammered into the ground. The first pontoon bridges were built of wooden boats, with a wood deck on top. This would allow farmers or tradesmen to cross the yellow river with their animals.

Conventional bridge designs can become expensive, and occasionally impossible to construct, when crossing deep fjords with poor waterbed conditions. Standard foundation cable-stayed bridges over one km long can become very costly[\[5\]](#), but since pontoon bridges are almost continually supported they are much more cost effective. Floating bridges can also be transported using tugboats, allowing the bridges to be moved after construction if necessary. One example of this took place in 1992 when the old Galata bridge[\[6\]](#) in Istanbul was badly damaged during a fire. The old floating bridge was towed up the river to be demolished. The new bridge was built just a few meters from the old one, this one was however not a floating bridge.

Unlike modern rock-foundations, a floating bridge moves during the tide. It is therefore important to calculate how much the bridge has to move to counteract deflections, and

design the pontoon draft accordingly. The tide acts as a 1000 km² wave, slowly lifting the supports for the bridge. In some parts of the world the difference from high tide to low can be over 11.7 meters^[8]. In Bjørnafjorden the tidal range is about 2.6 meters^[9], which induces tidal effects that cause significant impact on the structure.

Tidal variations are based around a mean tide level. The mean tidal level lies close to the average tidal height. Because the variation between high and low tide is mostly even, designing the bridge for zero deflection during a mean tide is a natural choice. However, large changes in the climate can raise future sea levels by 0.5-2 meters ^[10]. This combined with the change in tidal amplitude following an increased global water level will change the cost based analysis of floating bridges^[10].



Bergsøysund bridge^[11] - Picture^[12]

The 931 meter long bridge was, at its opening, the only floating bridge not transversally supported in the world. The seven concrete pontoons are replaceable, and are mounted on the steel truss bridge. All pontoons were produced locally, and the bridge was assembled nearby to

where it sits today. The whole bridge was then towed using tugboats to its final location.

Nordhordland bridge^[13] - Picture^[14]

This floating pontoon bridge is the second longest bridge in Norway. The bridge was opened in 1994, and consists of two parts. A cable-stayed bridge with a harp design allows larger ships to pass under its 32 meter tall clearance. The floating bridge with 10 pontoons crosses a 500 meter deep fjord, where a floating moored bridge would be near impossible. It is the longest floating bridge in



Europe, but costs for construction far exceeded the budget when it was built.

1.3 Research gaps and motivation

When surveying the existing literature, it was discovered that the amount of published articles regarding floating bridges in Norway mostly focused on wave-induced effects. While wave loads have been previously explored, there appears to be a significant research gap concerning tidal effects particularly in Norwegian water bodies. Furthermore, the effects of implementing the initial design draft for individual pontoons on bridges subjected to tidal variation is a topic where further research may be beneficial. The motivation of the thesis is to assess the use of floating bridges in areas with significant tidal variations and take a closer look at one of the planned bridges. Such a type of bridge can be the solution to improve the infrastructure in many parts of the world and may drastically reduce construction related costs.

1.4 Objective

The objective of the thesis work is to analyse one generic simple bridge and two of the proposed Bjørnafjorden floating steel pontoon bridge solutions. Their predetermined section parameters will be evaluated with respect to the impact of tidal variations and self-weight. Analytical research with focus on capturing the out-of-plane responses will be conducted using Matlab models. Maximum moment distributions, vertical displacements and rotations are to be examined along the bridge girder throughout several iterations in order to determine the optimal bridge configuration.

1.5 Scope and limitations

The scope of the thesis is limited by time and a high level of complexity. This entails several prerequisites and limitations. Several possible solutions have been discussed by the Norwegian Public Roads Administration, but it has been concluded that a bridge from Tysnes to Os is the best alternative [\[15\]](#). All environmental loads and conditions are limited to the Bergen area. The bridge has a tower section, defined as a high bridge, which will allow ships to pass. The high bridge part is not a floating section, and therefore not considered.

All of the bridge calculations are performed within the serviceability limit state, SLS, and are therefore left unfactored. SLS calculations enable the finding of deflections and moment responses under normal service conditions. Relevant checks of the structures in the ultimate limit state, fatigue limit state and the accidental limit state must be completed in a real design process to verify adequacy of the design. However, these checks are outside the scope of the study.

The loads examined in the thesis are the self-weight of the bridge deck, the pontoons, and tidal loads. The bridge that is planned across Bjørnafjorden is surrounded by mountains. Such covered fjords experience relatively calm wind conditions compared to open areas, such as over an open sea. Furthermore, the bridge's elevation is close to the sea level, where the wind speeds are naturally low. For that reason the wind loads are neglected in this study.

Table 1.A . Overview of significant limitations and neglections.

Factors	Relevancy	Considered
Tidal loads	High	Yes
Bridge design	High	Yes
Self weight	High	Yes
Wave loads	High	No
Current loads	Moderate	No
Wind loads	Low	No
Traffic loads	Low	No
Marine growth	Low	No
Hydrostatic water pressure	Low	No
Accidental loads	Moderate	No
Environmental effects	High	No
Cost efficiency & Aesthetics	High	No
Seismic loads	Low	No

Wave loads

While examining the fjord's wave conditions is highly relevant for the complete design process of the bridges, it is left outside of the scope for this thesis. Research has already been carried out on the wave conditions of Bjørnafjorden by the Department of Marine Technology at NTNU, where the effects of inhomogeneity were investigated [\[16\]](#). While conducting such wave computations is complex and requires sophisticated software, it must be addressed in an extensive analysis.

Traffic loads

Traffic loads are forces induced by cars and other vehicles traveling the bridge route. While being prominent for all sorts of operative bridges, traffic loads are varying heavily depending on the location and season. The Annual Average Daily Traffic, AADT, for the route across

Bjørnafjorden is estimated to be somewhere between 12000 and 14000 vehicles[\[17\]](#) by the year 2050 with a speed limit of 110 km/h. For comparison, the Nordhordland bridge AADT was 16206 in 2020[\[18\]](#). While these numbers are significant in the design process, the bridge's heavy self-weight is the greatest factor contributing to the load composition. For the purpose of this thesis, the traffic loads are neglected but simple deflection controls are performed within the SLS, based on the route's AADT and its corresponding maximum incline requirements. The Norwegian Public Road Administration "Håndbok N100 - Veg- og gateutforming"[\[19\]](#) provides standard requirements for different dimensioning classifications. As the estimated AADT surpasses 12000 with a speed limit of 110 km/h, the maximum incline is 5%.

Marine growth

Marine growth[\[20\]](#) is referring to problematic species that grow on underwater infrastructure. In the case of floating bridges, the growth may have a significant impact on the weight of the pontoons. Additionally, carefully estimating the mass of such growth may be crucial for certain structures due to high maintenance and removal costs. The Norwegian Public Roads Administration "Håndbok N400 - Bruprosjektering"[\[21\]](#) is providing indicative values for calculating the weight of the growth if no other values are documented. There are certain solutions to employ in order to reduce the impact of marine growth, with anti-fouling paint and the utilization of high quality steel for the pontoons being two viable options. Marine growth will therefore be neglected in the calculations in this thesis.

Seismic loads[\[22\]](#)

Earthquakes are the result of earth's moving continental plates. The border between these plates are called fault lines. As Norway does not lie close to a fault line there is a low risk of damage to infrastructure. For the purpose of this thesis, the seismic loads are neglected. However, it shall be mentioned that the Norwegian standard NS-EN 1998[\[23\]](#) addresses seismic loads as something that must be considered in a complete design process.

Current loads

Horizontal loads from current are highly relevant for continuously supported floating bridges as water currents are largest near the water surface[24]. The floating bridge designs considered in this thesis have large spans between discretely supporting pontoons. Therefore the relative cross-section of the pontoons compared to the bridge is low and the impact of current loads is assumed to be neglectable. Horizontal transversal loads are not considered as only the out-of-plane response is addressed in this thesis.

Hydrostatic water pressure

Pontoons are assumed to be able to withstand the static pressure from its designed draft.

Thermal stresses

Thermal stresses are caused by change in temperature of restrained material and can result in undesirable deformations and large internal stresses. The issue is prominent for all fixed or otherwise translation-restrained structures. Considering thermal stresses is highly relevant when designing steel bridges and other kinds of infrastructure in Nordic climate conditions as temperatures may vary greatly over the course of a day. A common solution is assembling expansion joints to avoid damage when the structure is expanding and contracting.

Calculations related to restraint forces are not addressed in this thesis, as the examined bridges are assumed to be simply supported at both ends according to the analytical model.

Sea level changes

Due to uncertainties in- and lack of data in the specific construction area, the future changes in sea level due to climate change are not considered in this thesis. It will however amplify a lot of the forces a bridge is put under during a tidal cycle. The chosen design return periods of tides are the largest recorded tides from the national mapping service of Norway.

It is important to stress that the mentioned neglected factors in [table 1.A](#) do have impact on the structure and therefore cannot be ignored. This is something that must be considered further in the dimensioning process.

Non-structural mechanics related factors

Environmental impact, sustainability and aesthetics are the greatest non-structural mechanics related factors that are not considered. Addressing such factors are comprehensive and would force the scope of the thesis to be expanded greatly.

1.6 Organisation of thesis

The first part of the thesis is the background chapter, aiming to give the reader an introduction to the purpose and motivations behind the project. The following part is a literature review with the purpose of providing the reader with the most useful research and theory regarding floating pontoon bridges. The literature review is followed up by a compilation of the discovered research gaps. Distinguishing such gaps is a requisite for the next part, which is formulating the objectives of the study, work scope limits and problem definition. After the problem is defined, various appropriate research methods and procedures are discussed.

An analytical solution for the analysis of floating bridges under varying water surface elevations is presented. Tidal effects on three different floating bridge designs will be examined, hence the calculations and results chapters are divided and concluded consecutively.

A 523.6 meter long generic bridge is examined first. Computations are executed in Matlab, and thereafter validated using the finite element method, FEM, software SAP2000. The relevant assumptions, parameters and conditions are presented in order to strengthen the replicability of the study. Similar setup is conducted for the remaining proposed Bjørnafjorden floating bridge where both a curved and a straight design option is evaluated, before proceeding to the discussion and conclusion chapters. The generalization of the results are discussed and possible calibrations of the models are explored. The discussion chapter is followed by a conclusion chapter, aiming to recapitulate and summarize the findings arising from the study on different floating bridge design options.

Chapter 2 Methods and models

Problem definition

The research question to be addressed in the study is: "How are long pontoon bridges affected by tidal variations". Additionally, the project includes subtasks such as developing a general understanding of pontoon bridges and executing bridge parametric studies based on the out-of-plane responses.

2.1 Overview of viable research methods

2.1.1 Quantitative and qualitative methods

There are several options to choose from when selecting research methods for a thesis. Quantitative and qualitative methods are both widely used. The former is often carried out by analysing large amounts of collected data, often by experimentation and taking measurements.

The qualitative research method is generally based on gaining a deeper understanding of the given topics in order to draw qualified conclusions. For this purpose, performing literature studies supported by one-on-one interviews with professionals may be an appropriate approach.

2.1.2 Case study and research by design

When conducting a case study, it is common to narrow down the scope of research to a single situation or project. This method can be beneficial in order to analyse an actual real-life structure, considering the fact that there are only a few floating bridges in Norway. However, this advantage does not come without any costs. It may be difficult to generalize and draw broader conclusions based on results from a case study. Therefore, such studies may preferably be complemented with additional research methods.

Research by design is a method based on the repeated process of creating, discarding and concluding different designs. This method is commonly utilized when trying to connect the design process closer to the customer's needs. While giving the opportunity to deeply explore and optimize different solutions, this method is based on several iterations and may therefore become costly in terms of time and effort. Certain elements of this method are implemented naturally in this project since the tidal effects and properties are investigated by several iterations.

2.2 Methodology

For the purpose of this thesis, conducting a mix of methods is a suitable choice. Different approaches may be utilized depending on the state of the project. The first step is to perform an early literature study on floating bridges in general. This is highly valuable considering the limited previous knowledge of the topic within the group. As has been mentioned, the research on floating bridges in Norway is limited. A quantitative analysis of data is therefore chosen for complementing the literature study, thus enabling more valid conclusions to be drawn on the issue.

Additionally, input from case studies will be considered. The most fundamental part of the project is exploring tidal effects on a 523.6 meters generic bridge and the Bjørnafjorden proposed floating bridges, by taking their determined properties into account.

The methods mentioned above all contribute to a composite approach that can be described as an analytical study.

2.2.1 Numerical implementation

Choosing suitable programs and formulations are essential to make sure that the analysis can be completed in a scientific and efficient way. Large amounts of data are to be collected and used to draw conclusions. Initial drafts and bridge properties must be calculated through satisfying amounts of iterations to accomplish the quantitative part of the thesis. The mentor

of this project is providing a feasible solution to this challenge.

The calculations are carried out in Matlab, using formulas that are based on trigonometric trial functions and are offering an approximate solution. A more thorough explanation of the method is presented in the Models and formula section [\(2.3\)](#). This is an analytical approach that has been found to be efficient in providing accurate results for simplified cases[\[25\]](#). Furthermore, the computational effort may be greatly reduced when compared to various advanced FEM-based programs that are available on the market. By utilizing this method, far less time is spent performing calculations when the parameters are adjusted.

This method works well with an approach where the results are analysed based on several iterations, with varying inputs. However, the Matlab code is running with a number of assumptions and neglections that are presented in [chapter 2.4](#). Given such simplifications, it is important to stress that the resulting forces and deflections obtained by this method are not completely identical to what a structure would experience in reality. Currently, this is the case for all structural analysis software that run simulations on floating bridges at various degrees. It is therefore common to split the analysis of a floating bridge into different parts. This technique enables the use of several softwares with their own specializations. Given the scope of this project, the chosen analytical method is sufficient to provide the necessary tools.

2.2.2 Numerical verification

Numerical validation, rather than hand calculations, is highly recommended given the great complexity of a floating bridge. For the purpose of this thesis, the FEM-based program SAP2000 is used to validate the collected data. SAP2000 is a structural analysis software with an intuitive user interface and strong engine[\[26\]](#). The combination of these two factors provides an efficient method of validation, without steep learning curves for the user. Similarly as for Matlab modeling[\[27\]](#), gaining experience by working with this program may be advantageous for future works given its relevance within the structural engineering field.

The various bridges are first modeled as Sap2000 structures, thereafter analysed within Matlab. Using the exact same parameters and simplifications are of most importance. The results are then compared in order to verify the accuracy of the Matlab results. Some deviations are expected since the programs are running the calculations based on different mathematical models. However, only the most simple cases will be compared, hence the deviations are expected to be neglectable if everything is executed correctly. The validation is also providing a crucial method of spotting potential input errors.

2.3 Models and formula

In order to calculate displacements, rotation and moments, a Matlab model was created using the methods shown in “Response of a floating curved pontoon bridge subjected to tide induced water surface variation: an analytical approach” (J. Dai et al., 2017)[\[25\]](#) based on the out-of-plane governing equations of motion (J. Dai, K.K. Ang, 2015) [\[29\]](#). The sign convention and direction of axes are presented in [figure 2.1](#), note that z refers to the longitudinal axis. This thesis presents an analytical approach to calculating the out-of-plane response of a long floating pontoon bridge.

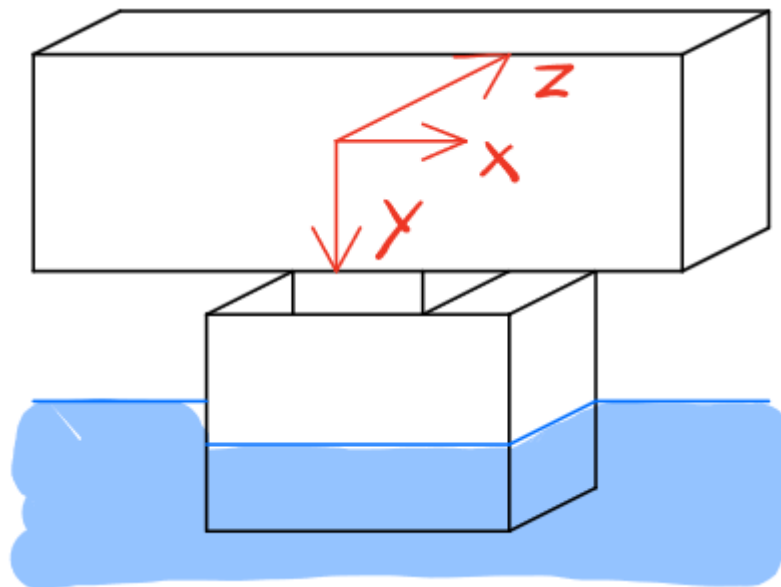


Figure 2.1. The sign convention used in the analytical model. The presented direction of the axes are considered to be positive.

The Mathematical formulation of the solution are presented as follows[25]:

A simply supported Euler beam with length L , radius R , cross-sectional area $A(z)$, flexural rigidity $EI_x(z)$ and shear rigidity $GJ(z)$ is considered. The beam is assumed to be restrained to torsion at the end supports and have constant curvature.

The governing equations for the out-of-plane response can be formulated as:

$$\frac{\partial^2}{\partial z^2} \left(EI_x(z) \frac{\partial^2 v}{\partial z^2} - \frac{1}{R} \beta \right) - \frac{GJ(z)}{R} \left(\frac{1}{R} \frac{\partial^2 v}{\partial z^2} + \frac{\partial^2 \beta}{\partial z^2} \right) + \sum_{k=1}^{N_p} k_{yk} (v - H_T - H_e) \delta(z - z_k) = \rho A(z) g \quad (1a)$$

$$\frac{EI_x(z)}{R} \left(\frac{\beta}{R} - \frac{\partial^2 v}{\partial z^2} \right) - GJ(z) \left(\frac{\partial^2 \beta}{\partial z^2} + \frac{1}{R} \frac{\partial^2 v}{\partial z^2} \right) + \sum_{k=1}^{N_p} k_{tk} \beta \delta(z - z_k) = 0 \quad (1b)$$

where v is the vertical displacement and β torsional deformation. The values k_{yk} and k_{tk} represent the vertical and torsional hydrostatic stiffness. N_p is the number of pontoons, H_t the tide induced surface elevation and H_e the water surface elevation in equilibrium.

Assuming displacements of the bridge as the summation of a series of sinusoidal functions, the following formulas can be derived where q_{vi} and $q_{\beta i}$ are the generalized coordinates of the i th mode.

$$v = \sum_{i=1}^{\infty} q_{vi} \sin \frac{i\pi z}{L} \quad \beta = \sum_{i=1}^{\infty} q_{\beta i} \sin \frac{i\pi z}{L} \quad (2)$$

Galerkin's approach is utilized to solve these coupled equations by computing the coefficients that satisfy the governing equations.

$$\sum_{j=1}^n a_{ij} q_{vj} + \sum_{j=1}^n b_{ij} q_{\beta i} = \rho g \int_0^L A(z) \sin\left(\frac{i\pi z}{L}\right) dz \quad (2a)$$

$$\sum_{j=1}^n c_{ij} q_{\beta j} + \sum_{j=1}^n d_{ij} q_{vi} = 0 \quad (2b)$$

The coefficients are computed as:

$$a_{ij} = \int_0^L \left[EI_x(z) \left(\frac{i\pi}{L}\right)^4 + \frac{GJ(z)}{R^2} \left(\frac{i\pi}{L}\right)^2 \right] \sin\left(\frac{i\pi z}{L}\right) \sin\left(\frac{j\pi z}{L}\right) dz + \sum_{k=1}^{N_p} k_{y,k} \sin\left(\frac{i\pi z_k}{L}\right) \sin\left(\frac{j\pi z_k}{L}\right) \quad (3a)$$

$$b_{ij} = \frac{1}{R} \left(\frac{i\pi}{L}\right)^2 \int_0^L (EI_x + GJ) \sin\left(\frac{i\pi z}{L}\right) \sin\left(\frac{j\pi z}{L}\right) dz \quad (3b)$$

$$c_{ij} = \int_0^L \left[\frac{EI_x(z)}{R^2} + GJ(z) \left(\frac{i\pi}{L}\right)^2 \right] \sin\left(\frac{i\pi z}{L}\right) \sin\left(\frac{j\pi z}{L}\right) dz + \sum_{k=1}^{N_p} k_{y,k} \sin\left(\frac{i\pi z_k}{L}\right) \sin\left(\frac{j\pi z_k}{L}\right) \quad (3c)$$

$$d_{ij} = \frac{1}{R} \left(\frac{i\pi}{L}\right)^2 \int_0^L (EI_x(z) + GJ(z)) \sin\left(\frac{i\pi z}{L}\right) \sin\left(\frac{j\pi z}{L}\right) dz \quad (3d)$$

To simplify this, the variables $A(z)$, $EI_x(z)$ and $J(z)$ are considered as a line integral of a function $f(z)$:

$$Q = \int_0^L f(z) \sin\left(\frac{i\pi z}{L}\right) \sin\left(\frac{j\pi z}{L}\right) dz \quad (4a)$$

When $f(z)$ is a constant, Q is given by:

$$Q = \begin{cases} \frac{fL}{2}, & \text{when } i=j \\ 0, & \text{when } i \neq j \end{cases} \quad (4b)$$

When $f(z)$ is symmetric with respect to the mid-span, Q is given by:

$$Q = \begin{cases} \int_0^L f(z) \sin\left(\frac{i\pi z}{L}\right) \sin\left(\frac{j\pi z}{L}\right) dz, & \text{when } |i-j| \text{ is even} \\ 0, & \text{when } |i-j| \text{ is odd} \end{cases} \quad (4c)$$

Once the coefficients are found, the generalized coordinates q_{vi} and $q_{\beta i}$ is computed by using $2n*2n$ matrix multiplication

2.4 Parameters, assumptions and idealization

The bridges are modeled as Euler-Bernoulli beams [28]. By utilizing such an idealization, it is assumed that the deflections are small relative to the length of the bridge and that the cross-section remains perpendicular to the deformed axis of the bridge. As the ratio between the length and height of the beam is large, shear deformation is neglected and pure bending is assumed.

Furthermore, a number of assumptions and simplifications are made when performing the following computations, including:

- Simple end supports with torsion restraints
- Constant density throughout the entire bridge and constant I_x , second moment of inertia about axis x , throughout the spans
- Neglection of waves and the other environmental loads presented in [chapter 1.5](#) "Scope and limitations"
- Homogeneous tidal variation across the water body
- Constant curvature
- Even pontoon spacing and uniform height throughout the entire length of the bridge
- The bridge girder is assumed to rest directly on the pontoons, eventual columns are neglected
- The pontoon weight is balancing itself through buoyancy action and is therefore not added to the total density of the structure
- The pontoon water plane moment of inertia is assumed to be zero

Chapter 3 Simple curved floating bridge

3.1 Introduction

A 523.6 m long generic curved floating bridge with arbitrary cross-section properties is examined. The formulations presented in the previous chapter are utilized for the following Matlab computations. It shall be noted that the corresponding calculations and validations of the following simple and draft cases have already been conducted earlier by Dai (2017)[\[25\]](#), but are repeated in this study to learn and verify the procedures. Gaining such knowledge is required to perform the subsequent tidal variation analysis.

The chapter is organized as follows. A short introduction is given before presenting the process of establishing the SAP2000 models, used for numerical verification of the analytical solution. The next part is computing the required initial drafts that results in neglectable relative deflections between the pontoons, a prerequisite for the bridge to be functional and operational. This part is accomplished by restraining the pontoon's vertical degree of freedom within the SAP2000 model. After the FEM model with corresponding computations are presented, the analytical study of the simple bridge is conducted using the mathematical formulation of the solution. A simple case without any initial draft is analysed in Matlab and validated. The analysis contains a convergence study for a homogeneous bridge, aiming to further limit the computational effort by restraining the calculations to the necessary amount of modes that gives accurate results.

A similar setup is adapted for two inhomogenous bridges. Convergence studies are executed for those bridges, and displacement discontinuities around the pontoons are displayed as the number of modes are adjusted.

The last part of the chapter is analysing how the three bridges behave under tidal variations, with extreme values found likely to occur within given return periods. The homogenous, as well as the two inhomogenous bridges are examined with varying properties. The results are then presented and the findings are finally summarized and concluded.

The presented bridge parameters are taken from J.Dai et al. (2017) [25]. The results can be validated with an external source by examining the simple bridges based on an identical setup.

The I_x values are scaled when computing the two inhomogenous cases according to the models presented in the SAP2000 section, [figure 3.3](#) and [figure 3.4](#).

Table 3.A. Simple bridge parameters

Parameter	Value
Length, L	523.6 m
Radius, R	500 m
Pontoon spacing	104.72 m
Deck sectional area, A	5 m ²
Deck height, h	12 m
Density bridge, d	11734.2 kg/m ³
Density water	1025 kg/m ³
E-modulus, E	2*10 ¹¹ N/m ²
Poisson ratio, ν	0.3
θ	60°
I_x	50 m ⁴
I_y^*	-m ⁴
Torsional stiffness, Kt	130 m ⁴
Pontoon waterplane area, A _p	1089.12 m ²

* This variable does not affect the out-of-plane responses, it is however included to ensure all values from the cited cross-section matches [\[25\]](#).

3.2 SAP2000 simple bridge models

3.2.1 Finite element method

SAP2000 is an analysis software based on the finite element method, widely referred to as FEM. The first development of the method began already in the 1940s[30], and has been further advanced ever since. The method provides invaluable assets within various engineering fields, including structural engineering. The method allows computers to perform highly complex computations with the help of embedded algorithms. When analysing a structural problem with the FEM, the structure or element is split into a large number of simpler finite elements, adding up to a mesh[31]. Every single element in the mesh is calculated and combined into the final result, using partial differential equations based on the boundary values.

3.2.2 Coordinates

The three simple bridges are assumed to have constant curvature and are modeled as circle segments, an example is shown in [fig 3.1](#). Since the radius and angle is given, the length of the segments can be computed as

$$L = \frac{2R\pi\theta}{360}$$

The pontoon and end support spacing are constant, hence the angles between the x-axis and the supports can be computed as

$$\theta n = \frac{n\theta}{x - 1}$$

where n is the support number, ranging between 0 and 5 while starting at A, and x is the total number of supports. The elevation is assumed to be constant along the whole length of the bridge, thus the vertical components are not computed.

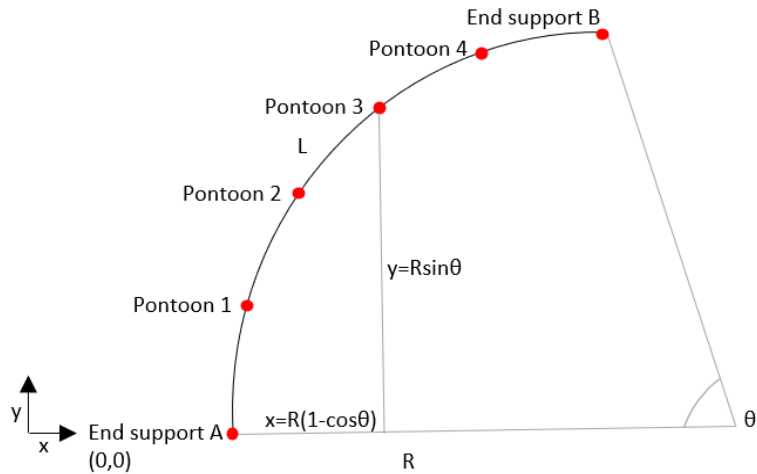


Figure 3.1. Simplified bridge model showing a method of determining the support and pontoon coordinates in the SAP2000 xy -plane, values shown in [table 3.B](#).

Table 3.B. Support and pontoon coordinates in the SAP2000 Simple curved bridge xy -plane.

Supports	x-coordinate (m)	z-coordinate (m)
End support A	0	0
Pontoon 1	10.9262	103.9558
Pontoon 2	43.2273	203.3683
Pontoon 3	95.4915	293.8926
Pontoon 4	165.4347	371.5724
End support B	250	433.0127

Procedures to determine coordinates are included in the Matlab models. However, the axes are different. The [xy-plane in SAP2000](#) is equivalent to the [xz-plane in Matlab](#).

3.2.3 Frame and support modeling

The simple bridges are modeled as continuous curved frames, divided into 5 spans. These 5 spans are further split into 20 segments each, adding up to a total of 100 joints. The frames are auto meshed at intermediate joints. Given the length of the bridge and the relatively low

complexity of the examined load cases, the presented setup is sufficient to provide accurate results. All properties are scaled with modifiers according to the corresponding Matlab parameters, except from the gravitational acceleration that is predetermined in SAP2000. Rectangular cross-sections are selected with dimensions equivalent to Matlab parameters and the shear areas are multiplied with zero in order to neglect shear deformations. The Homogeneous model is presented in [figure 3.2](#). Inhomogeneous symmetric model is presented in [figure 3.3](#), and Inhomogeneous non-symmetric model is presented in [figure 3.4](#).

The end supports are restrained in the 3 translational degrees of freedom, but are allowed to rotate freely about the vertical and perpendicular axes. The local axes at the end support B are rotated 30 degrees about the vertical axes to align axis 1(x) with the bridge's longitudinal one, thus allowing torsion to be restrained.

For the simple no draft cases, the pontoons are assigned as springs with vertical stiffness values of 10940.2 kN/m, calculated using Archimedes principle.

$$F = Ap * Z * \rho_{water} * g$$

The pontoons are assigned as roller supports for the initial draft cases. This implies that the vertical degrees of freedom are restrained, allowing the calculation of the required drafts that gives zero initial pontoon displacement by manipulating the formula above.

$$Z = \frac{F}{Ap * \rho_{water} * g}$$

The reaction forces with corresponding initial drafts can be found in [table 3.C](#).

The end support and pontoon configuration is identical for all three simple bridges. It is worth noting that SAP2000 considers the upward vertical direction as positive and the y-axis as the longitudinal one, unlike the Matlab model.

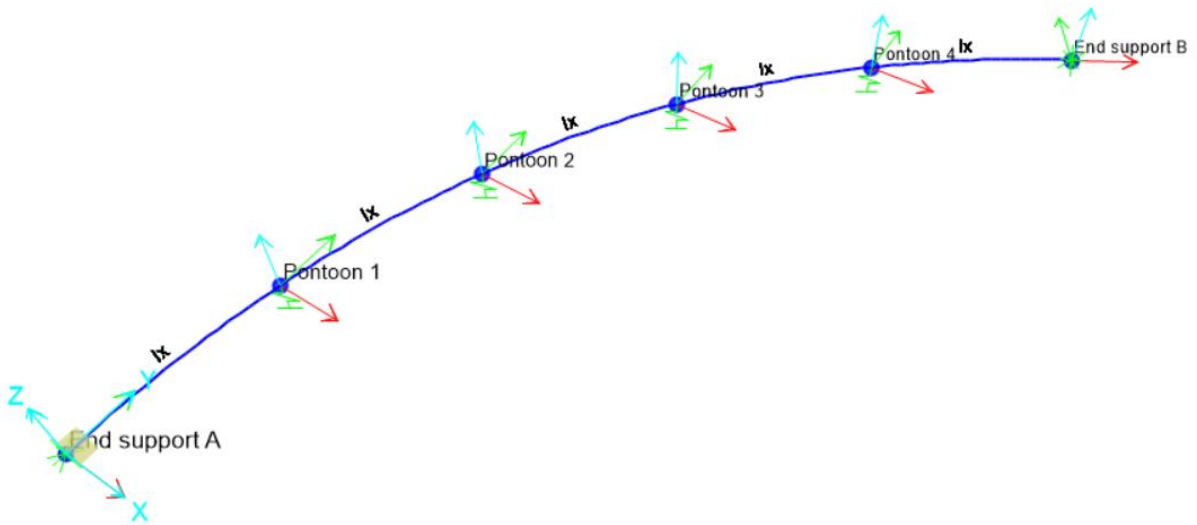


Figure 3.2. Homogeneous simple bridge model. Pontoons assigned as springs and the global and local joint axes visible.

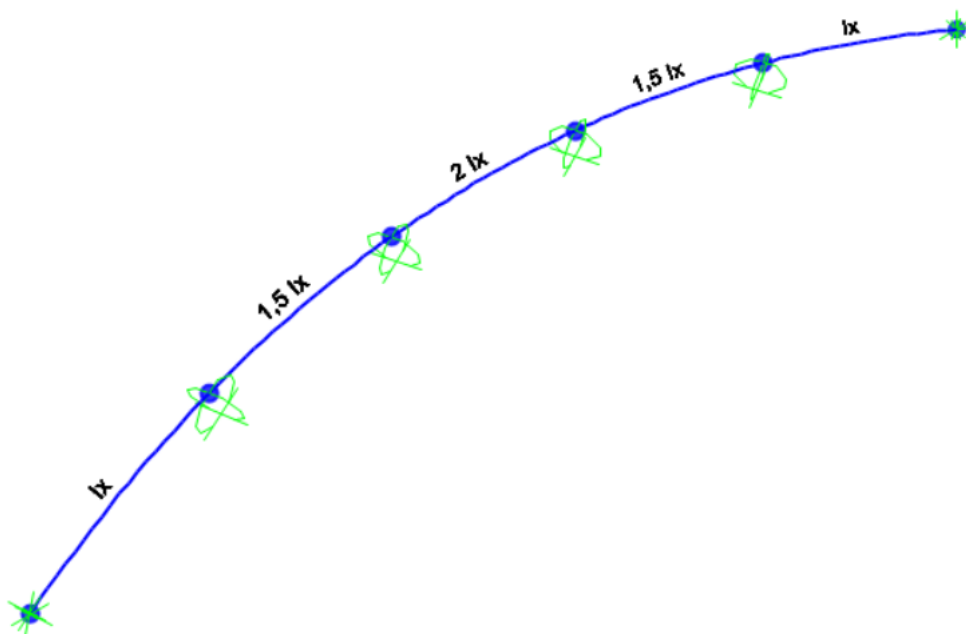


Figure 3.3. Inhomogeneous symmetric simple bridge model. Pontoons assigned as roller supports.

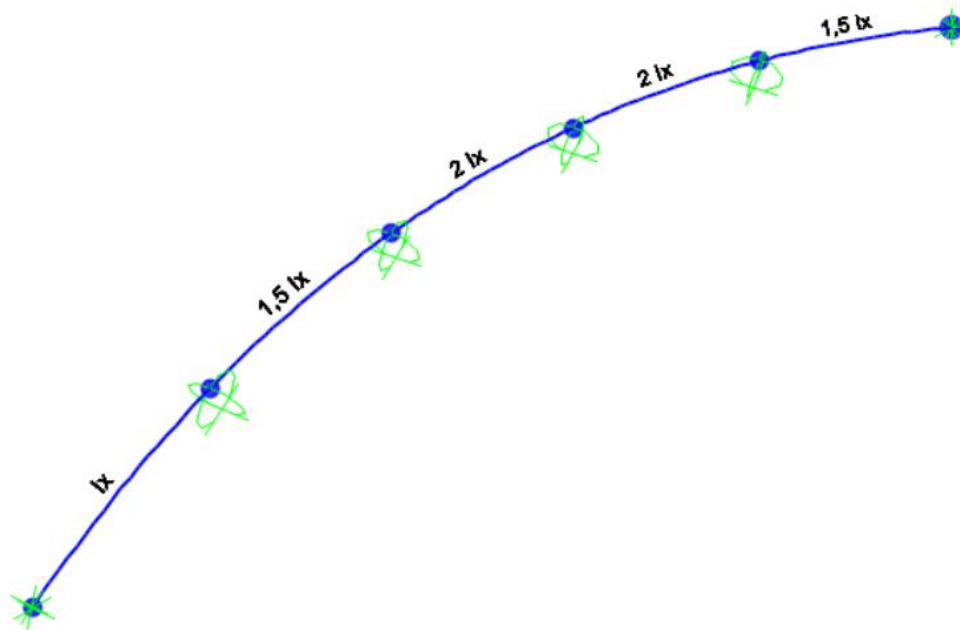


Figure 3.4. Inhomogeneous non-symmetric simple bridge model. Pontoons assigned as roller supports.

Table 3.C. Table of reaction forces and initial drafts for the simple bridges.

Support	Homogeneous symmetric		Inhomogeneous symmetric		Inhomogeneous non-symmetric	
	Reaction force (kN)	Initial draft (m)	Reaction force (kN)	Initial draft (m)	Reaction force (kN)	Initial draft (m)
End support A	23763.346	0	23511.663	0	23507.975	0
Pontoon 1	68216.259	6.235	68834.057	6.292	68567.803	6.268
Pontoon 2	58647.562	5.361	58281.446	5.327	58579.406	5.355
Pontoon 3	58647.562	5.361	58281.446	5.327	58135.019	5.314
Pontoon 4	68216.259	6.235	68834.057	6.292	68866.076	6.295
End support B	23763.346	0	23511.663	0	23598.055	0

3.3 Homogenous simple bridge with convergence study

It is essential to demonstrate that the results converge towards a solution or certain value, independent of the number of modes or mesh size[\[32\]](#). Without fulfilling this criteria, the results might not be accurate. While performing calculations with an infinitive large number of modes may provide a precise result, it is not a feasible solution considering the vast amount of computational effort required. The challenging part arises when performing calculations on complex cases that require those large mode numbers. Keeping a balance is key to secure efficiency. Conducting convergence studies allows the engineer to present accurate results with less time spent.

The calculations presented in figures [3.5](#) and [3.6](#) are performed without pontoon drafts using the analytical solution adapted into Matlab. This helps simplify the calculations. The figures show convergence and vertical displacement, respectively. The vertical displacements are calculated in both Matlab and SAP2000 to verify the accuracy of the model. The following convergence study is conducted in Matlab with an intel core i7-4790 processor and 8 gb RAM. The homogeneous cases are examined with the numbers of modes varying between 1 and 30.

3.3.1 Results and discussion

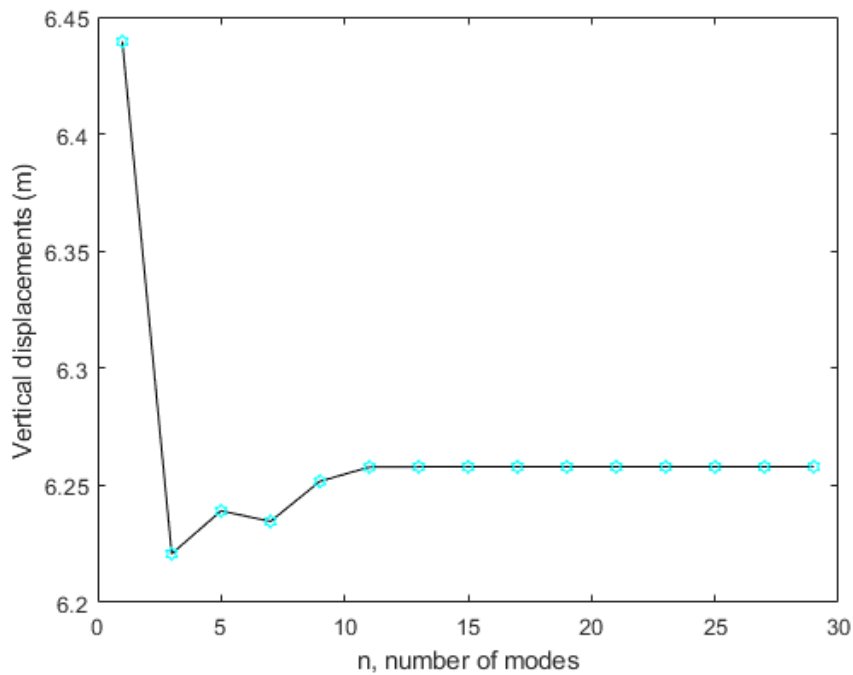


Figure 3.5. Convergence study on the homogeneous simple bridge. Maximum displacements calculated with varying numbers of modes. The CPU time remains at approximately 1 second as the modes are increasing from 1 to 30.

As displayed in [figure 3.5](#), the maximum displacements are converging rapidly when the numbers of modes exceed 7. However, the computational effort is not noticeably increasing thus 30 modes are chosen for further homogeneous calculations.

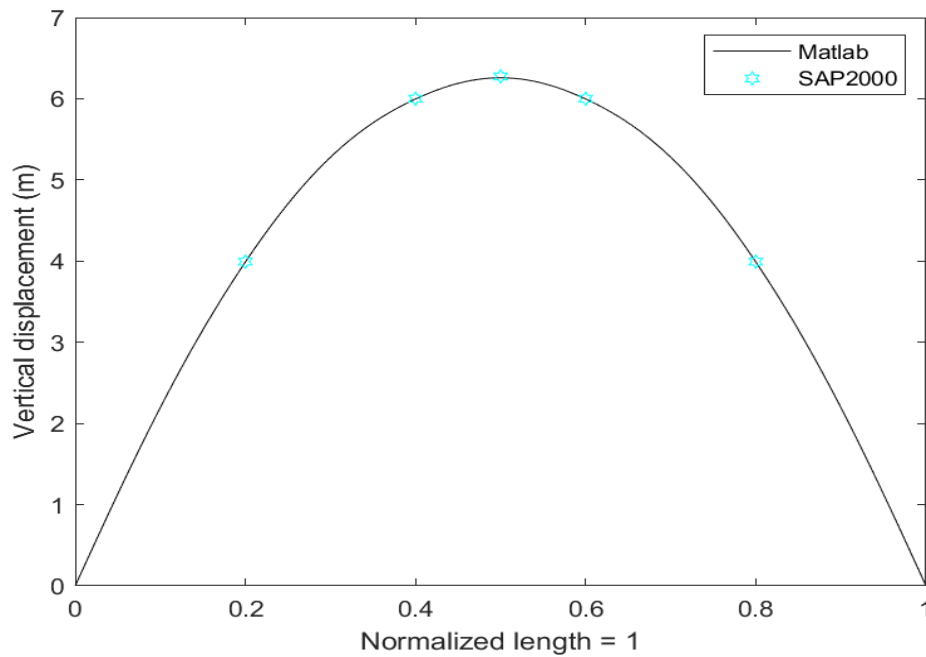


Figure 3.6. Homogenous simple bridge with 30 modes. Vertical displacements over the whole length of the bridge with the SAP2000 pontoons assigned as springs. Pontoon displacements obtained in SAP2000 marked in blue.

The maximum displacement value obtained in Matlab is 6.258 m, found at the midspan. The maximum value in the SAP2000 model is 6.275m. The deviation is close to zero at the pontoon levels, while the midspan value deviates with 17mm, the difference is small. [Figure 3.6](#) shown above visualises the difference between the models. In order to more easily compare the different bridge properties, most of the figures have a normalized length equal to one.

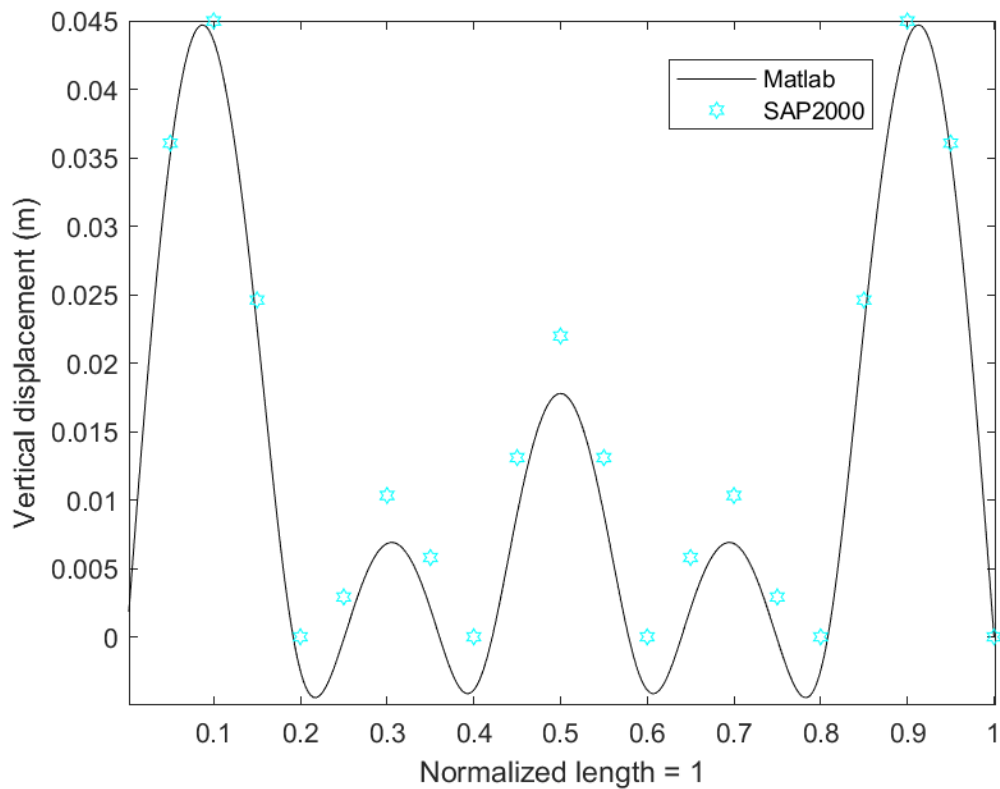


Figure 3.7. Homogenous simple bridge with 30 modes. Vertical displacements calculated with initial pontoon draft precalculated, maximum value of 0.0446m. Displacements obtained by the SAP2000 model are discretized into twenty parts, as shown in blue.

As shown in [figure 3.7](#), the SAP2000 results deviate from the results found in Matlab at several of the examined points. The greatest deviation is found in the middle span of the bridge. The displacement at this point, calculated in Matlab, is 17,8 mm while the corresponding SAP2000 joint has a value of 22 mm, resulting in a deviation of 4,2 mm. It is worth noting that some sources of error are found. The gravitational acceleration constant is set to 9.8 in Matlab, while the predetermined constant in SAP2000 has a value of 9.80665. Considering the length and high density of the bridge this difference might interfere with the calculated buoyancy forces, thus slightly altering the results. Furthermore, deviations might occur to some extent considering that SAP2000 is performing the computations based on numerical FEM while the Matlab code is utilizing the analytical solution.

3.4 Inhomogeneous simple bridges

3.4.1 Convergence and discontinuities

Similarly as for the previous case, convergence study and SAP2000 validation is conducted to verify the accuracy of the models. In addition to finding the required number of modes, the convergence study is further utilized for spotting discontinuities. Such interferences might occur, for inhomogeneous bridges, because of the sudden change in rigidity as the l_x values differ discretely for the spans. The discontinuities from large changes in stiffness is assumed to be because the matlab model uses trigonometric trial functions. Sudden changes in stiffness are difficult to model using these functions without increasing the number of modes significantly. The calculations are performed by the same computer as for the homogeneous case and with implemented drafts presented in [table 3.C](#).

3.4.2 Inhomogeneous symmetric

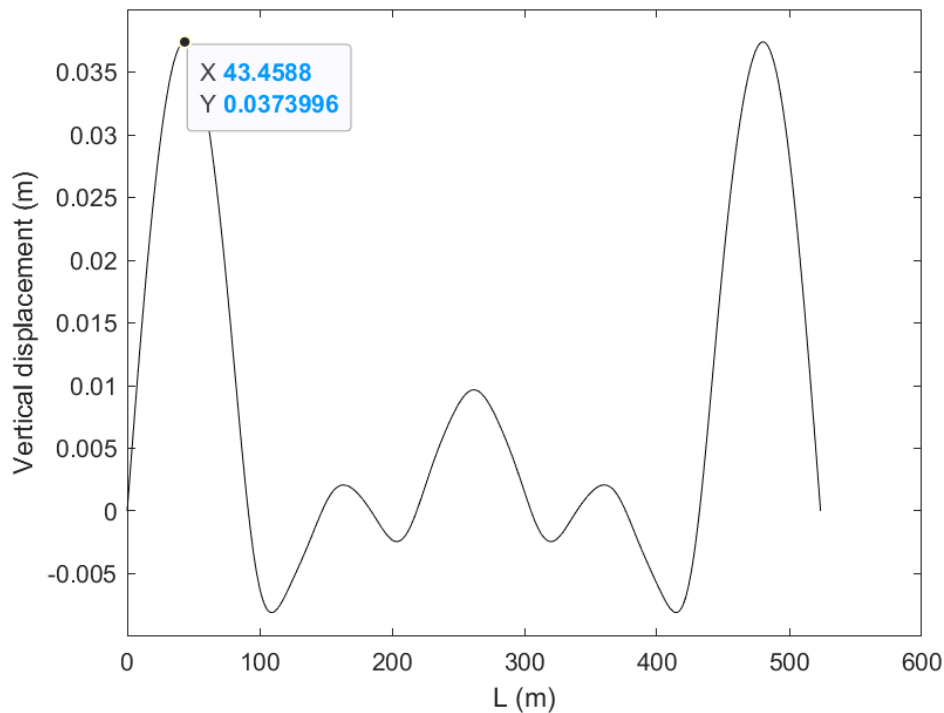


Figure 3.8. Inhomogeneous symmetric with 30 modes. CPU time 0.645477 seconds.

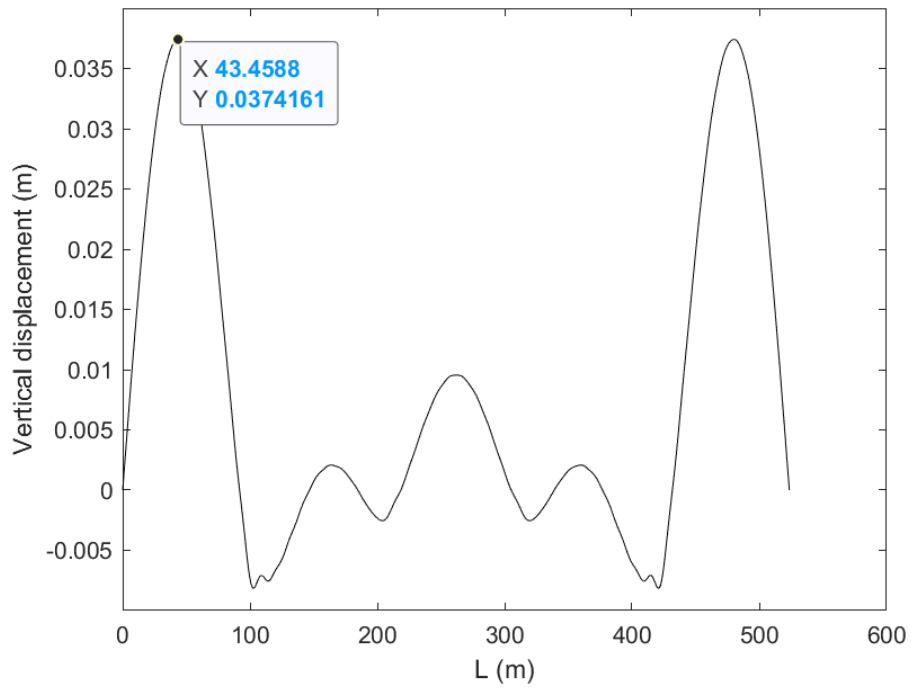


Figure 3.9. Inhomogeneous symmetric with 100 modes. CPU time 5.832653 seconds.

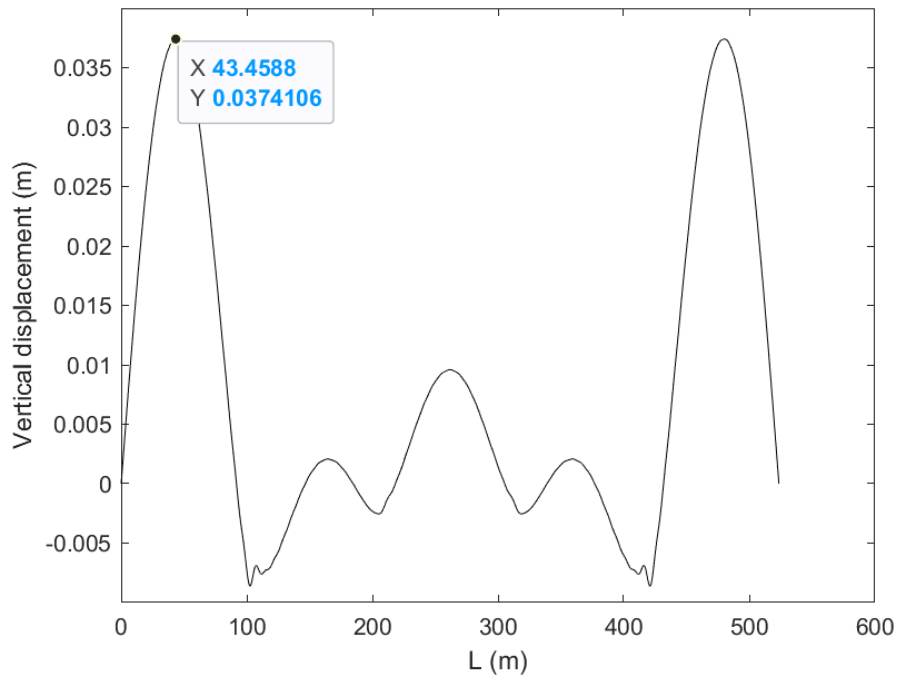


Figure 3.10. Inhomogeneous symmetric with 150 modes. CPU time 17.470773 seconds.

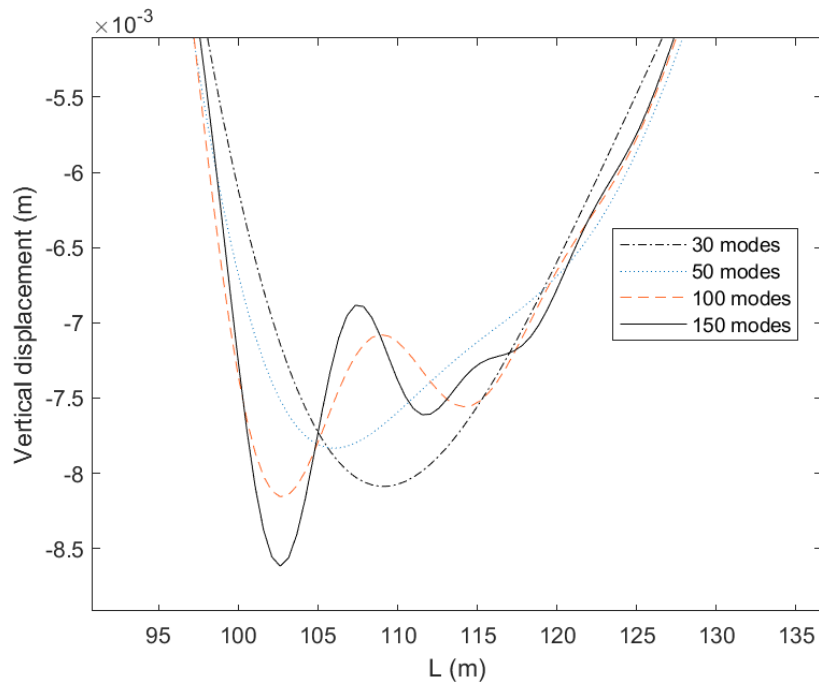


Figure 3.11. Inhomogeneous symmetric. Effect of number of modes on the vertical displacement of bridge girder near point of property discontinuity.

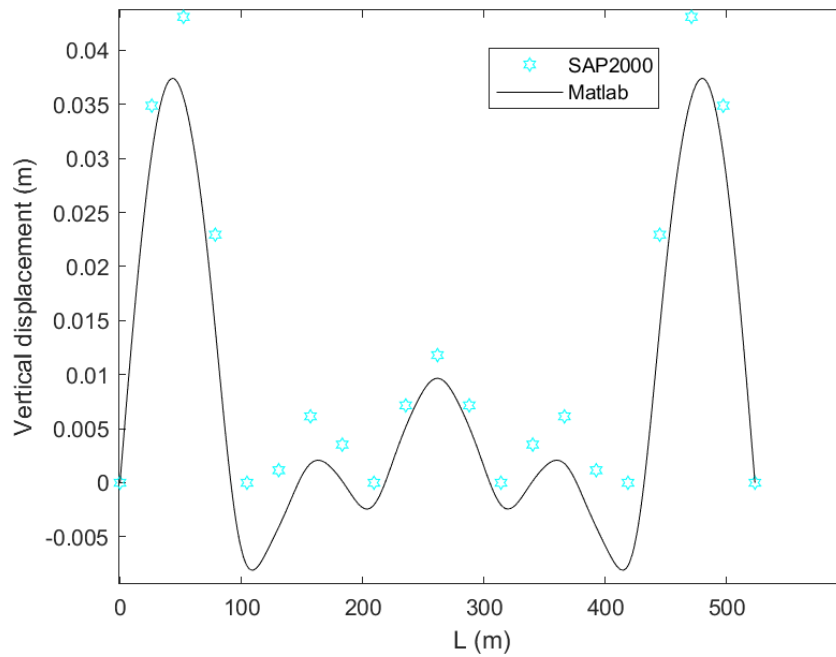


Figure 3.12. Inhomogeneous symmetric simple bridge with 30 modes. Vertical displacements calculated with initial pontoon draft precalculated, maximum value of 0.0374m. Displacements obtained by the SAP2000 model are discretized into twenty parts, as shown in blue.

It is clear when comparing [figure 3.8](#) to [figure 3.9](#) and [3.10](#) that the first pontoon location has a discontinuity when exceeding 30 modes. [Figure 3.11](#) shows the zoomed in location, with [figure 3.12](#) visualising the proximity of the Matlab model to the SAP2000 model.

3.4.3 Inhomogeneous non-symmetric

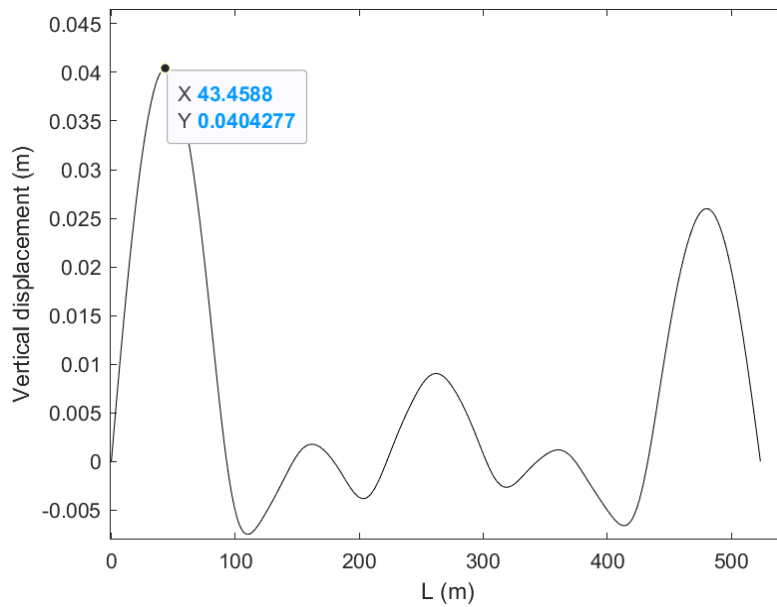


Figure 3.13. Inhomogeneous non-symmetric with 30 modes. CPU time 1.250737 seconds.

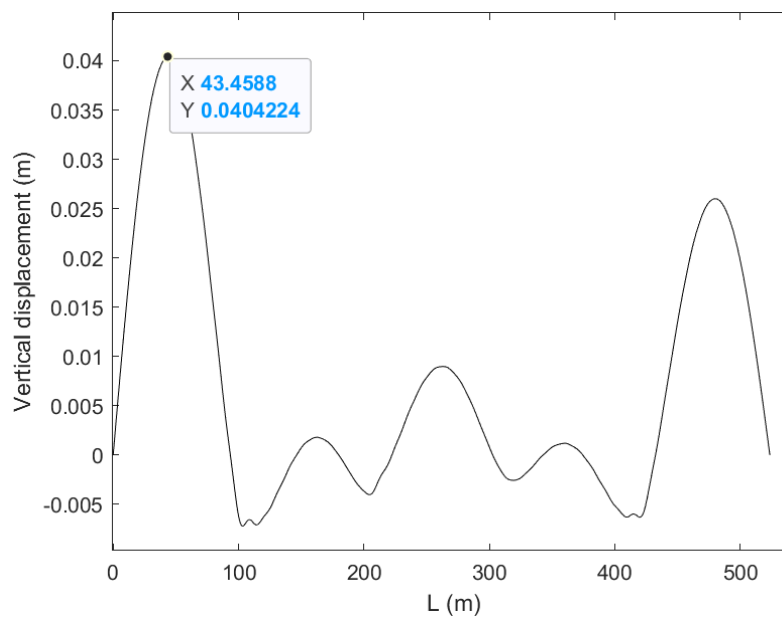


Figure 3.14. Inhomogeneous non-symmetric with 100 modes. CPU time 13.711692 seconds.

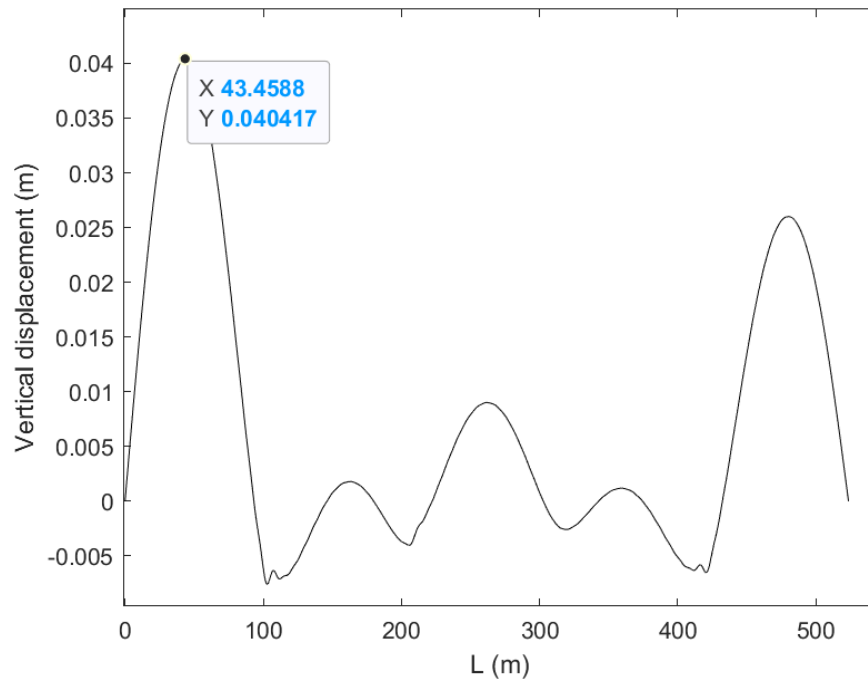


Figure 3.15. Inhomogeneous non-symmetric with 150 modes. CPU time 33.705703 seconds.

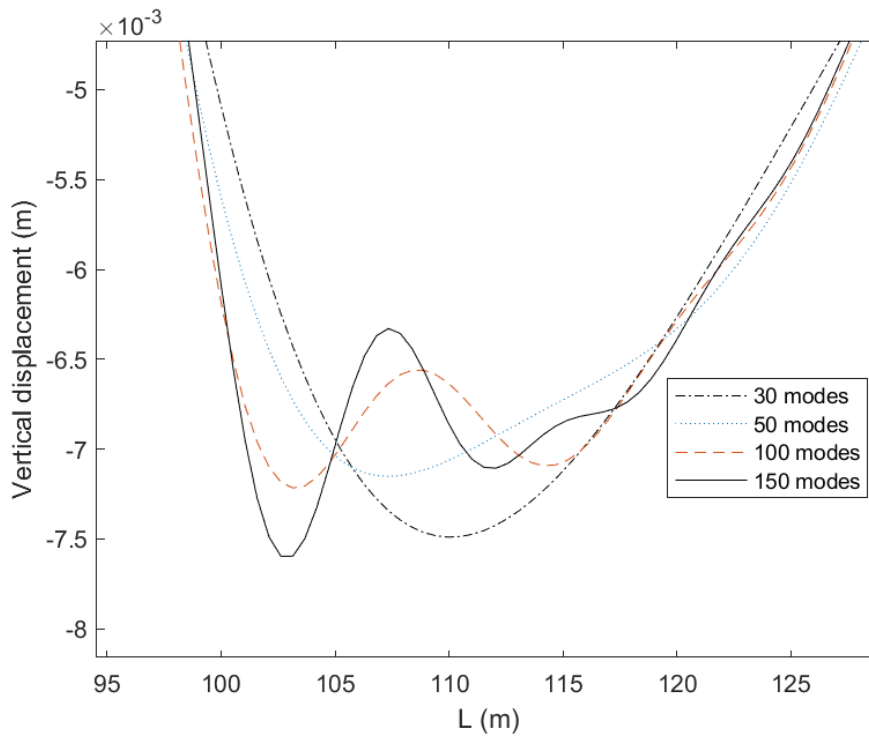


Figure 3.16. Inhomogeneous non-symmetric. Effect of number of modes on the vertical displacement of bridge girder near point of property discontinuity.

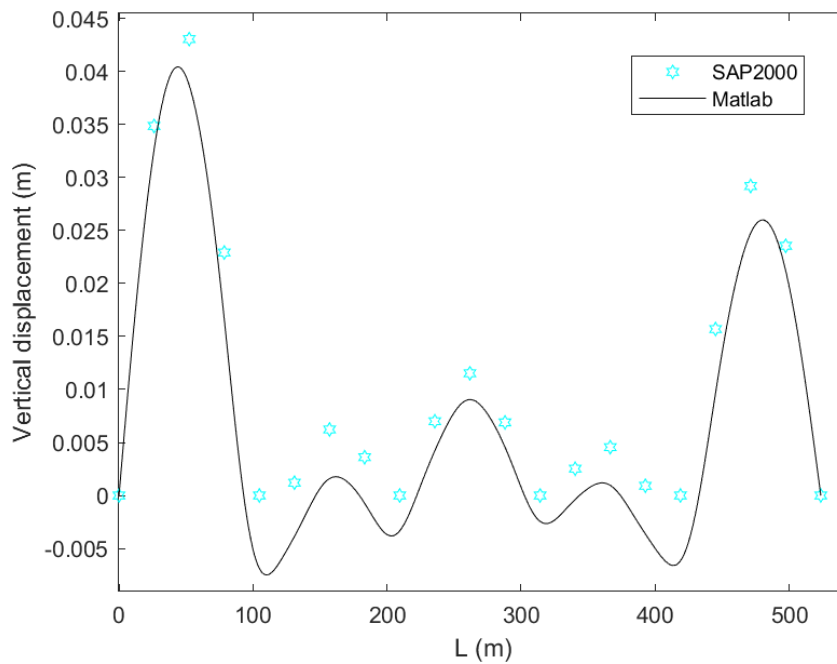


Figure 3.17. Inhomogeneous non-symmetric simple bridge with 30 modes. Vertical displacements calculated with initial pontoon draft precalculated, maximum value of 0.0404m. Displacements obtained by the SAP2000 model are discretized into twenty parts, as shown in blue.

Discontinuity around the pontoons occurs (shown in [figures 3.13, 3.14, 3.15](#)) as the number of modes exceeds 30, at a similar rate as for the inhomogeneous symmetric. The maximum displacements for the symmetric and non-symmetric cases are 37.4 and 40.4 mm respectively at 30 modes, and are unaffected when increasing the numbers. However, when compared to the homogeneous case, the computational effort is increasing much faster given the greater complexity.

3.5 Tidal variations

The next part examines how the presented simple bridge configurations are affected when subject to tidal variations. The out-of-plane response is considered and maximum moments, displacements and rotations are compared.

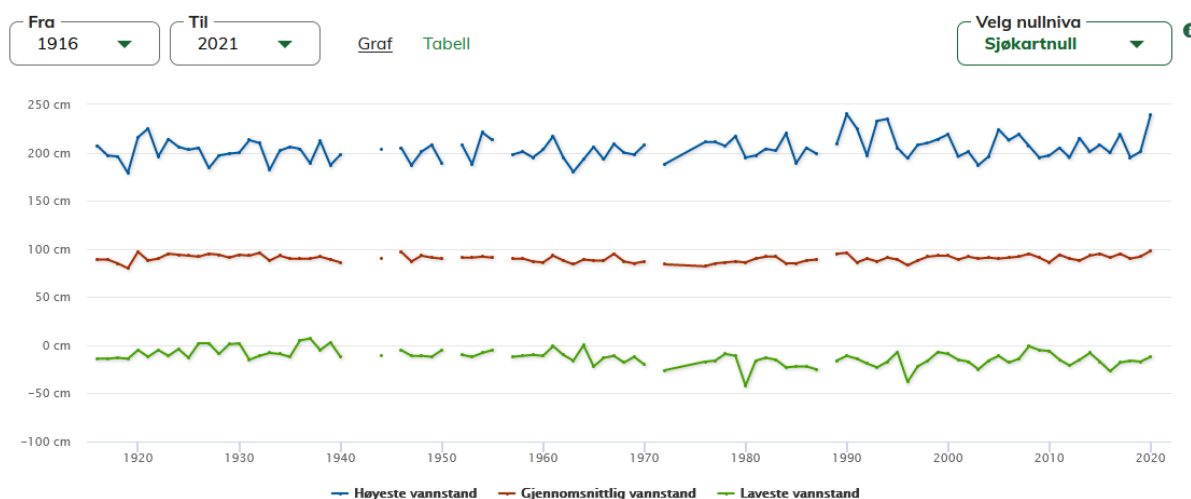


Figure 3.18. Tidal variations in Bergen over the last 100 years. [33]

The blue line represents the annual highest tide. The red line represents the average tide, and the green line represents the lowest annual tide.

Floating pontoon bridges are subject to tidal variations more than a conventionally designed bridge would be. The pontoons move vertically with the tide, but the end supports remain still as they are fixed to the shore. If a pontoon bridge is designed to remain flat during a high tide, the low tide will cause the bridge to sag. It is therefore important to manipulate the way a bridge acts during tidal variations by changing the design parameters of the bridge, or by adding ballast[34] to the pontoons.

Another essential part of designing a floating bridge is to make sure that the lowest possible internal forces and stresses occur during the mean tidal positions. If this criteria is not fulfilled, the initial deflections will be large and further amplified during the tidal cycle. This could in the worst case scenario lead to rupture. It is equally important to ensure that the end supports are properly hinged or simply supported. The internal stresses induced by the tidal variation would become huge if the end supports are not allowed to rotate.

As the considered simple bridges are fictive and arbitrarily placed, tidal variations with magnitudes found in Bjørnafjorden are explored instead. The Norwegian mapping authority keeps track of the tidal variations in the nearby city of Bergen. Mean tide in the area is 97cm above the lowest astronomical tide, with a max of 229cm and a min of -28cm^[35] (the 100 year max and 20 year minimum). The maximum value is found within a 100-year return period while the minimum value has been extracted from a shorter 20-year return period. While not resulting in an optimal setup, these are the values that are available by the time this study is conducted, thus chosen for the following computations. The maximum, average and minimum tides are visualised in [figure 3.18](#).

3.5.1 Method

The three bridges are designed with the initial drafts equal to the required zero pontoon displacement, occurring at the mean tide and presented in [table 3.C](#). As previously discussed, the mean tide is a critical state to design for in order to minimize the overall stresses and deflections during the cycle. Computations are then performed on the bridges simulating the low and high tide respectively, resulting in six examined cases.

3.5.2 Tidal variation results

Homogeneous

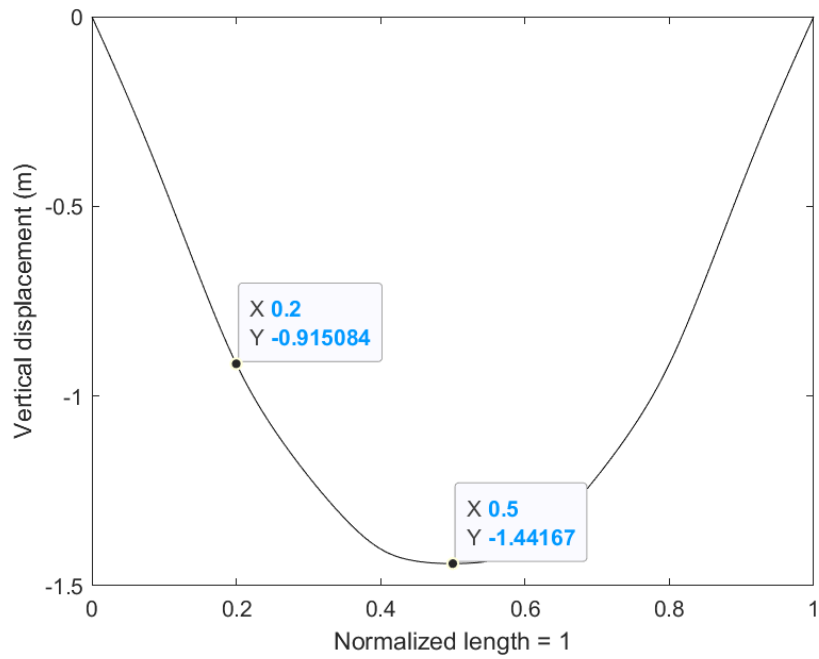


Figure 3.19. Homogeneous simple bridge with 30 modes. High tide of 229 cm, which corresponds to a relative tide of 132 cm from mean.

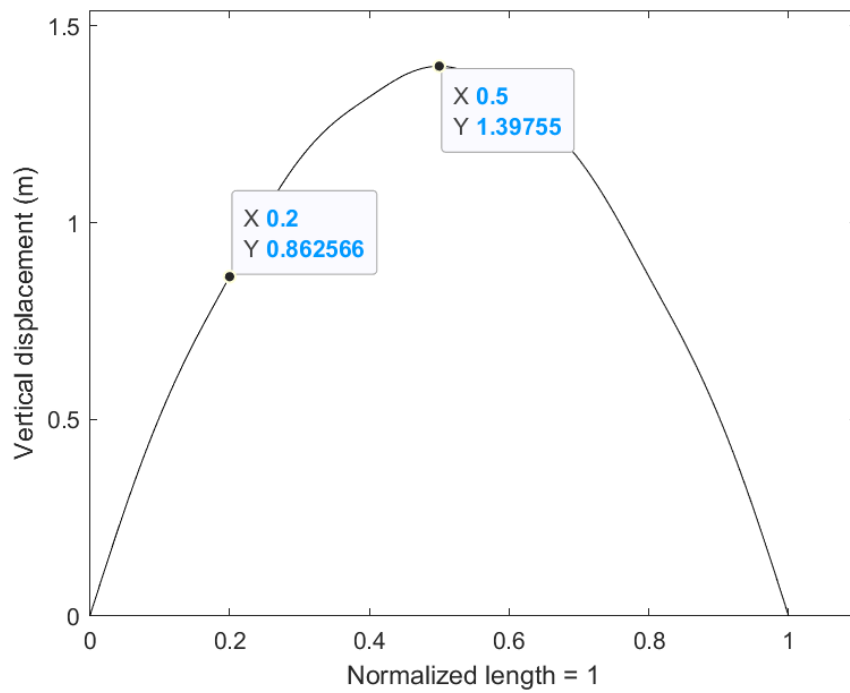


Figure 3.20. Homogeneous simple bridge with 30 modes. Low tide of -28 cm, which corresponds to a relative tide of 125 cm from mean.

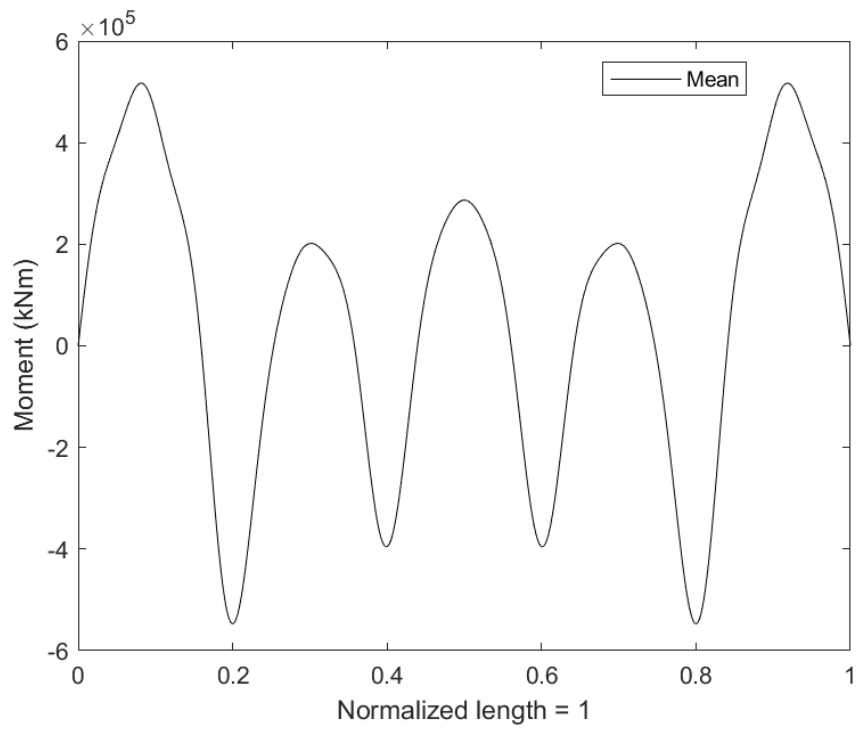


Figure 3.21. Moment distribution for the homogeneous simple bridge with 30 modes during mean tide.

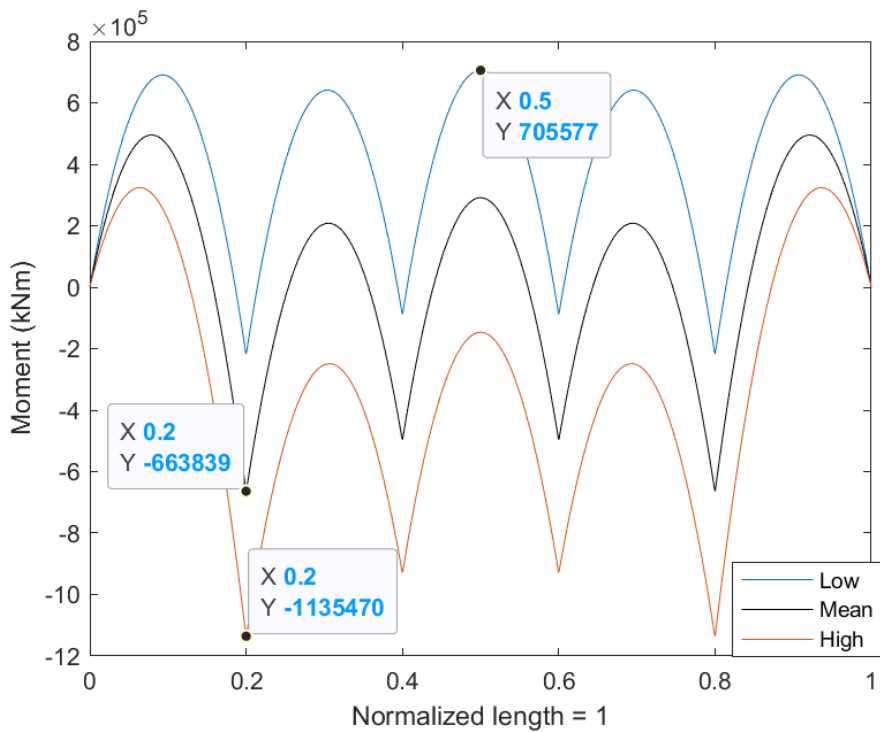


Figure 3.22. Moment distribution during low, mean and high tide for the homogeneous simple bridge with 1000 modes. Maximum moments marked.

Inhomogeneous symmetric

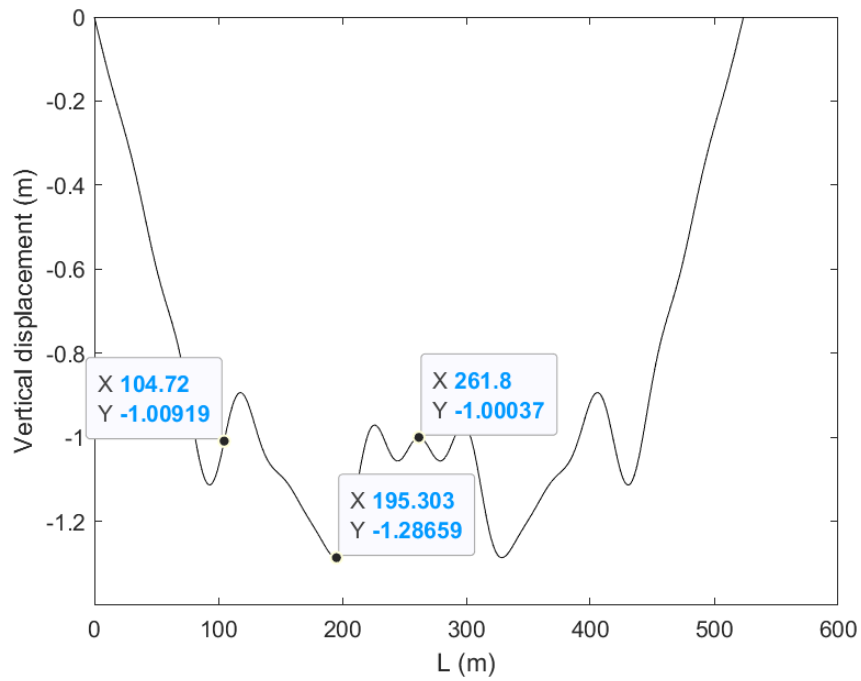


Figure 3.23. Inhomogeneous symmetric simple bridge with 30 modes. High tide of 229 cm, which corresponds to a relative tide of 132 cm from mean.

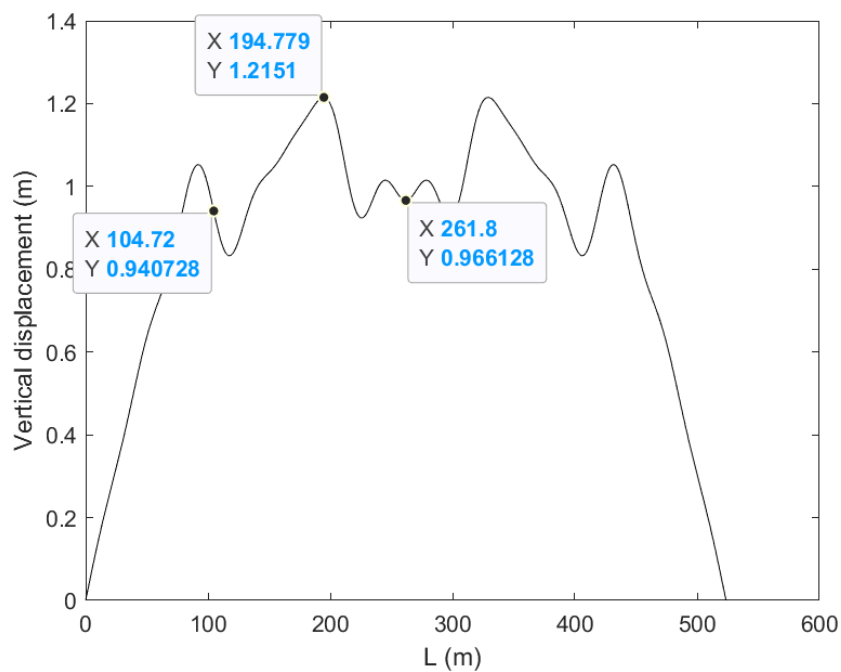


Figure 3.24. Inhomogeneous symmetric simple bridge with 30 modes. Low tide of -28 cm, which corresponds to a relative tide of 125 cm from mean.

As shown in [figure 3.23](#) and [3.24](#), the vertical displacements change abruptly. The cross-section becomes stiffer towards the middle of the bridge, which causes steep areas around the pontoons due to change in stiffness.

Inhomogeneous non-symmetric

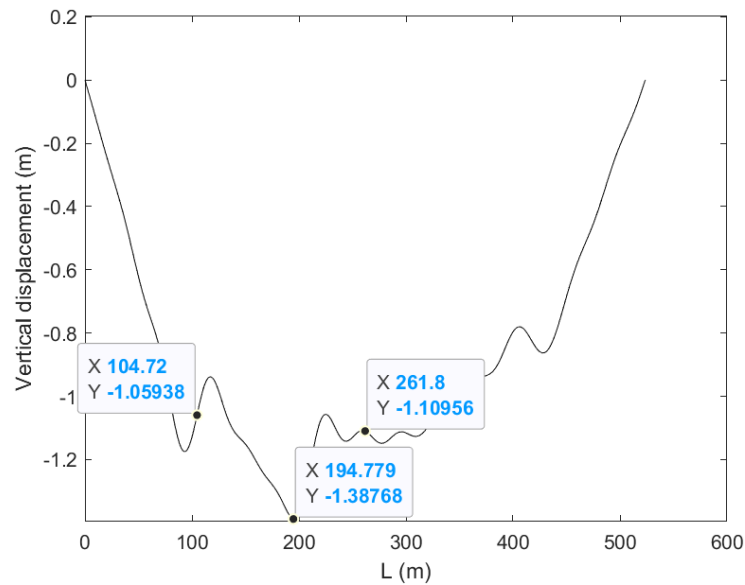


Figure 3.25. Inhomogeneous non-symmetric simple bridge with 30 modes. High tide of 229 cm, which corresponds to a relative tide of 132 cm from mean.

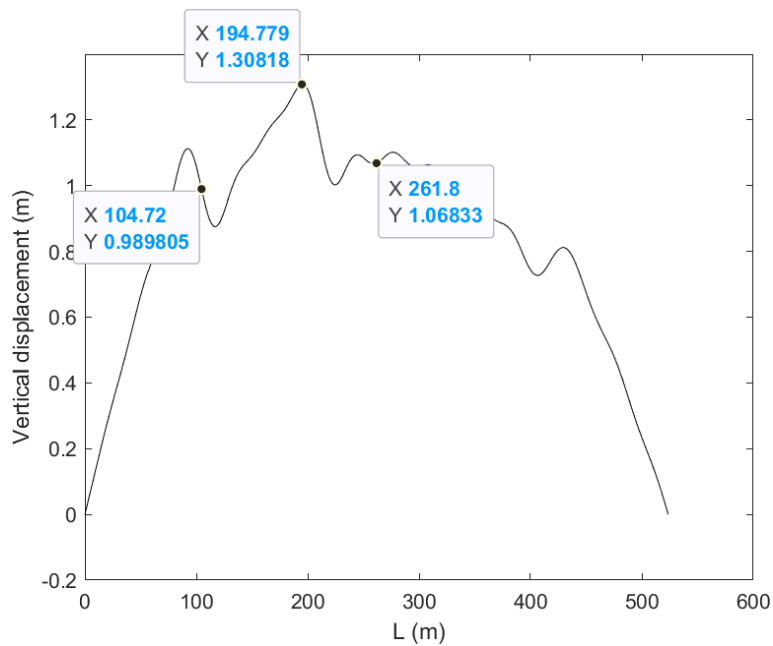


Figure 3.26. Inhomogeneous non-symmetric simple bridge with 30 modes. Low tide of -28 cm, which corresponds to a relative tide of 125 cm from mean.

The non-symmetric inhomogeneous bridge presented in [figure 3.25](#) and [3.26](#), experiences the same irregularities as the symmetric bridge. This configuration as shown in [figure 3.4](#) has lower displacements towards end support B (right side of the figure), as this section is stiffer.

3.6 Simple bridge concluding remarks

The results show a satisfying agreement between the Matlab and SAP2000 computations, validating the accuracy of the analytical model. The deviations are somewhat larger in the inhomogeneous models, this might occur due to more complex stiffness distributions as the sudden changes in stiffness might interfere with the trigonometric trial functions used in Matlab. The deflection results are converging already as of 30 modes for all three bridges. The computational effort is low throughout the entirety of the 30 modes calculations, further enhancing the usability of the model. For moment calculations 1000 modes give a clearer figure, as large changes in moments are expected over pontoons. The relative vertical displacement between the pontoons and end supports are low when designed with the calculated initial draft parameters. However, as the bridges are subjected to the extreme tide values, larger out-of-plane deflections are shown and the maximum moments are varying heavily across the spans. While observing the homogeneous cases, it is found that the maximum moment value during high tide is approximately twice as large as the corresponding mean tide maximum ([figure 3.22](#)).

During a high tide the moment over the support pontoons are the limiting factor. High tides combined with a storm surge can raise floating bridges more than the 1000year return period[\[36\]](#), as seen during the Vivian storm[\[37\]](#). Therefore it might be relevant to use the highest recorded tide when calculating the maximum moment of a floating bridge. This concept is further investigated in [chapter 4.7](#) (alternative tide design).

Designing a floating bridge with a non-homogeneous stiffness for a low tide might be simpler, as the maximum moment lands under the bridge elements. So adding stiffness to a singular bridge element where necessary, during the design process, is simple.

However a bridge subject to a high tide places the maximum moments over the support pontoons. As the weakest element's capacity is the designing factor of the transition's moment capacity. Combining two different cross-sections provides no additional strength during a high tide.

While the inhomogeneous bridges results are showing lower maximum displacements than the homogeneous counterpart, the tidal variations in the examined area contribute to significant effects upon all of the examined bridges. The inhomogeneous bridge girders experience large vertical displacement abruptions between the pontoons during the considered tidal-cycle. Parametric studies may preferably be executed in a design process in order to optimize a bridge section that withstands the conditions based on specific requirements.

Further research may explore the effects of changing the abutment height to be closer to the high tide values, rather than the mean tide. This may help reduce those extreme moments and displacements that might occur within a long return period. However when considering the significant fatigue induced by the daily tidal cycle, using the mean tide value is likely beneficial in most cases. An exception would be when designing for ultimate limit stresses under extreme weather conditions. An alternative tidal reference study is presented in [chapter 4.7](#).

Chapter 4 Bjørnafjorden curved floating bridge

4.1 Background Bjørnafjorden curved and straight bridge

Two proposed fjord crossing solutions are examined. The Norwegian Public Roads Administration assigned teams of suitable entrepreneurs in 2018[\[38\]](#). The objective was to survey the various options and determine the overall strongest solution. The chosen end anchored curved floating bridge and an alternative moored straight floating bridge were found to be feasible options. However, the end anchored curved floating bridge was favored mainly due to it being a robust and cost-efficient solution.

Information by the administration was published in may 2021[\[39\]](#) and revealed that the bridge structure, including the pontoons, will be built in steel. While concrete is the general building material for pontoon design, steel provides significantly lower self weight for the buoyancy to counteract. Additionally, substituting concrete in large structures is a critical step towards the reduction of CO2 emissions by the construction industry.

Extensive articles have been published regarding the two bridge solutions and the study presented in this thesis is based on parameters found when reviewing those articles[\[40\]\[41\]](#). Including both a curved and a straight bridge option allows a more comprehensive study to be conducted, where comparing the effects of tidal variation on two different viable bridge designs is a major part.

Looking at inhomogeneity, such as for the simple bridges, would have expanded the scope beyond the comparison of the proposed sections and are left out.

The Bjørnafjorden bridge study is split into two chapters based on the mentioned solutions, with the curved bridge being presented first. The setup is very similar for both cases as the majority of the parameters and assumptions are the same for both bridges. This is also true for the used methods and approach. Thus, all identical information is presented in this chapter and deviations are accounted for in the following chapter.

4.2 Organization of chapter

The chapter is organized as follows. An introduction is presented including important information such as bridge parameters, conditions and assumptions. The SAP2000 bridge model is described briefly, as the modeling process has already been shown in chapter three. An identical approach is conducted within the software where the pontoons are assigned as roller supports, allowing the required initial drafts to be found. A simple convergence check is completed to distinguish the required number of modes before proceeding into a tidal variation study. The bridge is examined while subjected to the mean, high and low tide conditions found close to Bjørnafjorden and presented in chapter three. The incline requirement is controlled with respect to the highest relative displacement acquired. A parametric study with the goal of determining how different sections withstand the out-of-plane response induced by tide is performed. An alternative tidal reference is explored, aiming to optimize the abutment height to reduce the extreme high tide moments.

4.3 Introduction

The bridge spans about 4600 meters, and consists of a high bridge and a floating bridge supported by 19 pontoons. The floating part is divided into a support section, S1, and span section, F1. The high bridge consists of a back and main span with a total length of about 860 meters and a tower with 80 cables to carry the girder. This part is intended to make it possible for ship traffic to cross the bridge. However, modeling and performing calculations on this non-floating part of the structure is highly complex and left outside of the scope of this thesis. The transition between the tower and the floating bridge is considered to be the entry part, meaning that the tower is modeled as the southern end support. Additionally, the transition span is reduced to the same length as the pontoon spacing in order to simplify the calculations.

The elevation between the floating part and the tower is neglected. The support conditions are identical as for the case with the previously addressed simple bridge. On the north side, the bridge is anchored to the abutment. Both ends are assumed to be simply supported, fixed in translational degrees of freedom with torsion restraint. The bridge girder consists of two

connected box cross-sections, but is herein modeled as one rectangular cross-section with equivalent properties.

In the articles [40][41], the bridge spans are designed as piecewise selected sections with varying properties. However, in this study, two of those determined sections are assumed to span the entire length homogeneously. Additionally, equivalent sections corresponding to the piecewise configuration are examined. Such homogeneity will simplify the calculations drastically and reduce the computational effort when performing the parametric studies. The three cross-sections are compared in order to evaluate the optimal solution.

All additional assumptions and idealization that are listed in [chapter 2.4](#) hold true for the examined Bjørnafjorden bridges.

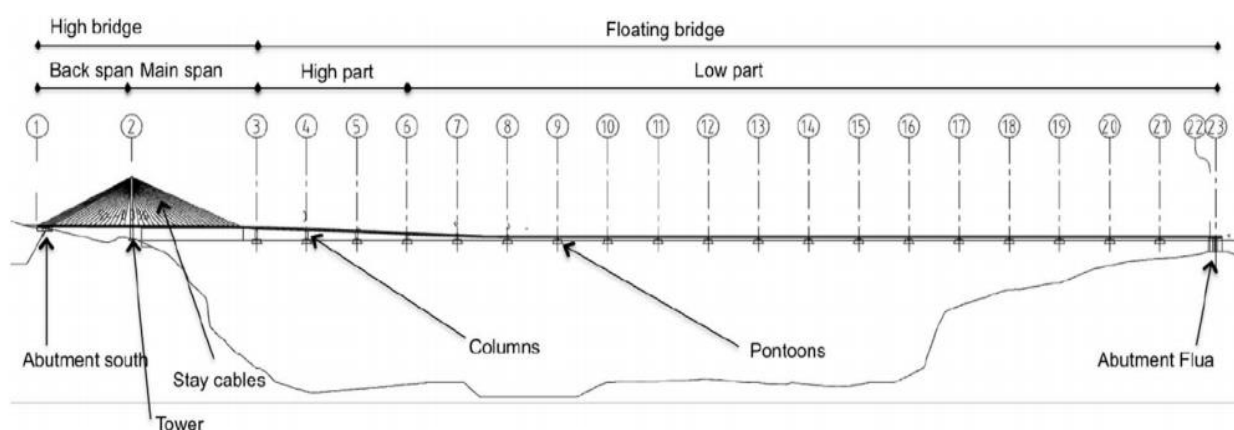


Figure 4.1. Curved floating bridge concept. Illustration by The Norwegian Public Roads Administration[42].



Figure 4.2. Curved floating bridge across Bjørnafjorden. Illustration by The Norwegian Public Roads Administration[43].

Table 4.A. Bridge parameters for three analysed curved floating bridge sections.

Parameter	Initial section F1	Most stiff section S1	Eqv. Curved
Length, L	3940 m	3940 m	3940 m
Radius, R	5000 m	5000 m	5000 m
Pontoon spacing	197 m	197 m	197 m
Deck height, h	6.5 m	6.5 m	6.5 m
Density bridge, d	14 162 kg/m ³	12 480 kg/m ³	27 449.8 kg/m ³
Density water	1025 kg/m ³	1025 kg/m ³	1025 kg/m ³
Sectional area, A	1.85 m ²	2.5 m ²	1 m ² (unit area)
E-modulus, E	2.1*10 ¹¹ N/m ²	2.1*10 ¹¹ N/m ²	2.1*10 ¹¹ N/m ²
Poisson ratio, v	0.3	0.3	0.3
θ	45.15°	45.15°	45.15°
I _x	737.9 m ⁴	1037 m ⁴	994.3 m ⁴
I _y *	13.16 m ⁴	18.34 m ⁴	-
Torsional stiffness, K _t	35.9 m ⁴	45.8 m ⁴	38.2 m ⁴
Pontoon waterplane area, A _p	1735.75 m ²	1735.75 m ²	1735.75 m ²

* This variable does not affect the out-of-plane responses, it is however included to ensure all values from the cited cross-section matches [\[40\]\[41\]](#).

4.4 SAP2000 and initial draft

The bridge is modeled using the same procedures as reported earlier in [chapter 3.3](#) visualised in [figure 4.3](#). The number of linear segments is set to 2000 because of the approximately ten times greater length compared to the simple bridge. Increasing the number of segments is important in order to secure an accurate curvature and even pontoon spacing. [Table 4.B](#) shows that there are tiny deviations between the reaction forces for pontoon number 7 to 13, thus identical initial drafts are set for those supports in Matlab.

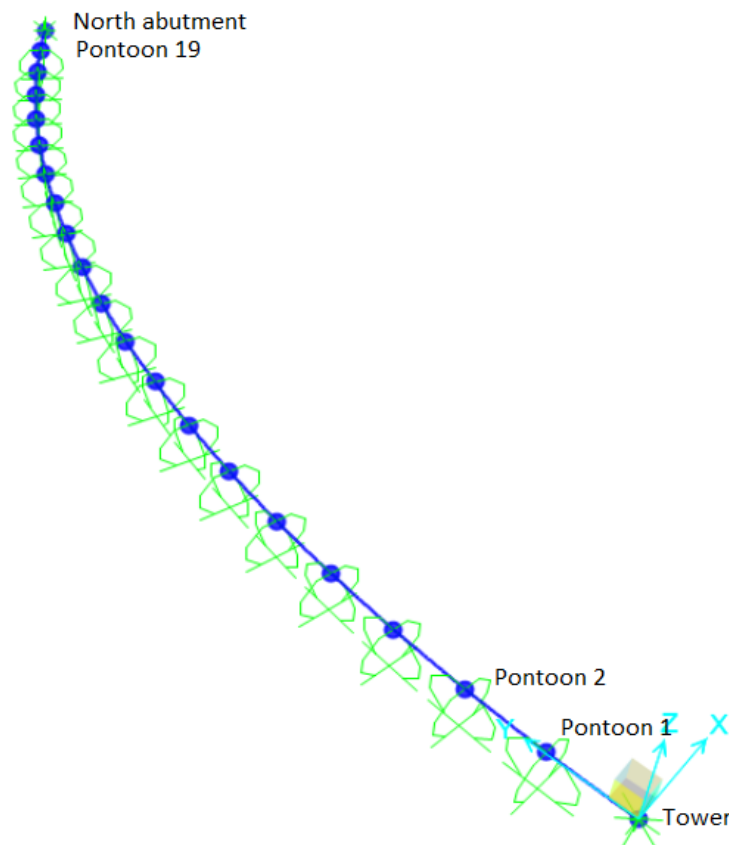


Figure 4.3. SAP2000 model of the Bjørnafjorden end anchored curved bridge with pontoons assigned as roller supports, for coordinates see [figure A.1](#).

Table 4.B. Reaction forces for the curved bridge obtained in SAP2000 with their corresponding initial draft values.

	Reaction force (kN)			Initial Draft (m)		
	Initial cross-section, F1	Strong cross-section, S1	Eqv. cross-section	Initial cross-section, F1	Most stiff cross-section, S1	Eqv. cross-section
Pontoon 1	57416.764	68378.512	60147.579	3.293	3.922	3.450
Pontoon 2	48780.165	58089.012	51090.877	2.798	3.332	2.930
Pontoon 3	51105.89	60861.192	53532.860	2.931	3.491	3.070
Pontoon 4	50479.703	60114.461	52874.588	2.895	3.448	3.033
Pontoon 5	50648.375	60315.711	53052.154	2.905	3.459	3.043
Pontoon 6	50602.995	60261.549	53004.341	2.902	3.456	3.040
Pontoon 7	50615.245	60276.182	53017.275	2.903	3.457	3.041
Pontoon 8	50611.962	60272.262	53013.811	2.903	3.457	3.041
Pontoon 9	50612.876	60273.355	53014.778	2.903	3.457	3.041
Pontoon 10	50612.578	60272.999	53014.461	2.903	3.457	3.041
Pontoon 11	50612.881	60273.361	53014.778	2.903	3.457	3.041
Pontoon 12	50611.974	60272.276	53013.811	2.903	3.457	3.041
Pontoon 13	50615.261	60276.201	53017.275	2.903	3.457	3.041
Pontoon 14	50603.03	60261.591	53004.341	2.902	3.456	3.040
Pontoon 15	50648.379	60315.717	53052.154	2.905	3.459	3.043
Pontoon 16	50479.87	60114.663	52874.588	2.895	3.448	3.033
Pontoon 17	51105.519	60860.754	53532.860	2.931	3.491	3.070
Pontoon 18	48781.881	58091.064	51090.876	2.798	3.332	2.930
Pontoon 19	57410.843	68371.475	60147.582	3.293	3.921	3.450

4.5 Tidal variations including a simple convergence study

A no draft case during high tide is computed in Matlab with varying numbers of modes. The results (fig 4.4 and 4.5) show that the vertical displacements are converging at approximately 100 modes, while the moment calculations require 250 modes to reach satisfying convergence. The latter is thus chosen for examining the response during the tidal cycle with implemented drafts. It is important to increase the number of modes when looking at bridges with more complex stiffness distributions and increased number of supports. In figure 4.4 below, thirty modes simply do not represent the actual moment distribution.

Convergence results

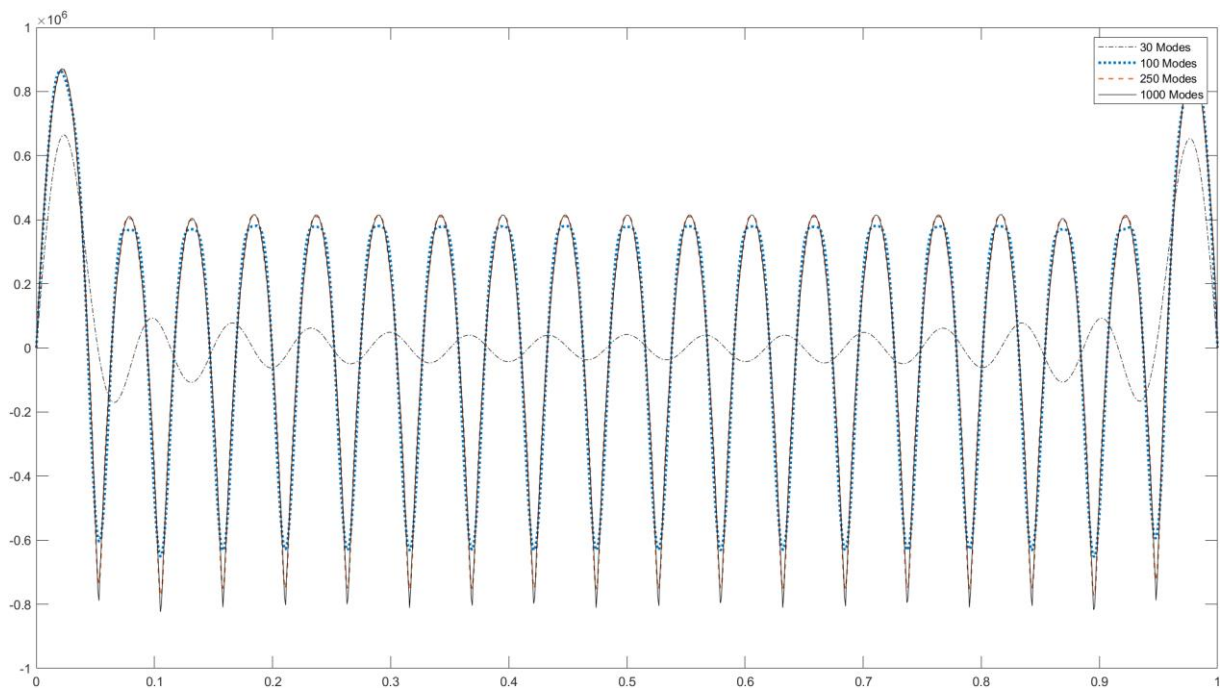


Figure 4.4. F1 Curved bridge no draft case with moments throughout the entire length of the bridge. High tide of 229 cm, which corresponds to a relative tide of 125 cm from mean. kNm is the y-axis unit of measurement. The normalized girder length is the x-axis unit of measurement.

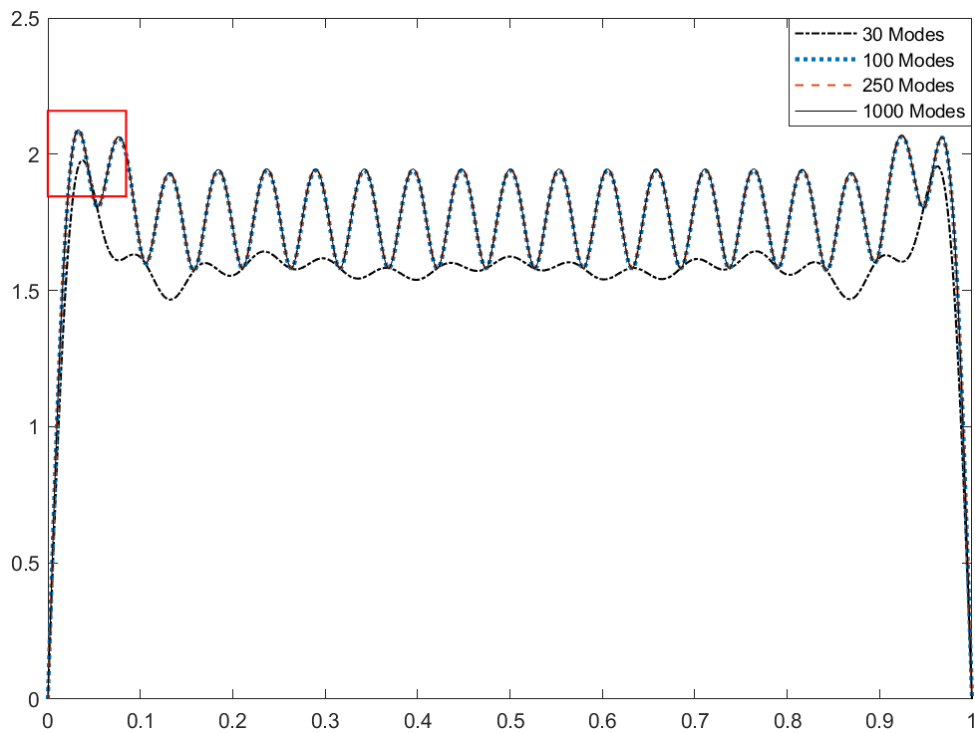


Figure 4.5. F1 Curved bridge no draft case with vertical displacements throughout the entire length of the bridge. High tide of 229 cm, which corresponds to a relative tide of 125 cm from mean. Meters is the y-axis unit of measurement. The normalized girder length is the x-axis unit of measurement.

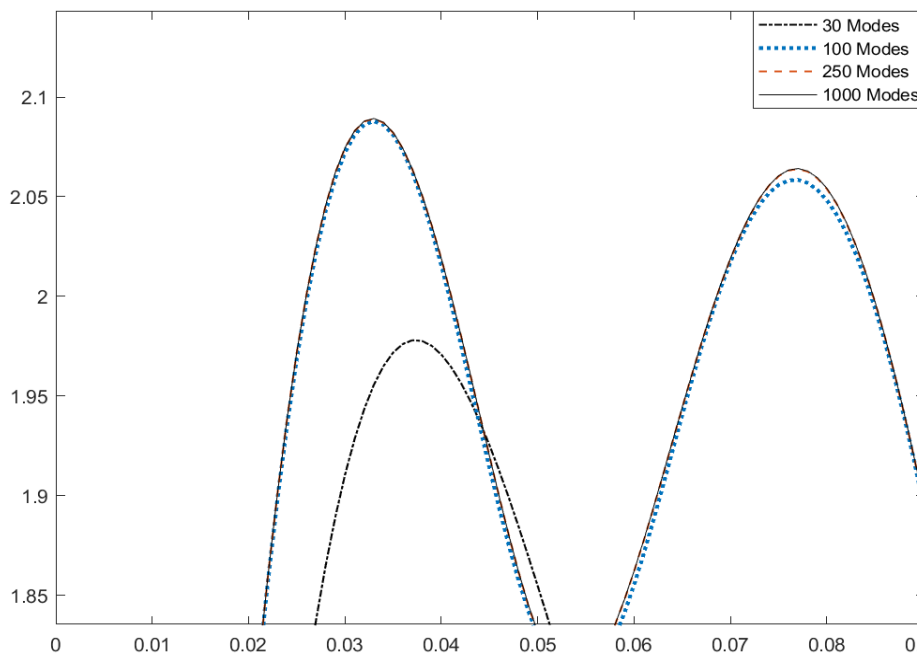


Figure 4.6. F1 Curved bridge no draft case with vertical displacements zoomed in. High tide of 229 cm, which corresponds to a relative tide of 125 cm from mean.

4.5.1 Tidal variation results

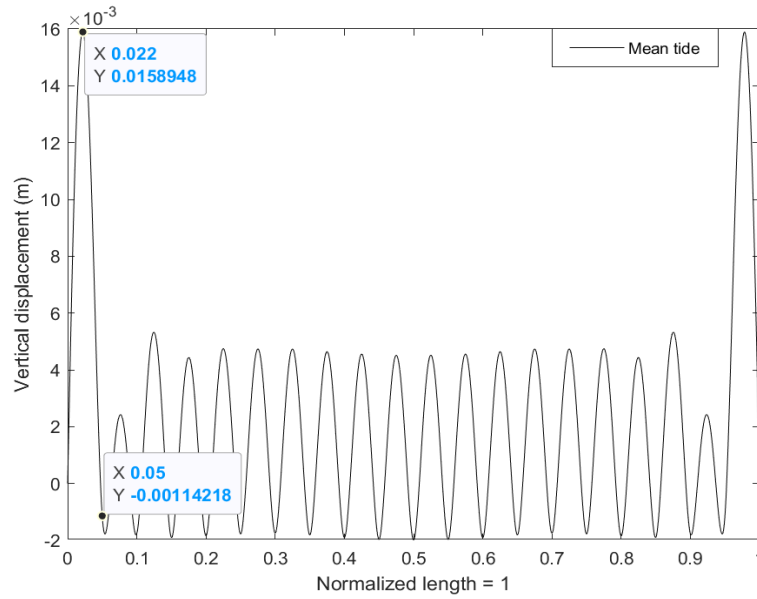


Figure 4.7. F1 Curved bridge with initial draft corresponding to reaction forces on mean tide.

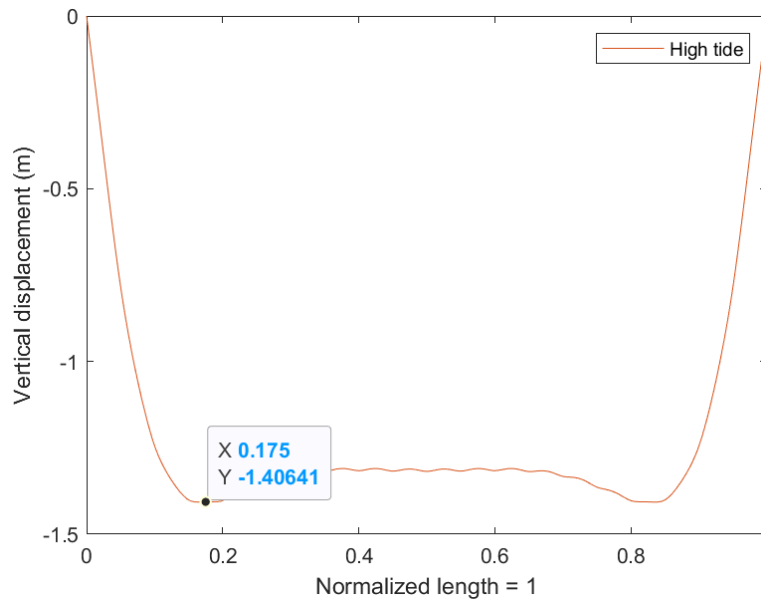


Figure 4.8. F1 Curved bridge with initial draft corresponding to reaction forces. High tide of 229 cm, which corresponds to a relative tide of 132 cm from mean.

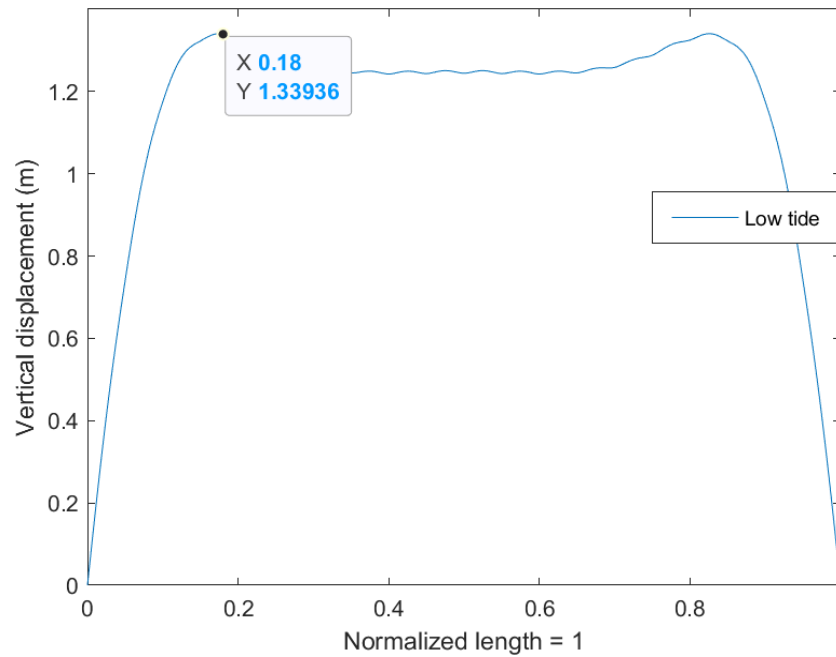


Figure 4.9. F1 Curved bridge with initial draft corresponding to reaction forces. Low tide of -28 cm, which corresponds to a relative tide of 125 cm from mean.

[Figures 4.8](#) and [4.9](#) show how little relative displacement occurs between pontoons during high and low tides. The deflection from the abutment to the first pontoon is much larger, and therefore might cause the incline to increase above the required maximum of 5%. This is further investigated in figure [4.13](#).

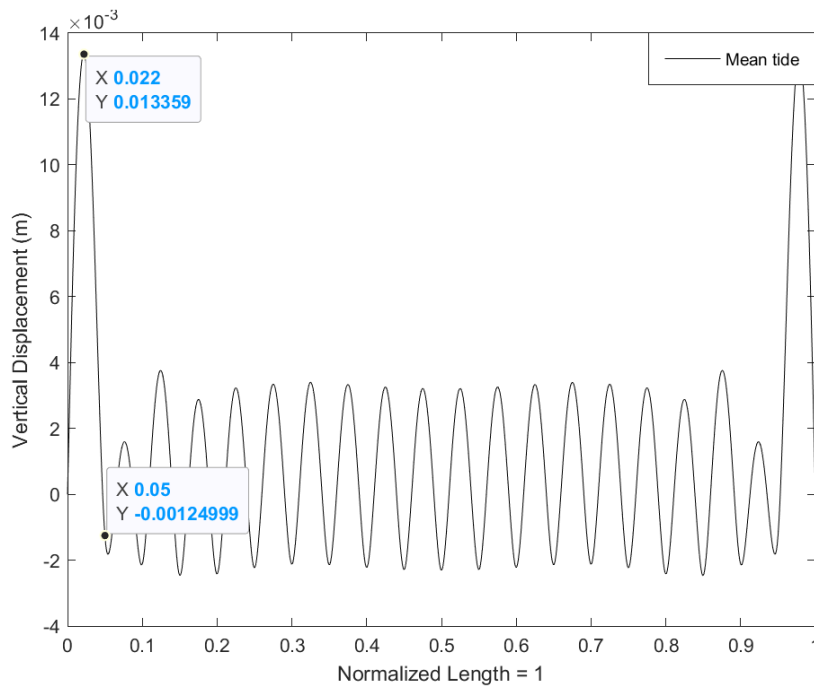


Figure 4.10. S1 Curved bridge with initial draft corresponding to reaction forces on mean tide.

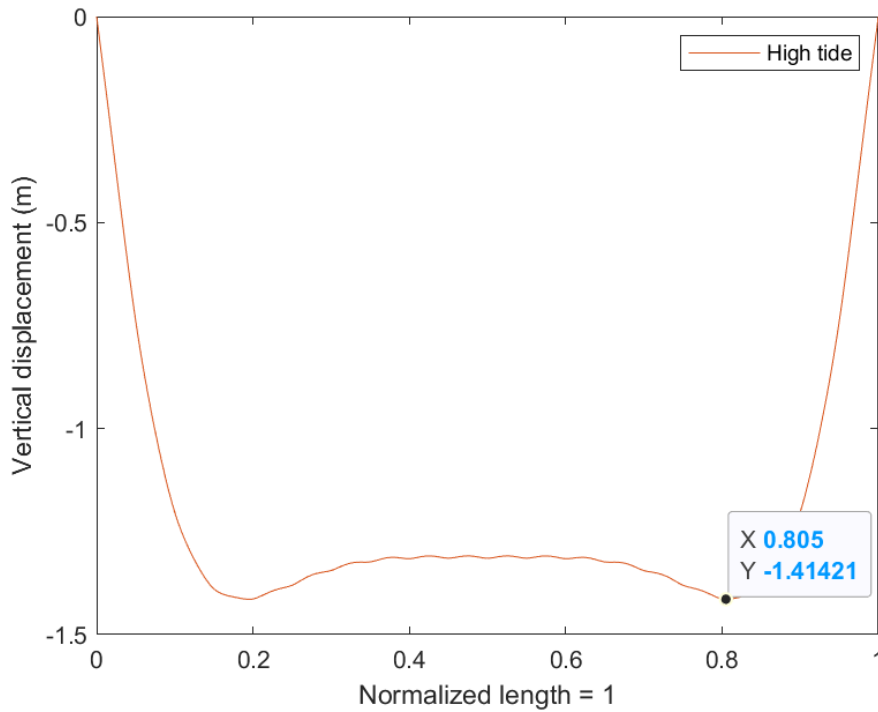


Figure 4.11. S1 Curved bridge with initial draft corresponding to reaction forces. High tide of 229 cm, which corresponds to a relative tide of 132 cm from mean.

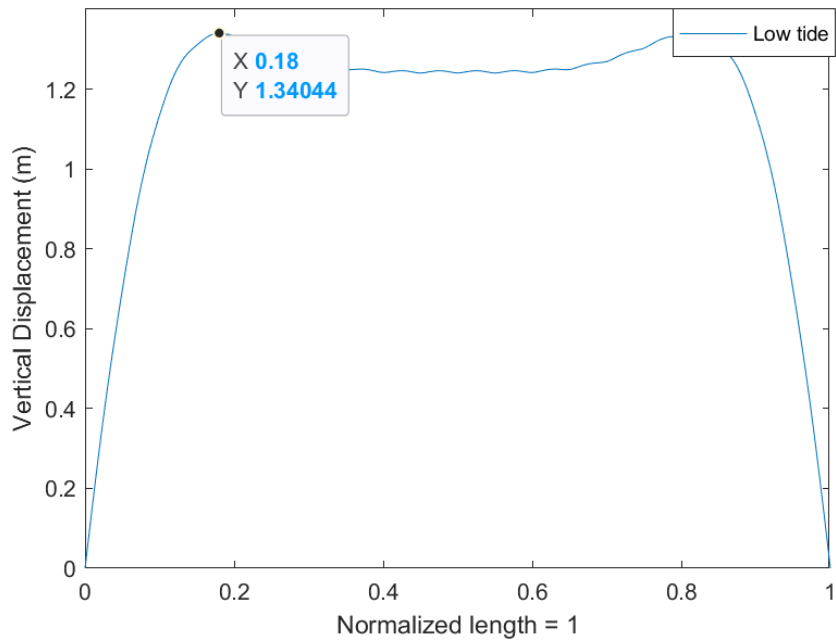


Figure 4.12. S1 Curved bridge with initial draft corresponding to reaction forces. Low tide of -28 cm, which corresponds to a relative tide of 125 cm from mean.

Figure 4.10 indicates that the pontoon displacements are approximately zero, while mid-spans are deflected relatively. The whole girder moves with the tide, with small inclines for the internal pontoons (figure 4.11 and 4.12).

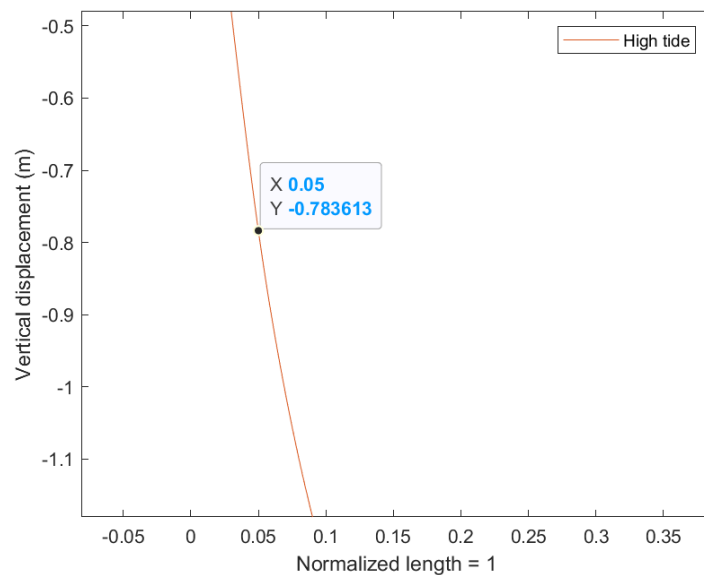


Figure 4.13. Maximum relative displacement found at F1 curved bridge during high tide. Zoomed in at the first pontoon. As the vertical displacement at the tower is zero, the incline over the 197 m long span is calculated to be 0.4%.

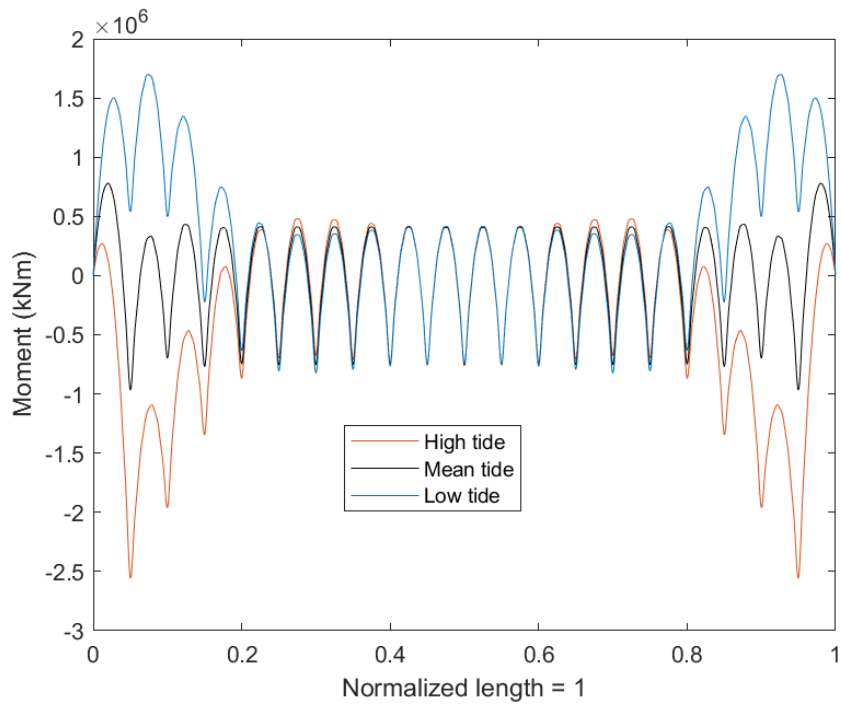


Figure 4.14. Moment distribution during low, mean and high tide for the F1, Bjørnafjorden curved bridge with 250 modes.

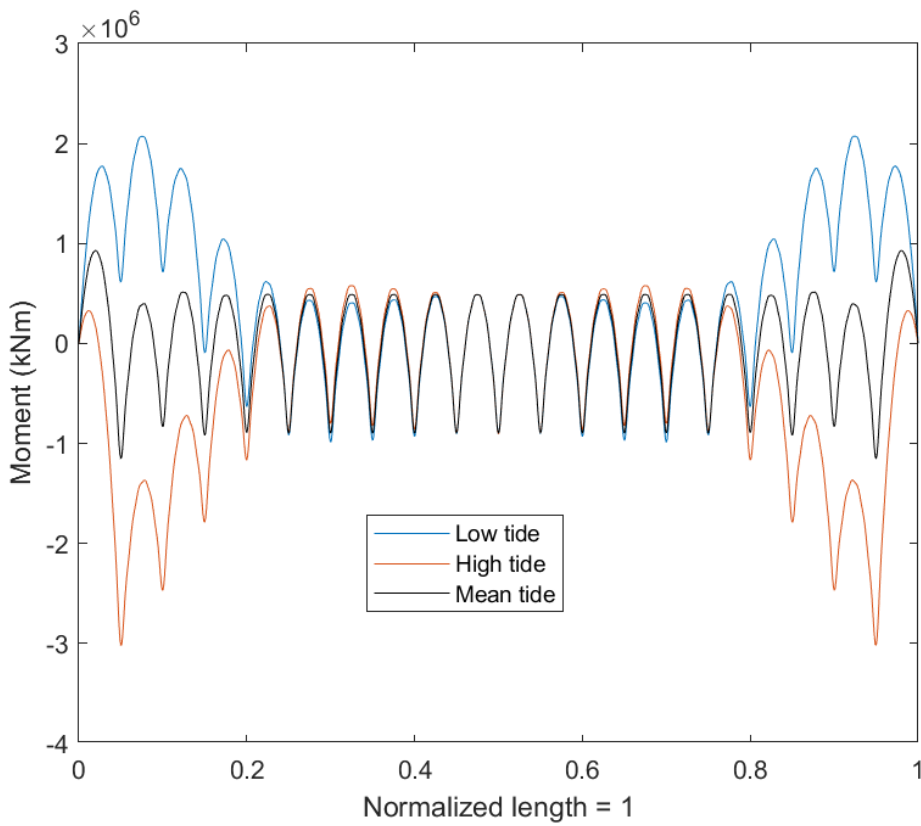


Figure 4.15. Moment distribution during low, mean and high tide for the S1, Bjørnafjorden curved bridge with 250 modes.

Moment distribution of two of the examined cross-sections, F1 and S1 ([figure 4.14](#) and [4.15](#)). The figures highlight that the internal pontoons are subjected to approximately the same moments during low, mean and high tide.

4.6 Parametric study

Girder properties

The bridge girder is considered a continuous beam, spanning over all of the pontoons. A continuous beam is a beam that crosses multiple supports as one unit. One of the advantages of using continuous beams is that they can provide high stiffness to the structure compared to multiple single beams. Specifically, less bending and deflections, and better resistance to buckling. It is also important that the girder is continuous so that the arch-action is maintained and the transverse forces are transferred to the ends of the bridge. The bridge girder is a vierendeel beam, consisting of two steel boxes. The steel boxes are regularly supported by crossbeams over the entire length of the bridge.

Approach

The presented tidal results are examined during the tidal cycle with the initial and most stiff section respectively. The deflections, moments and rotation profiles are compared during meantide as examining the response at this state is relevant due to the fatigue that the bridge would experience caused by daily tidal cycles. An equivalent section-cantilever beam formula is utilized to control the usability in terms of rotation if the piecewise selection of sections were chosen. After comparing the results, a simplified convergence study is conducted aiming to explore how efficient it would be to adjust the I_x if the most stiff section were to cross the whole span.

Equivalent section-cantilever beam formula

If the southmost span is solely considered and cut in half, the support within this cut can be assumed to be fixed. Standard beam deflection tables shows that the maximum deflection can be computed as

$\delta = \frac{qL^4}{8EI}$, where δ is the deflection at the free end and q is the equivalent uniform load, herein the self-weight of the examined span.

As δ and I are the two unknown variables, the equivalent second moment of inertia can be found by fixing δ to any absolute value.

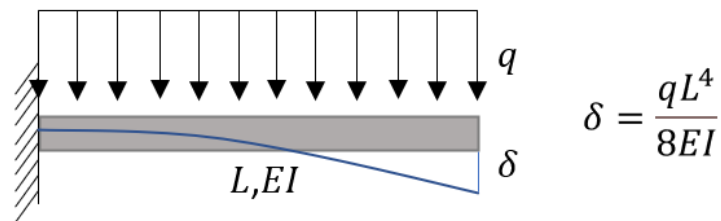


Figure 4.16. Maximum beam deflection formula for a cantilever beam subject to uniform load

By following the piecewise section configuration of the low part of the bridge, but implementing this sequence throughout the entire length, the sequence repeats as follows for every single span and a SAP2000 model is designed thus.

S1(24.625m) -> F1(147.75m) -> S1(24.625m)

This repetition is visualised in [figure 4.18](#).

The formula in [figure 4.16](#) is then utilized in order to find the equivalent stiffness of the southmost split span with the obtained deflection values obtained in the software model. The full reaction force table with corresponding initial drafts can be found in [table 4.B](#).

The midspan vertical displacement value is 0.01516m shown in [figure 4.17](#), giving the composite section an equivalent I_x value of 994.3m⁴

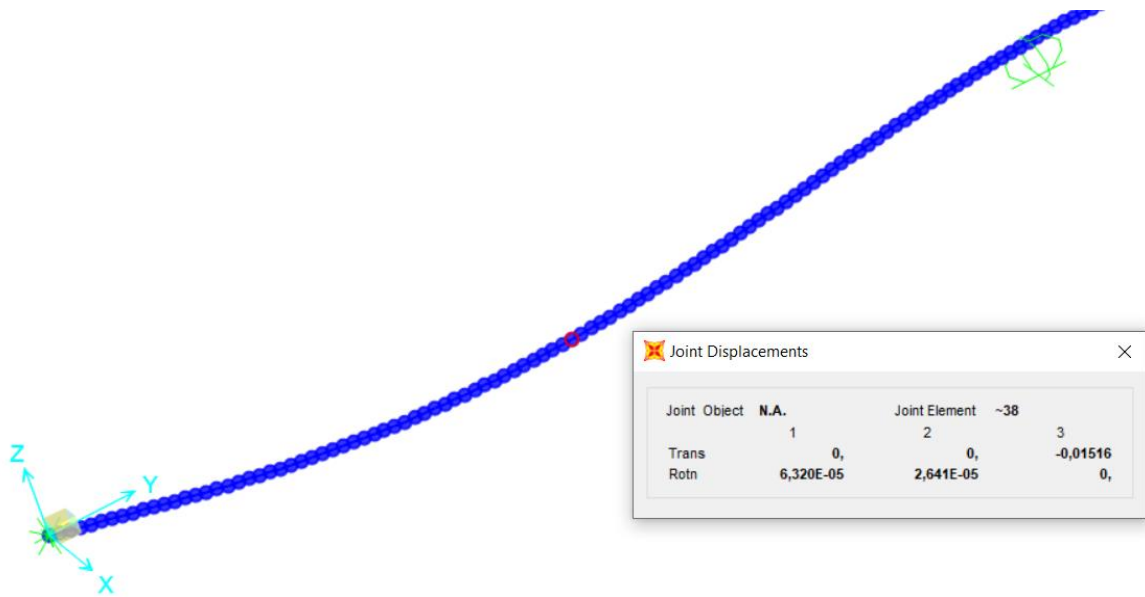


Figure 4.17. Curved bridge maximum displacement at the southmost span when the piecewise section configuration is considered.

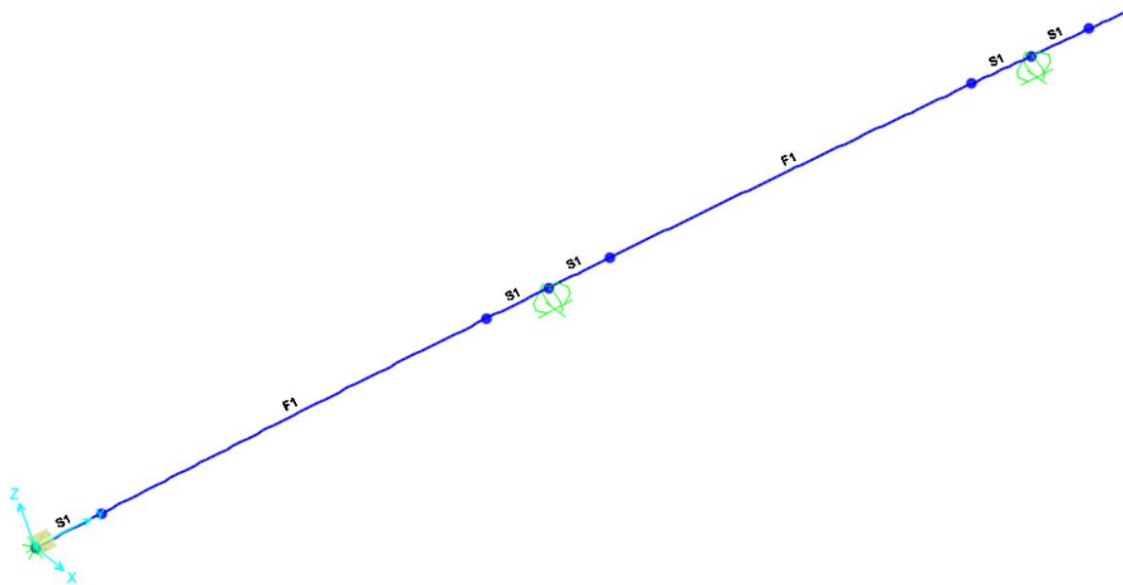


Figure 4.18. Cut showing the curved bridge section configuration model.

The same SAP2000 model is used to calculate the equivalent torsion constant J , by computing the formula,

$$\theta = \frac{TL}{GJ}$$

where θ is the angle of rotation about the longitudinal axis of the beam, T is the applied

torque, L is the length of the considered span and G is the shear modulus, a material property computed as

$$G = \frac{E}{2(1 + \nu)}$$

By applying a torsional moment of -10^7 kNm at the first pontoon and extracting the rotation of -0.63865 radians, the equivalent J is equal to 38.2 m^4

The ratio between F1 and S1 is 3:1 along the span length, giving the composite girder an average density of 27449.8 kg per unit length with an equivalent area equal to one square meter.

4.6.1 Parametric study results

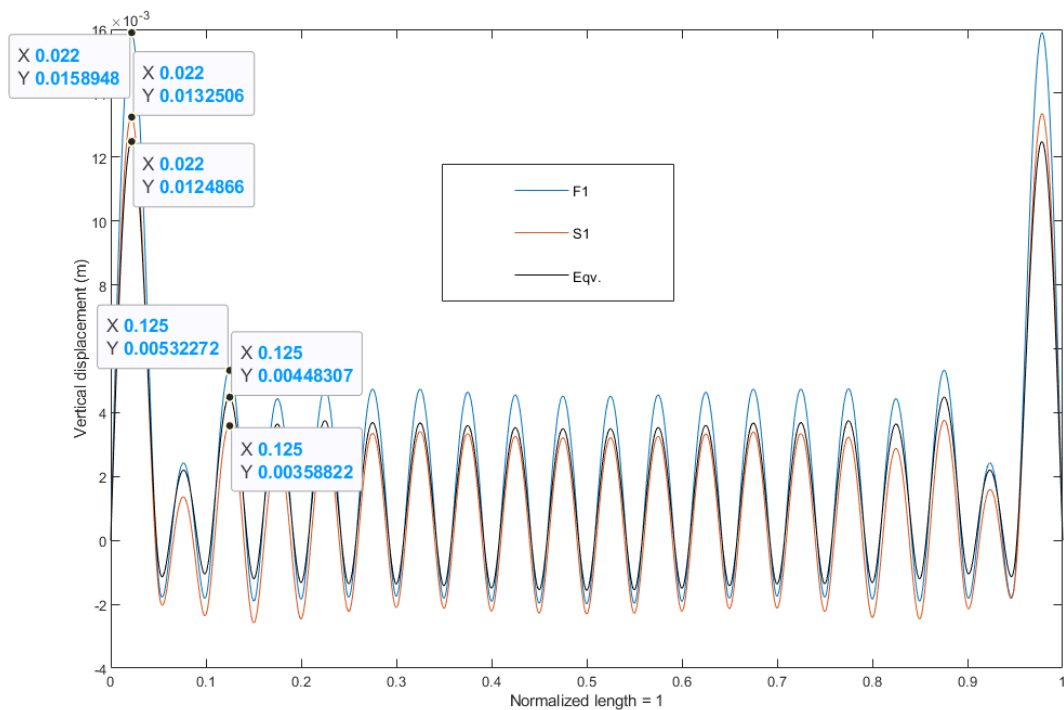


Figure 4.19. Curved bridge vertical displacements for F1, S1 and equivalent sections during mean tide. Maximum values marked.

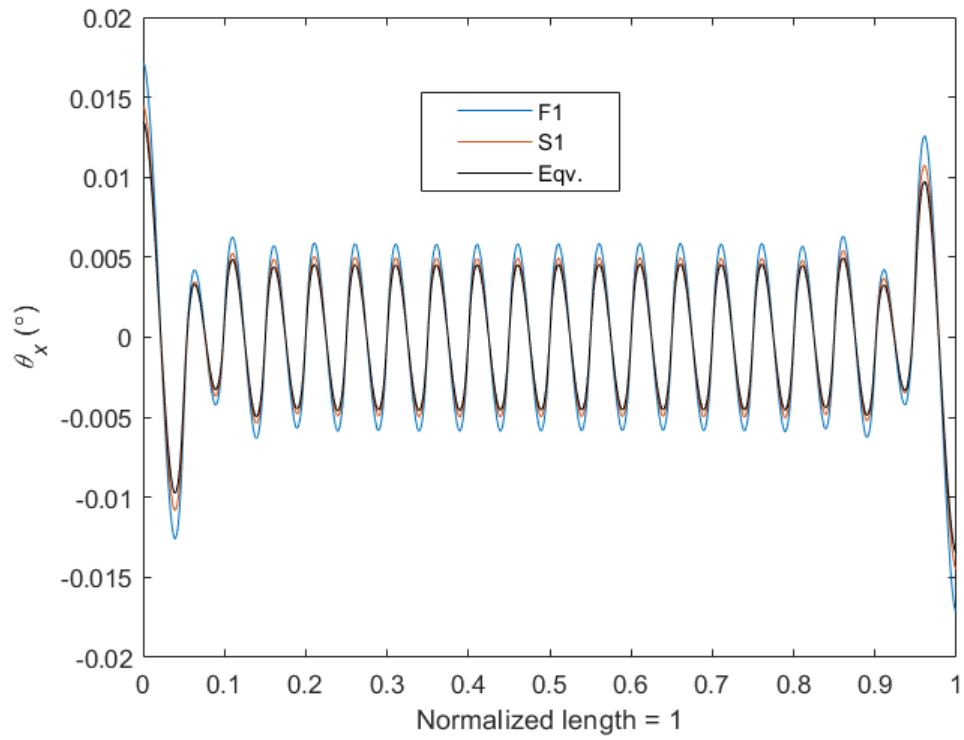


Figure 4.20. Rotation profile for F1,S1 and the equivalent sections during mean tide.

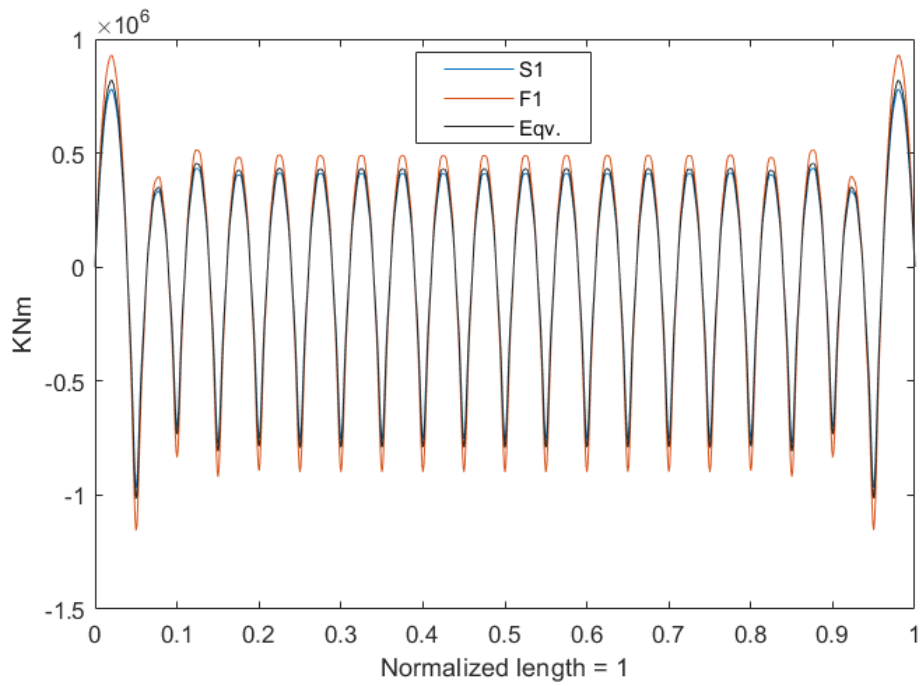


Figure 4.21. Moment profile for F1 and S1 sections during mean tide.

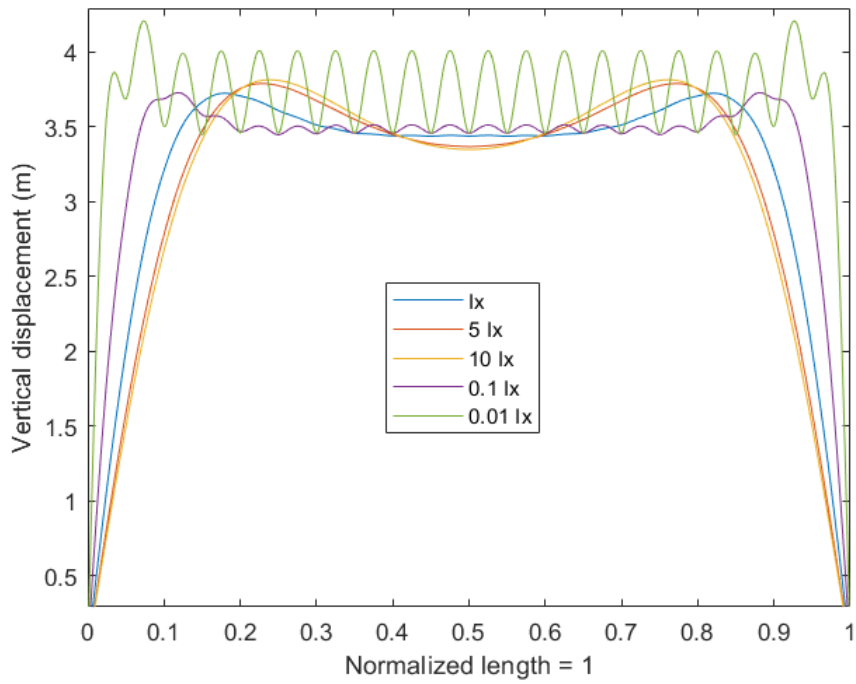


Figure 4.22. Simple convergence study showing the S1 curved bridge vertical displacement with zero initial draft and zero tide. The l_x values are scaled according to the figure.

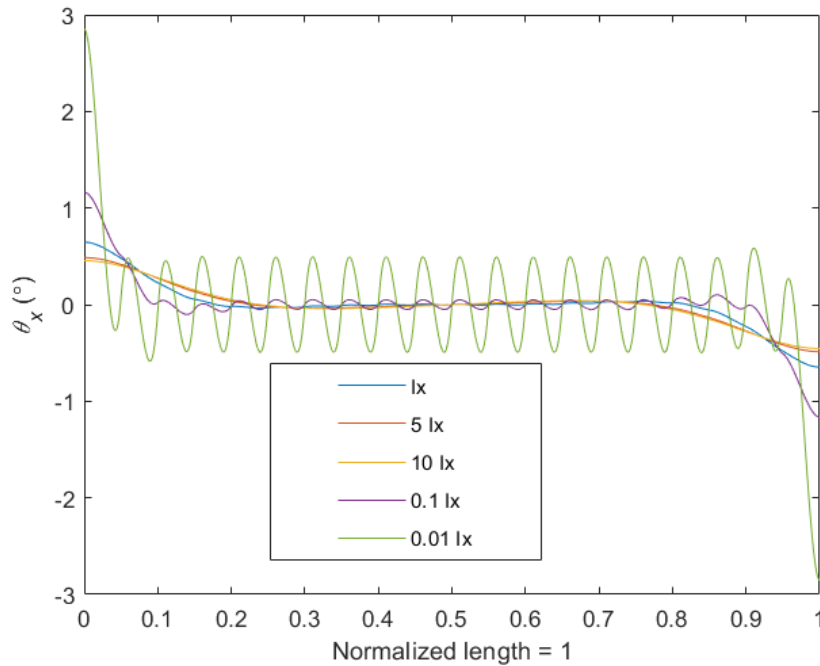


Figure 4.23. Simple convergence study showing S1 curved bridge rotation profile with zero initial draft and zero tide. The l_x values are scaled according to the figure.

4.7 Alternative tide design

Because fixed beams create higher support moments than mid-span moments, the mean tide is not a perfect reference for tidal variations. By running a theoretical modified tide of one meter from mean, both high and low, the maximum moments always occur on the outermost pontoons during a high tide, shown in [figure 4.24](#).

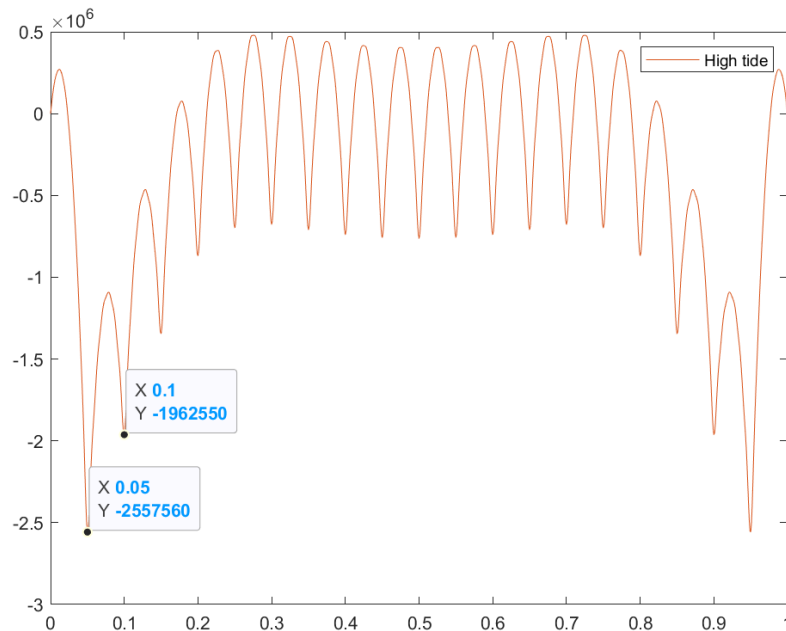


Figure 4.24. F1 curved bridge moment diagram designed for zero deflection at mean tide. The largest moment of all tidal variations occurs during high tide at the first and last pontoon. In this case a 132 cm high tide from mean.

By designing the bridge for a 25% high tide as mean, the highest moments are lowered by 13.8%. The theoretical one meter high and low tide is used to approximate the daily tidal variations that lead to fatigue. This is visualised as a four panel figure in [figure 4.25](#).

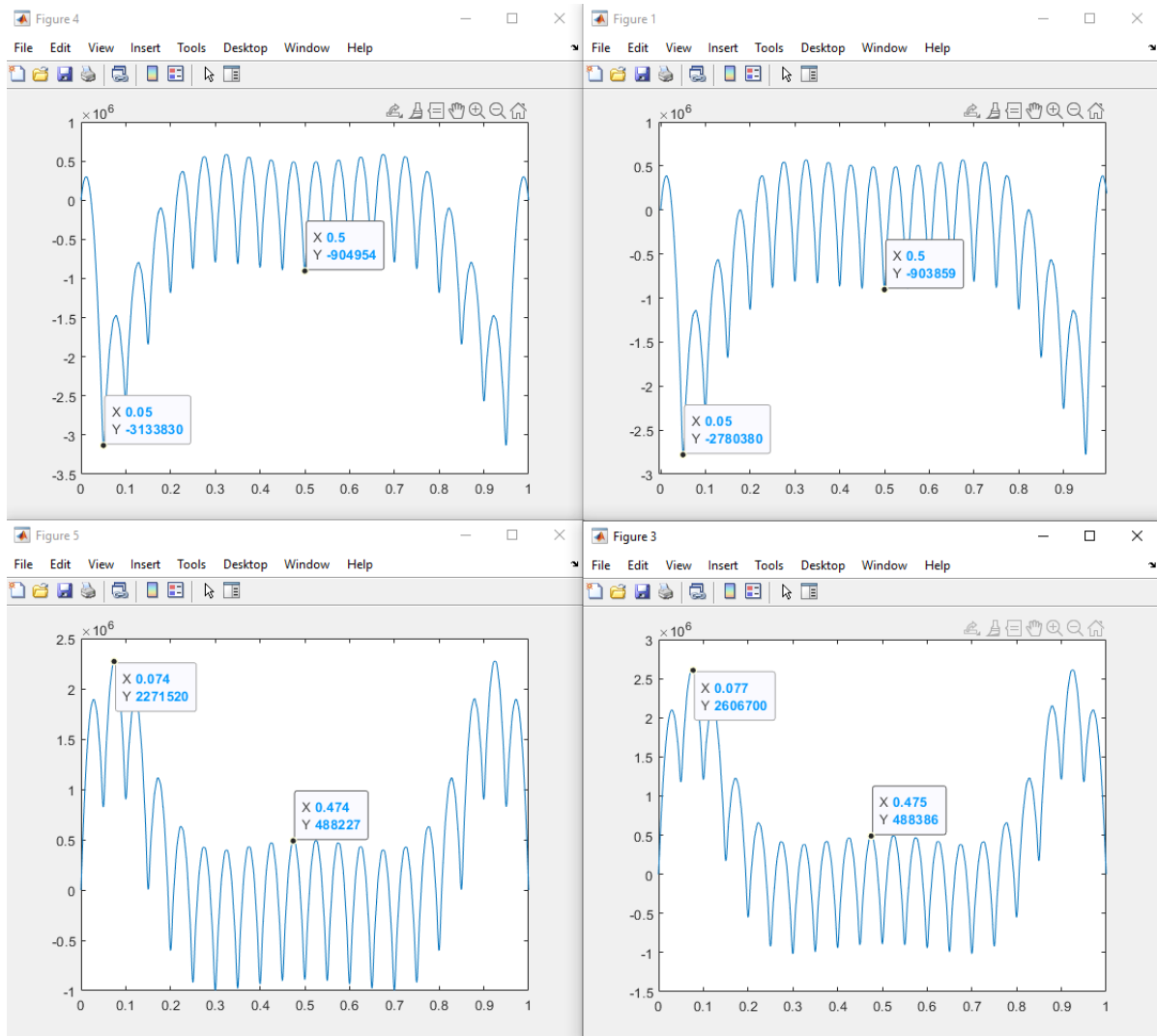


Figure 4.25. S1 curved bridge moment diagrams.

Top left: 1 meter high tide. Top right: 0.75 meter high tide. Bottom left: 1m low tide. Bottom right: 1.25 m low tide.

Looking at the extreme cases, the decrease in max moments proves even more prevalent. In Bergen the highest recorded tide was 143cm above mean, while the lowest was 139cm below mean. Using 140cm as the normalized maximum tide from mean, the high tide moment max is 3.1×10^6 kNm. The low tide moment max is comparably lower at 2.3×10^6 kNm.

Table 4.C. All figures are based on S1 Curved bridge with initial drafts from [table 4.B](#)- S1 cross-section.

		Normal case (kNm)	Modified case (kNm)	Change
Mean tide moment max	Span	929413	1077210	+ 15.9%
	Supports	-1154490	-801036	- 30.6%
Average high tide moment max	Span	446450	548564	+ 22.9%
	Supports	-2568310	-2214850	- 13.8%
Average low tide moment max	Span	1735780	2070970	+ 19.3%
	Supports	-969894	-988011	+ 1.9%
Highest recorded tide moment max	Span	582950	566158	- 2.9%
	Supports	-3133830	-2780380	- 11.3%
Lowest recorded tide moment max	Span	2271730	2609220	+ 14.9%
	Supports	-998880	-1017000	+ 1.8%

4.7.1 Alternative tide design conclusions

Designing the bridge to sag at mean tides but level around 25% of daily high tides can even out the moment forces by 11.3% of the design max moment, in this given example. The lower forces during a daily tidal cycle can also reduce fatigue. The usability of the bridge for vehicles is barely affected, with the maximum incline increasing from 0.4% to 0.47%.

4.8 Bjørnafjorden curved bridge concluding remarks

Increasing the cross-sectional properties from F1 to S1 also increases the moments ([figure 4.21](#)), while only reducing the displacements by a neglectable amount. For the purpose of decreasing the effect of tidal variations, there seems to be no purpose in increasing the stiffness beyond F1. However, the rotation angles ([figure 4.20](#)) are smaller along the whole length. This section is well-balanced since it provides a lower density than S1, without compromising significantly on I_x . This gives the smallest deflections between pontoons and mid-spans of all three evaluated cross-sections, hence the minimum rotations, given that the slope is the first derivative of the deflections with respect to length according to the adapted Euler-Bernoulli beam theory.

The calculated maximum incline of 0.4% satisfies the presented max requirement of 5%. However it shall be highlighted that the 5% requirement includes traffic, which is neglected in this study, but the calculated value indicates that the bridge would perform well in terms of serviceability even if a heavy traffic load case would be considered.

Long floating curved bridges subjected to tidal variations are mostly affected in the outermost few pontoons. The first bridge spans have an increased incline and therefore also larger moments. After the bridge has flattened out the spans and pontoons act as they would during zero tide. [Figure 4.24](#) shows that the outermost three pontoons have significantly higher moments than the middle pontoons. The first and last pontoons are the most affected with three times the moment.

For a homogenous long floating bridge the design moment occurs during a high tide, it is possible to reduce this amount significantly. Changing the reference tidal level can potentially even out outliers in the moment distribution. However more calculations and research should be completed to validate this theory.

The parametric study results show that the equivalent cross-section's displacements mid-span on the internal pontoons are located between F1 and S1 ([figure 4.19](#)). This result is as

expected, because the two stiffnesses are combined. However, the displacements between the end supports and outermost pontoons are noticeably lower than the calculated values for both F1 and S1. While S1 provides roughly 4% increased I_x compared to the equivalent section, the density is almost 14% higher. This gives a significant impact on the displacements due to the heavy self-weight of the girder. It could be investigated if the deviations are greater along the outermost spans because of the lack of buoyancy forces between pontoons on both sides, forces that give a stabilizing effect. Another reason might be that Matlab only has one input for density, and thus the distribution is incorrect.

As shown in [figure 4.22](#), the already predetermined I_x value of 1037 m^4 is an appropriate choice if S1 was to span the entire length and no initial draft or tide are considered. Lowering the value allows greater relative vertical displacements between the pontoons to arise. Increasing the I_x does not seem to improve the overall deflection results of the bridge, but would rather lead to a cost inefficient solution. The rotation profile in [figure 4.23](#) shows that slightly increasing the I_x would lead to higher bridge performance in terms of useability, as the maximum and relative rotations are decreased. However, when considering the magnitude of the rotations relative to the length of the spans, adjusting the size or geometrical shape of the cross-section might lead to an expensive solution that does not noticeably improve the serviceability of the bridge when only self-weight is considered.

Furthermore, the flexibility of the girder is a concern that must be addressed if the rigidity of the bridge is to be increased. It is essential that the bridge is allowed to flex sufficiently during the whole tidal cycle to prevent large restraint stresses. It is found that changing the I_y value does not impact the rotation and vertical deflection of the bridge. This is expected, considering that only the out-of-plane response is addressed and the horizontal forces are neglected.

Chapter 5 Bjørnafjorden straight bridge

5.1 Introduction

Another solution that has been presented is a straight side-anchored floating bridge [44]. The extent of this bridge is the same as for the curved, with a total length of about 4600 meters with a floating part of 3840 meter. The torsional constant input can be determined with an arbitrary value. No torsional moment occurs for a straight bridge if only vertical loading is included, with its mass assumed to be evenly distributed along the width of the cross-section. Additionally, the curvature is set to zero. The floating bridge is supported by 19 pontoons with a spacing of 192 meter. In order to provide an adequate comparison with the curved floating bridge, the same parameters from [table 4.A](#) are carried over, except from the equivalent section parameters that are presented in the parametric study ([chapter 5.5](#)). Reduction in the bridge length compared to the curved counterpart reduces the spacing slightly.

In the presented solution, the translational degree of freedom is free in the longitudinal direction at the north support in order to avoid restraint stresses, such as thermal stresses. This solution is preferred since the straight bridge solution does not utilize arch action to transfer forces, but in these computations both ends are assumed to be restrained to provide an identical support configuration for comparison with the curved bridge. The bridge is provided with four clusters of mooring lines, connecting the pontoons to the seabed, in order to withstand transverse loading from waves. However this is neglected in this study since the out-of-plane response is considered solely.



Figure 5.1 Straight floating bridge across Bjørnafjorden [45].

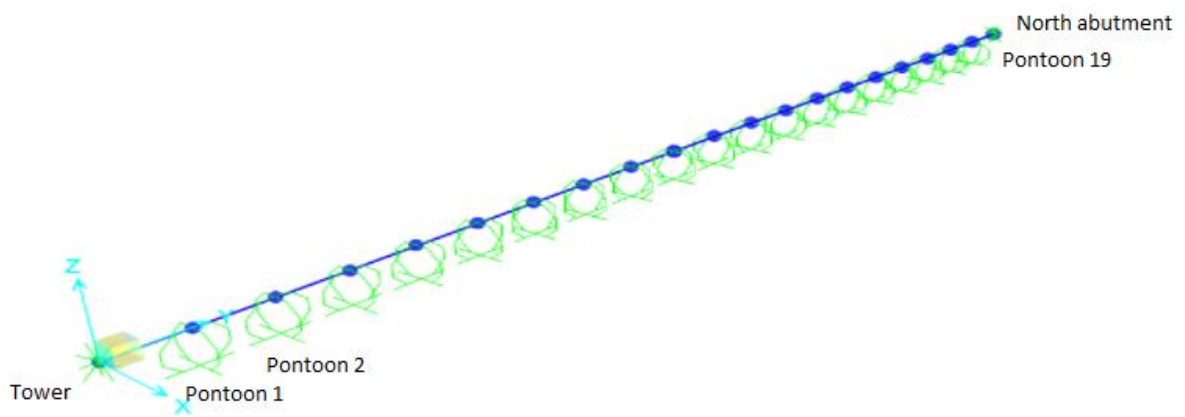


Figure 5.2. SAP2000 model of the Bjørnafjorden end anchored straight bridge with pontoons assigned as roller supports, for coordinates see [figure A.2](#).

5.2 Parameters

Table 5.A. Reaction forces for the straight bridge (shown in [figure 5.2](#)) obtained in SAP2000 with their corresponding initial draft values.

	Reaction force (kN)			Initial draft (m)		
	Initial cross-section, F1	Strong cross-section, S1	Eqv. cross-section	Initial cross-section, F1	Most stiff cross-section, S1	Eqv. cross-section
Pontoon 1	55936.868	66613.535	58660.803	3.208	3.821	3.364
Pontoon 2	47557.348	56634.617	49873.229	2.728	3.248	2.860
Pontoon 3	49802.633	59308.460	52227.852	2.856	3.402	2.996
Pontoon 4	49201.011	58592.006	51596.933	2.822	3.360	2.959
Pontoon 5	49362.215	58783.979	51765.987	2.831	3.371	2.969
Pontoon 6	49319.021	58732.540	51720.689	2.829	3.369	2.966
Pontoon 7	49330.596	58746.324	51732.828	2.829	3.369	2.967
Pontoon 8	49327.490	58742.626	51729.571	2.829	3.369	2.967
Pontoon 9	49328.337	58743.634	51730.459	2.829	3.369	2.967
Pontoon 10	49328.055	58743.298	51730.163	2.829	3.369	2.967
Pontoon 11	49328.337	58743.634	51730.459	2.829	3.369	2.967
Pontoon 12	49327.490	58742.626	51729.571	2.829	3.369	2.967
Pontoon 13	49330.596	58746.324	51732.828	2.829	3.369	2.967
Pontoon 14	49319.021	58732.540	51720.689	2.829	3.369	2.966
Pontoon 15	49362.215	58783.979	51765.987	2.831	3.371	2.969
Pontoon 16	49201.011	58592.006	51596.933	2.822	3.360	2.959
Pontoon 17	49802.633	59308.460	52227.852	2.856	3.402	2.996
Pontoon 18	47557.348	56634.617	49873.229	2.728	3.248	2.860
Pontoon 19	55936.868	66613.535	58660.803	3.208	3.821	3.364

5.3 Method

Displacements, moments and rotations are calculated during the tidal cycle and a parametric study is conducted in order to compare how the different sections affect the results. The initial number of modes is set to 250, which is assumed to be sufficient for the straight bridge given the convergence results obtained in the curved bridge study.

5.4 Tidal variation results

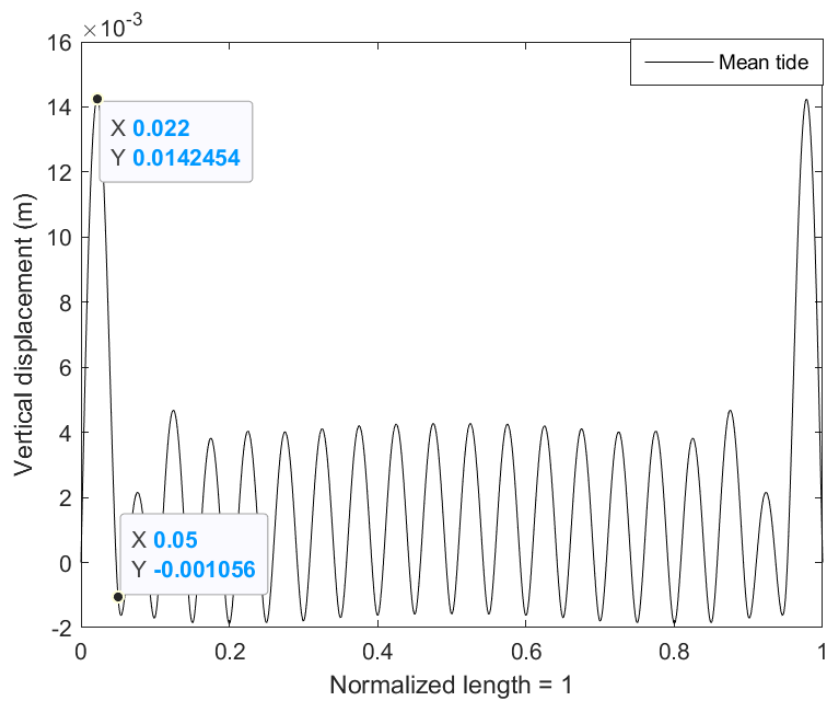


Figure 5.3. F1 straight bridge with initial draft corresponding to reaction forces on mean tide.

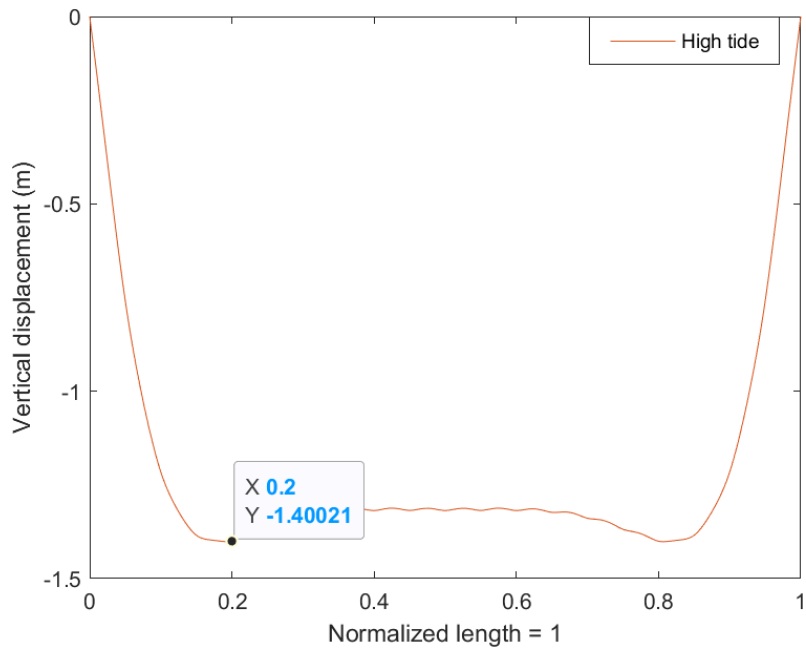


Figure 5.4. F1 straight bridge with initial draft corresponding to reaction forces. High tide of 229 cm, which corresponds to a relative tide of 132 cm from mean.

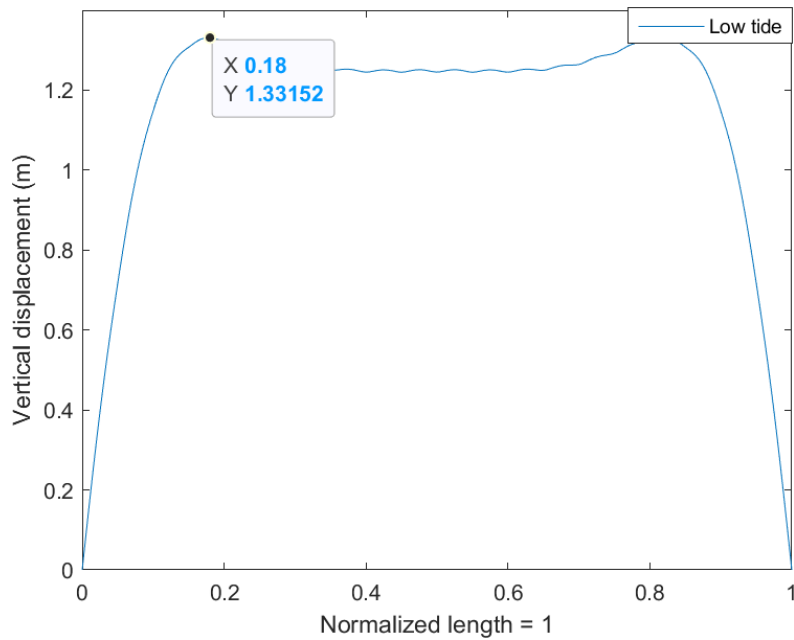


Figure 5.5. F1 straight bridge with initial draft corresponding to reaction forces. Low tide of -28 cm, which corresponds to a relative tide of 125 cm from mean.

Figure 5.3, 5.4 and 5.5 shows the displacement of the F1 cross-section during three tidal positions. Low tide displacement is slightly higher than during a high tide, and mean tide deflection is negligible.

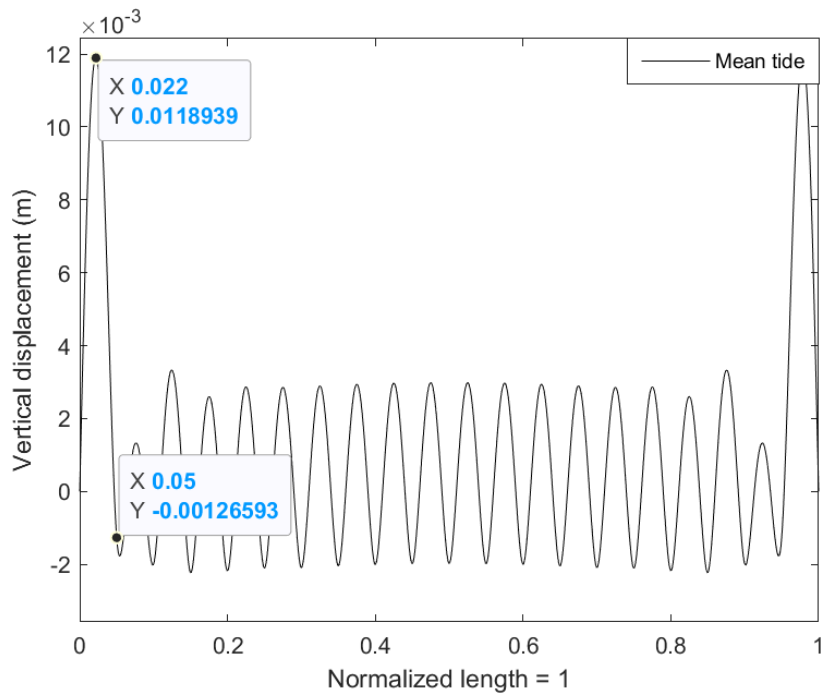


Figure 5.6. S1 Straight bridge with initial draft corresponding to reaction forces on mean tide.

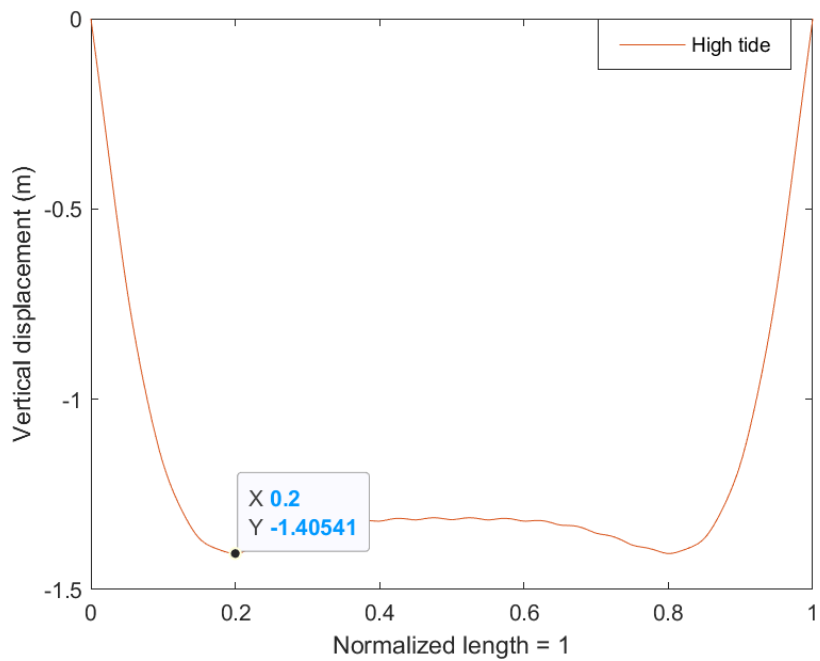


Figure 5.7. S1 straight bridge with initial draft corresponding to reaction forces. High tide of 229 cm, which corresponds to a relative tide of 132 cm from mean.

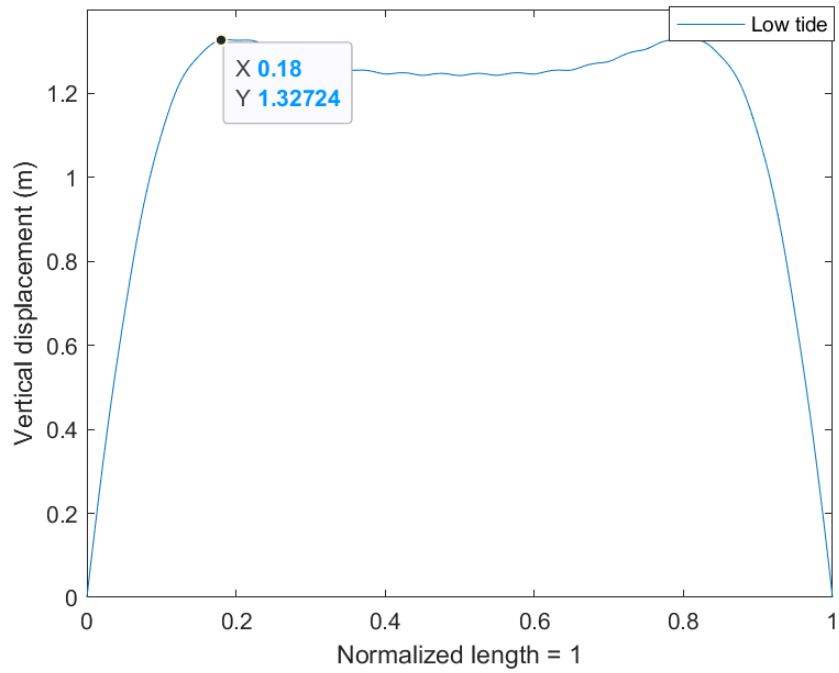


Figure 5.8. S1 straight bridge with initial draft corresponding to reaction forces. Low tide of -28 cm, which corresponds to a relative tide of 125 cm from mean.

Compared to the figures for the F1 cross-section, Figure 5.6, 5.7 and 5.8 show slightly lower deflection during a low tide, but no difference in the mean and high tide graphs.

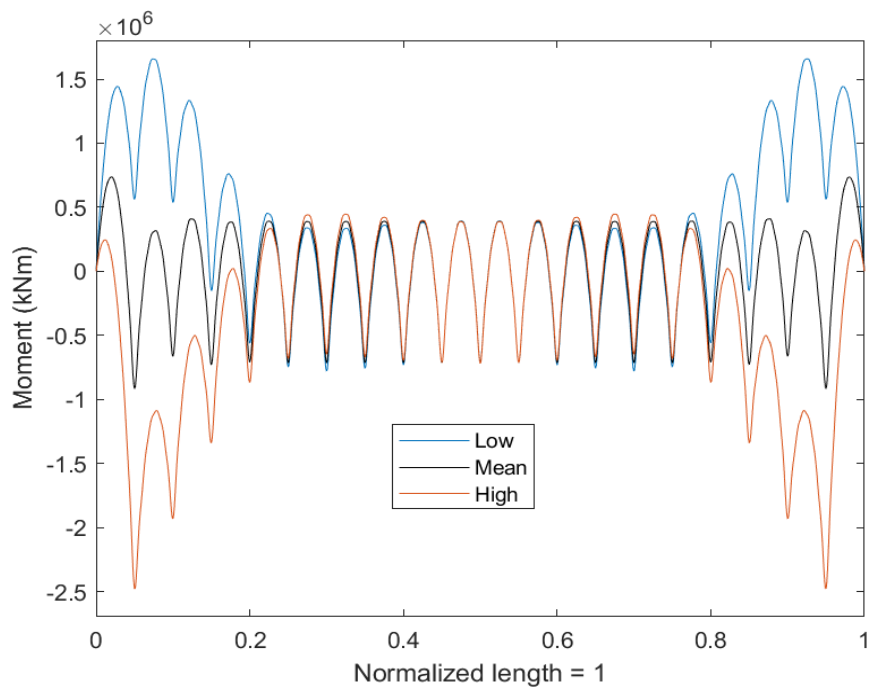


Figure 5.9. Moment distribution during low, mean and high tide for the F1, Bjørnafjorden straight bridge with 250 modes.

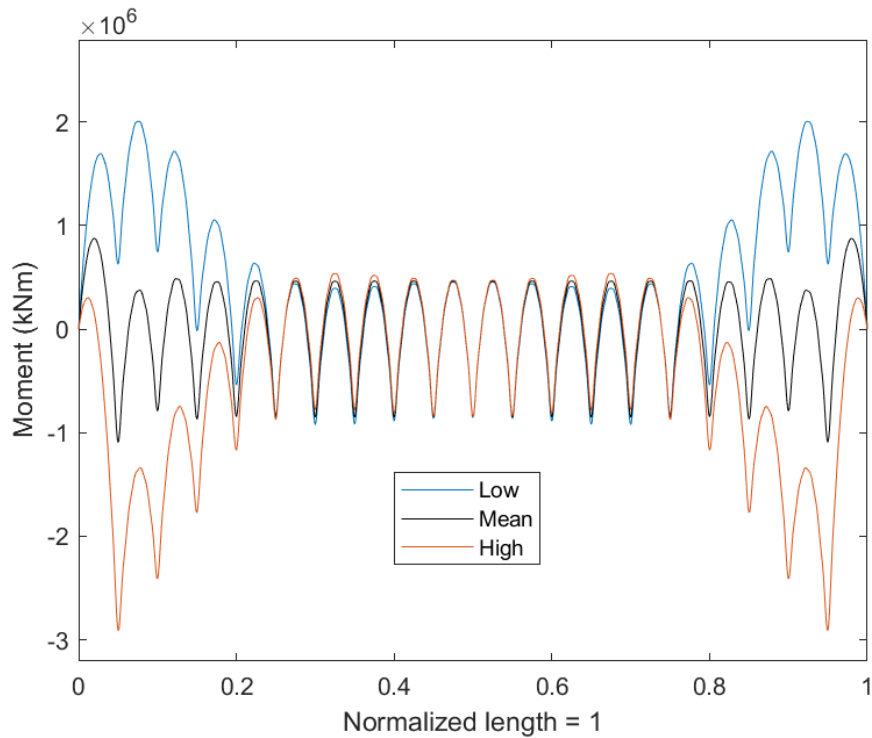


Figure 5.10 . Moment distribution during low, mean and high tide for the S1, Bjørnafjorden straight bridge with 250 modes.

Figure 5.9 and 5.10 shows the moment distribution for F1 and S1 respectively. The figures indicate that the outlier three pontoons are subjected to higher moments during low and high tide, compared to mean.

5.5 Parametric study

The exact same procedures are executed to obtain results that can be compared with the curved bridge. The average density of the composite girder is 27482,3 kg per unit length and the vertical displacement in the middle of the southmost span is 0.013642 m, giving an equivalent I_x of 998.11m⁴

5.5.1 Parametric study results

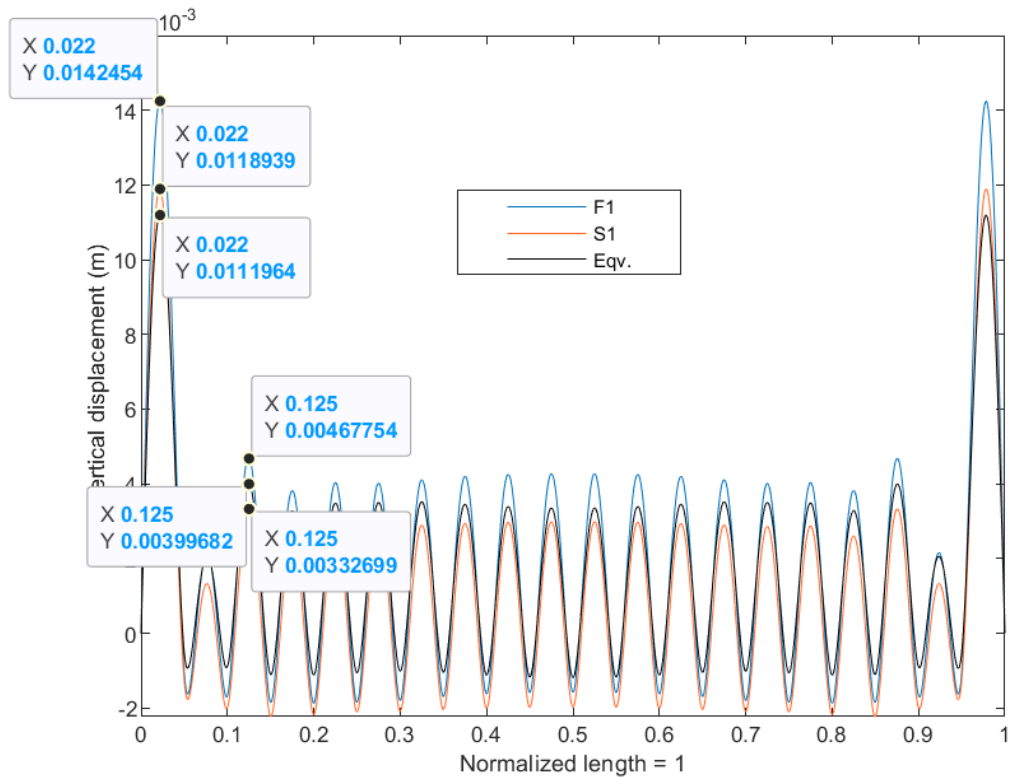


Figure 5.11. Curved bridge vertical displacements for F1 and S1 sections during mean tide. Maximum values marked.

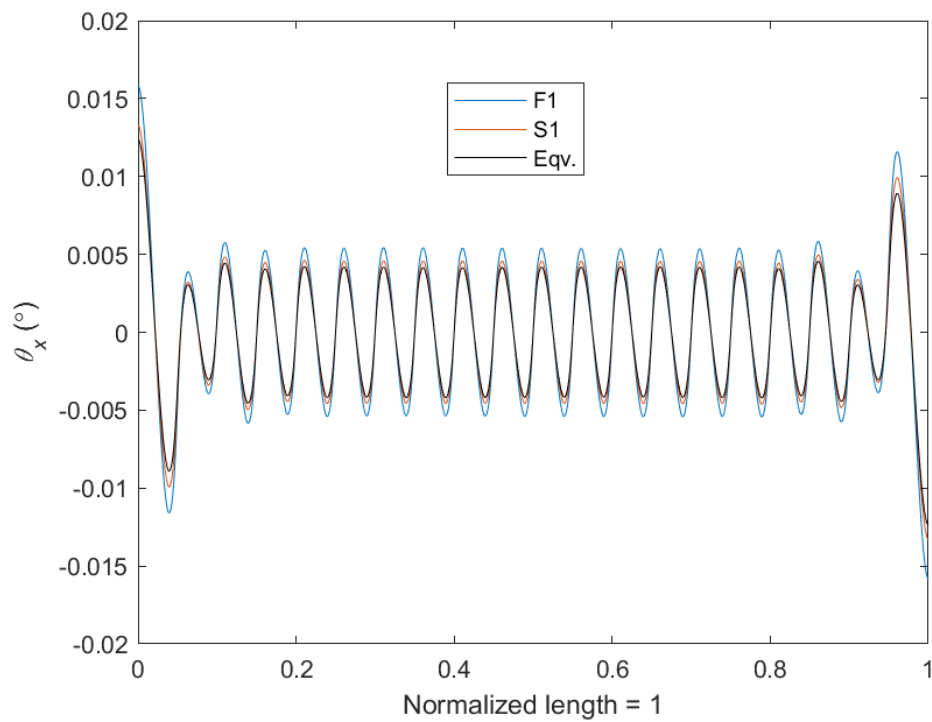


Figure 5.12. Rotation profile for F1, S1 and the equivalent sections.

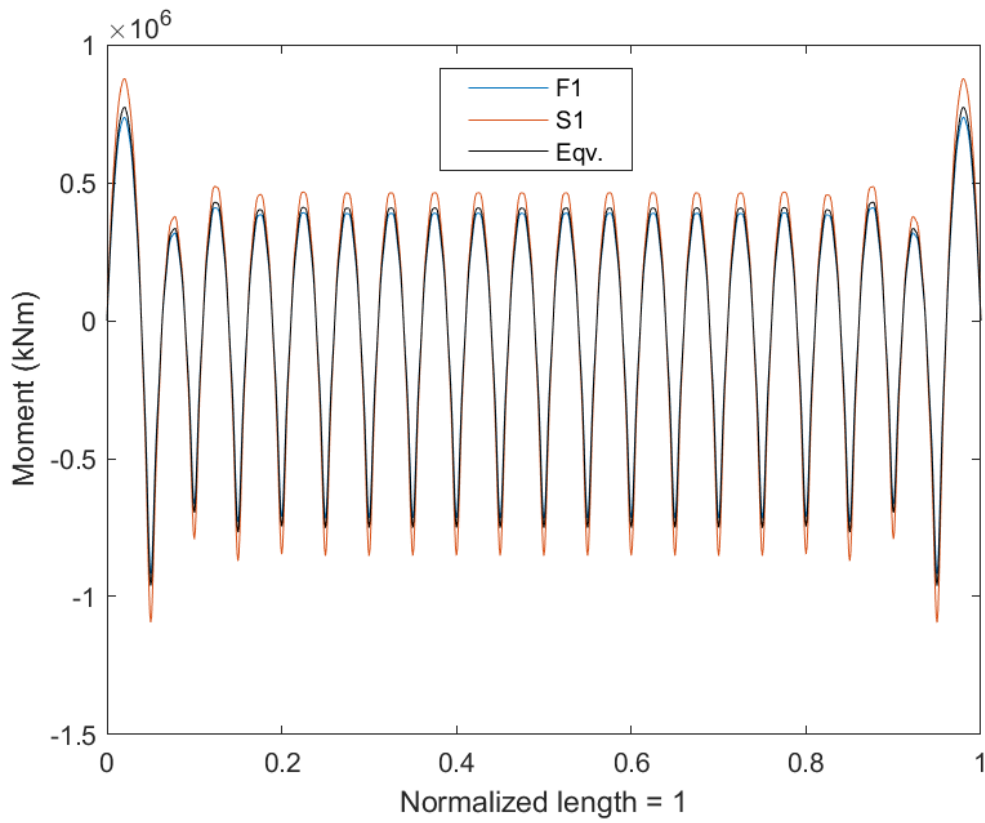


Figure 5.13. Moment profile for F1 and S1 sections during mean tide.

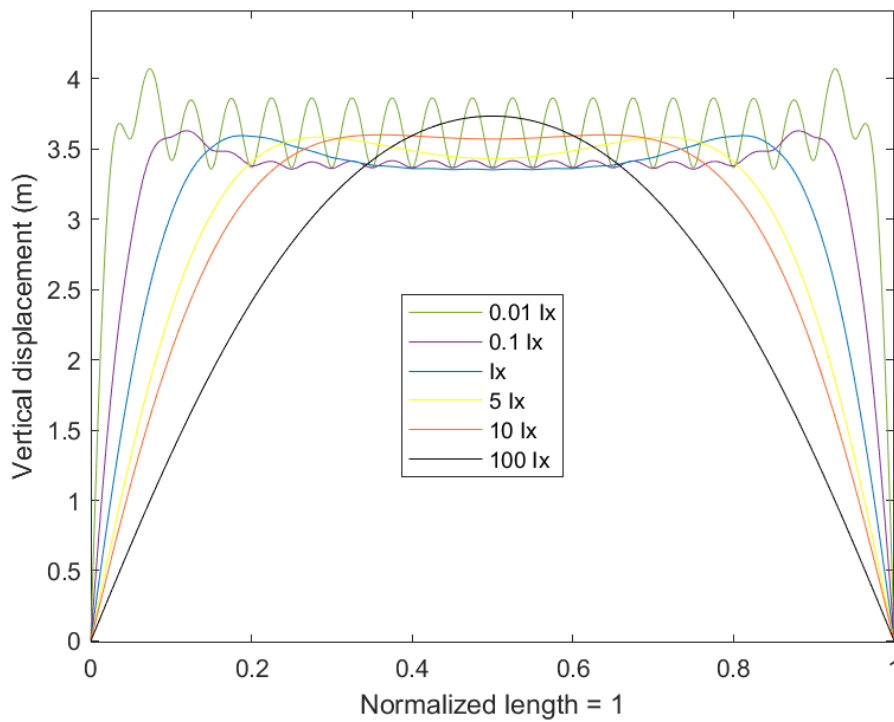


Figure 5.14. Simple convergence study showing the S1 straight bridge vertical displacement with zero initial draft and zero tide. The l_x values are scaled according to the figure.

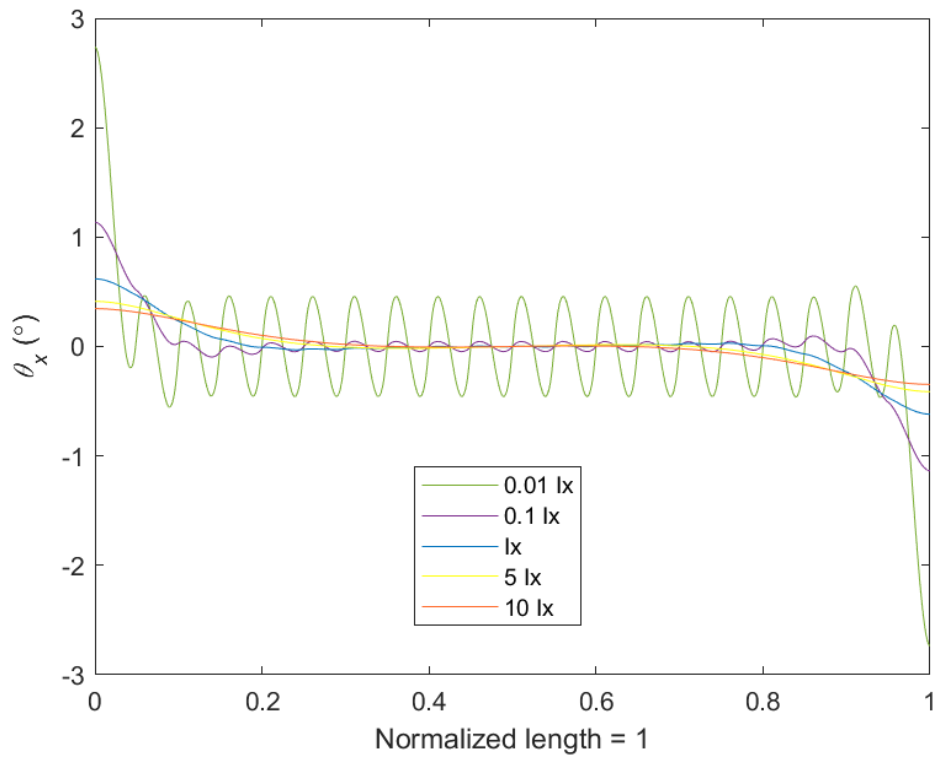


Figure 5.15. Simple convergence study showing S1 curved bridge rotation profile with zero initial draft and zero tide. The I_x values are scaled according to the figure.

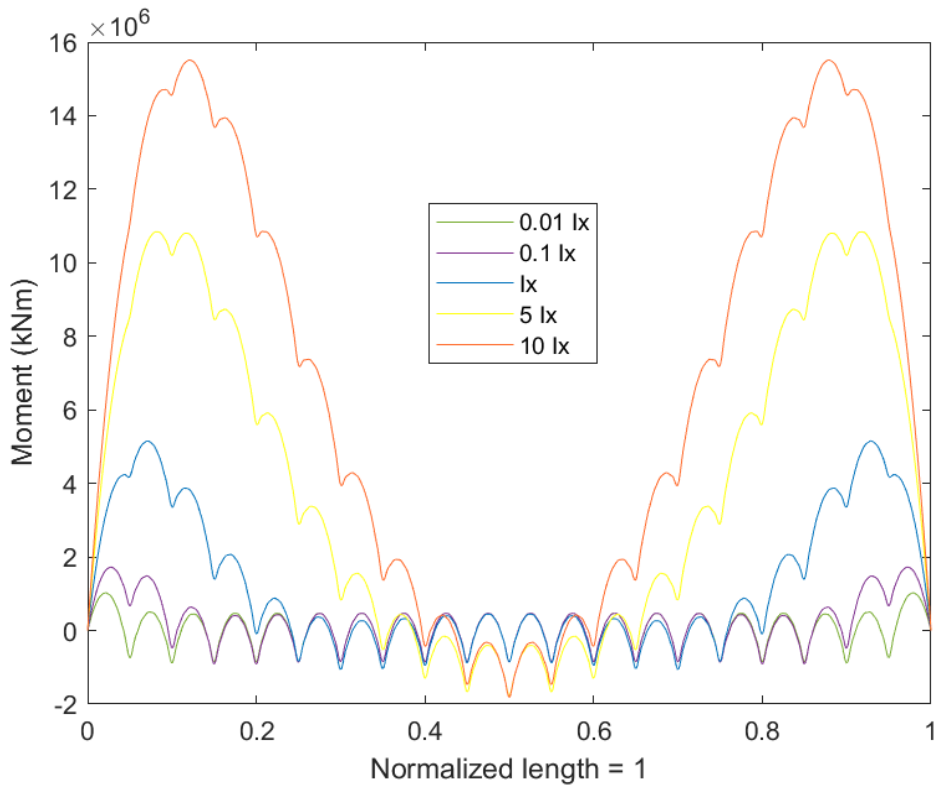


Figure 5.16. Simple convergence study showing S1 curved bridge moment profile with zero initial draft and zero tide. The I_x values are scaled according to the figure.

5.6 Bjørnafjorden straight bridge concluding remarks

The incline requirements are assumed to be well satisfied, even in a heavy traffic case, as the straight bridge's maximum and relative displacements are slightly smaller than the curved bridge's values.

Based on the [figures 5.3](#) and [5.6](#) of the various cross-sections, F1 and S1, there are relatively small pontoon displacements. The calculations are conducted in Matlab with initial pontoon draft, and on the basis of a SAP2000 model. The displacements are about two millimeters for both cross-sections, which is rather satisfactory. Although the goal is zero vertical movement of the pontoons, the displacements are marginal. The results show a good agreement between the two softwares. The difference in displacements for the two sections are small during the extreme tide and are neglectable.

The presented moment [figures 5.9](#) and [5.10](#) show that pontoons number 1 and 19, on the x-axis at 0.05 and 0.95 respectively, absorb large moments relative to the internal pontoons. This is expected since both of the end supports are free to rotate about x, and therefore all moments are transferred to the end pontoons and further distributed inwards. These moments are increased as the stiffness increases, further amplifying the effect. If S1 were to span the entire length, the max moment occurring at pontoon 1 would increase by about 20% compared to F1 without noticeably improving serviceability. This is due to increased reaction forces since S1 has higher density.

During mean tide, S1 is performing slightly better in terms of resisting displacements ([figure 5.11](#)). F1 mid-span displacement between second and third pontoon is approximately one and a half times greater than the corresponding S1 displacement. However, the magnitude of the displacements are very low compared to the length of the spans, indicating that both sections would provide sufficient resistance when traffic is added. The results for the equivalent cross-

section are similar to the curved bridge. The vertical displacement and moment ([figure 5.13](#)) profiles, displays that the equivalent cross-sections performance lies in between the initial and most stiff cross-sections. [Figure 5.12](#) shows that the equivalent cross-section provides the smallest rotations, as for the curved bridge.

As the end supports, tower and north abutment, are not rotationally restrained about the longitudinal axis, the whole girder will move vertically during change of tide. When the stiffness of the girder varies, the pontoon deflections ([figure 5.14](#)) and rotations ([figure 5.15](#)) change relative to each other. Adjusting the I_x value directly affects the magnitude of the deflections between adjacent pontoons due to self-weight, thus altering the serviceability of the bridge. Reducing I_x results in larger fluctuations, and opposite when it is increased.

When I_x becomes extremely large the bridge's displacement diagram converges towards a parabola. The entire bridge deforms as a unit. A consequence is that the pontoons are forced to move along with the girder, and fail to remain at an even water depth. The I_x might increase as a result of reshaping or increasing the area of the cross-section. Given that the material is unchanged, an increase in area will also lead to greater dead load and reaction forces. The distribution of the reaction forces are also affected by the change of I_x . When I_x increases, the pontoons closest to the ends are subjected to an increased reaction force relative to the internal pontoons. The result is large moments and abrupt changes as shown in [figure 5.16](#). The rotation profile in [figure 5.15](#) indicates that the predetermined I_x value provides sufficient resistance to bending if S1 were to span the entire length, similarly as for the curved bridge configuration.

5.7 Bjørnafjorden curved and straight comparison

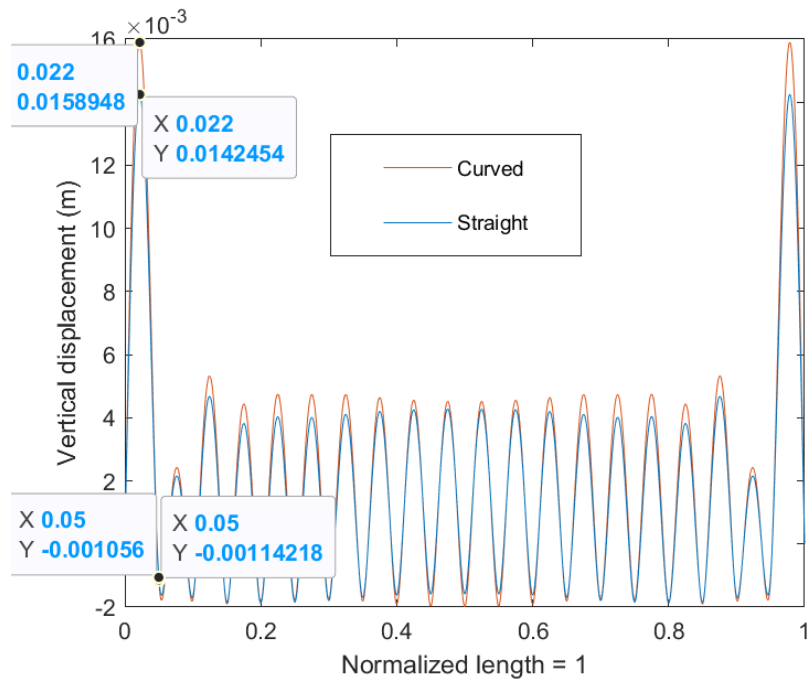


Figure 5.17. F1 straight and curved bridge with initial draft corresponding to reaction forces on mean tide.

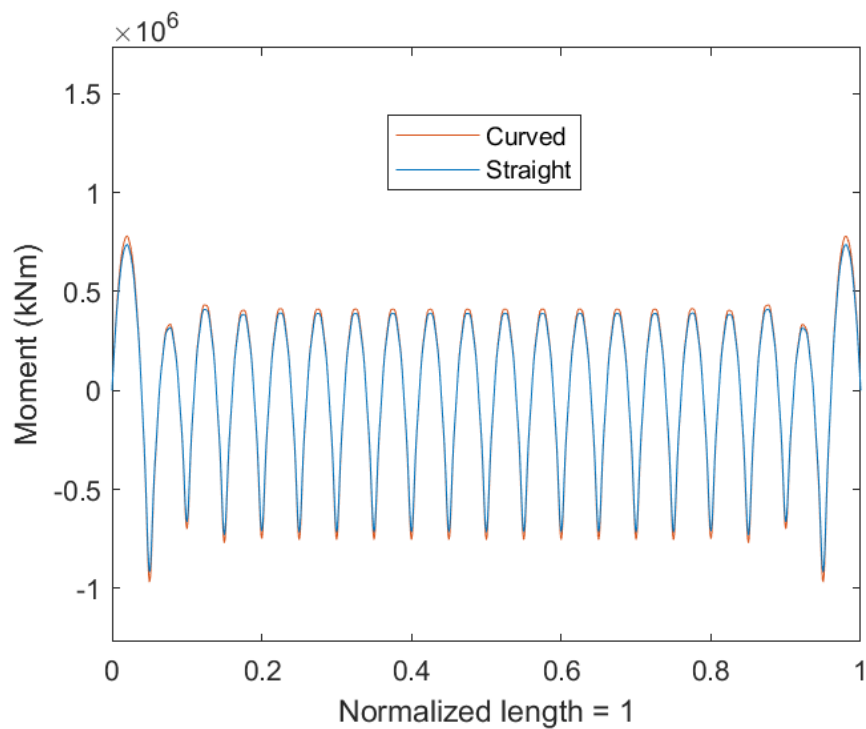


Figure 5.18. F1 straight and curved bridge moment on mean tide.

Figure 5.19. F1 straight and curved bridge with initial draft corresponding to reaction forces. Low tide of -28 cm, which corresponds to a relative tide of 125 cm from mean.

5.7.1 Curved and straight comparison conclusions

A direct comparison of the bridges presented in the previous chapters are shown in [figure 5.17](#), [5.18](#) and [5.19](#). The result shows that the straight bridge is subjected to slightly smaller displacements and moments. Due to the arch, the curved bridge spans 100 meter longer than the straight one. The extra length provides more dead load, which in response causes higher displacements and moments. Neither bridge has short enough spans to have any problem with incline. The almost 200 meter long space between pontoons ensures the tidal effects only slightly (<1%) increase the incline.

Chapter 6 Discussion and conclusions

6.1 Discussion

6.1.1 Calibrations

One of the primary assets of the chosen analytical method proved to be the ability to easily calibrate a range of parameters based on needs. While this method provides useful information regarding a range of variables, the Matlab code can be further developed in order to explore different related topics. However, performing such development requires great skill. Mathematical and structural engineering understanding, combined with sufficient Matlab coding skills are necessary.

6.1.2 Generalizability

The tide effects vary greatly depending on the geographical location. Some coastal areas experience neglectable tidal variations, while others are affected by variations that range up to approximately 12 meters[\[46\]](#). The results acquired in this study are therefore generalizable to locations with similar conditions, assuming the variations can be taken as homogenous across the examined water bodies. The study may be further expanded by vastly increasing the input tidal range. Consequently, different locations may then be analysed. This would allow for observation of recurring patterns in order to generalize the impact of tidal variations more extensively.

Another factor that is important to discuss is that the thesis has only examined a few bridge designs. While increasing the replicability of the conducted studies, it decreases the generalizability of the findings. Properties such as modulus of elasticity, cross-section and density do all have direct impact on the resulting deflections and rotations, hence only an identical setup will give the exact same results.

An idea for further generalization of the study is to analyze tidal effects on bridges with additional simplifications. For example, one could model unit bridges with the exact same properties except a few carefully chosen ones. By creating models more uniform, comparing

the effect of varying tidal ranges would be easier. This approach could help draw more extensive conclusions.

6.2 Conclusions

The purpose of the thesis was to examine long floating bridges subject to tidal variations. Several moment, vertical displacement and rotation calculations were performed. The goal was exploring the relationship between different sectional parameters and the tide-induced out-of-plane responses.

The thesis has covered five chapters on floating bridges. Chapter one consists of background information, facts and objectives for the thesis, and is followed by a chapter on the methodology conducted. In the remaining parts of the thesis, three different cases have been addressed. A generic simple bridge, a curved and a straight bridge over the Bjørnafjord were examined. The results collected in this study may prove useful in the optimization process, with the alternative tide design and the curved versus straight bridge comparison being most relevant. Based on the results presented in this thesis, four main conclusions can be drawn.

- 1) It was found that as the whole bridge girder moved with the tide, vertical deflections and rotations only deviated slightly between the different bridge designs and sections. This holds true during the entirety of the considered tidal cycles. However, the extreme moments varied greatly when different configurations were examined. The maximum moments during high tide occurred in the bridge girder over the pontoons, while the midspans between pontoons experienced the greatest impact at low tide.
- 2) F1 is found to be a better solution than S1, because F1 provides lower moments relative to displacements. As highlighted in the two previous chapters, the equivalent cross-sections results lie between F1 and S1. This cross-section is a good alternative, especially when the rotation angles along the whole length are considered. The displacement values are located close to S1 while the moments are close to F1, indicating a strong overall solution. However, given the great length of the bridges,

employing F1 along the whole bridge would be the most cost-efficient solution if only the observed factors are considered. The displacements and rotations are very similar for all three options regardless of stiffness, further emphasizing that F1 is a suitable section with the lowest extreme moment values during the effect of tide.

- 3) Long floating pontoon bridges subjected to tidal loads are at risk of two major issues. The first problem is the change in incline from the abutment to the first floating pontoon under a large tide. The simple bridge results show that if a bridge has short spans between pontoons and a low vertical stiffness the incline can cause a bridge to become too steep for heavy traffic. The second problem floating bridges encounter is restraint forces from high tides. Because the abutment is a fixed point regardless of tidal height, it can counteract the buoyancy forces from a high tide. These forces create a large outlier moment in the girder over the outermost pontoons. Because tidal cycles repeat every day, these forces lead to fatigue. The data obtained in chapter 4 show that by changing the reference tidal height a bridge is designed to be level at, it is possible to reduce these outlier moments by a significant amount.
- 4) The optimal fjord crossing is a straight bridge. As described in [chapter 5.7.1](#) this bridge design provides a slightly better overall performance. The straight bridge is subject to somewhat smaller displacements and moments due to shorter spans. Further analysis that takes waves and current loads into account will likely show that a curved bridge is more suitable if applying a mooring line system is unfeasible or less cost-efficient.

6.3 Recommendations for future work

Research shows that tidal effects will be amplified significantly in some parts of the world with the rising sea levels from global warming. Optimizing future floating bridge design based on those effects can be relevant in locations where the impact of changing sea level have been previously neglectable.

The examined floating bridges were strictly subjected to tidal effects and self-weight. Further research can be conducted addressing aspects like combinations of various environmental loads or traffic. Other bachelor level projects that would be highly relevant for today's society, could address problems such as - "How will floating bridges compete in the future, influenced by more extreme climate and weather conditions?" Or, -"How does floating bridges compete in terms of environmental sustainability, when compared to conventional bridge designs?"

References

- [1] S. Vegvesen. "Ferjefri E39." (accessed 21.05.2021)
<https://www.vegvesen.no/vegprosjekter/ferjefriE39/nyhetsarkiv/videreutvikler-de-matematiske-beregningsmetodene-for-bolger-og-strom>
- [2] S. Vegvesen. "Ferjefri E39." (accessed 21.05.2021)
<https://www.vegvesen.no/vegprosjekter/ferjefriE39>
- [3] W. Contributor "Archimedes's principle (accessed 21.05.21)
https://en.wikipedia.org/wiki/Archimedes%27_principle
- [4] W. Contributor "Pontoon bridge" (accessed 21.05.2021)
https://en.wikipedia.org/wiki/Pontoon_bridge
- [5] W. Contributor "List of longest cable-stayed bridge spans" (accessed 21.05.21)
https://en.wikipedia.org/wiki/List_of_longest_cable-stayed_bridge_spans
- [6] W. Contributor "Galata bridge" (accessed 21.05.21)
https://en.wikipedia.org/wiki/Galata_Bridge
- [7] W. Contributor "Tidevann" (accessed 21.05.21)
<https://no.wikipedia.org/wiki/Tidevann>
- [8] NOAA "Highest tides" Nova Scotia (accessed 21.05.2021)
<https://tidesandcurrents.noaa.gov/faq2.html#26>
- [9] Norwegian National Mapping Service "Tidevann og observert vannstand fra bergen" (accessed 21.05.21)
<https://www.kartverket.no/til-sjos/se-havniva/resultat?id=9000002>
- [10] M.D. Pickering et.al "The impact of future sea-level rise on the global tides (accessed 21.05.21)
<https://www.sciencedirect.com/science/article/pii/S0278434316304824>
- [11] S. Vegvesen. "Bergsøysundet bru" page 25 (accessed 21.05.2021)
https://web.archive.org/web/20071030024535/http://www.vegvesen.no/aktuelt/nasjonal_verneplan/enkeltobjekter_131-158_w.pdf
- [12] W. Contributor "Bergsøysundbrua" photograph by Cato Edvardsen(2011) (accessed 21.05.2021)
https://no.wikipedia.org/wiki/Bergs%C3%B8ysundbrua#/media/Fil:Bergs%C3%B8ysundbrua_01.jpg
- [13] S. Vegvesen Hordaland "Nordhordlandsbrua" (accessed 22.05.2021)
https://www.nb.no/items/URN:NBN:no-nb_digibok_2014081906042?page=1
- [14] "Nordhordlandsbrua" photograph by Ovesen (2010). (accessed 22.05.2021)
https://no.wikipedia.org/wiki/Nordhordlandsbrua#/media/Fil:Nordhordlandsbrua_towards_north.jpg
- [15] S. Vegvesen. "Fjordkryssing – Bjørnafjorden"(accessed 22.05.2021)
<https://www.vegvesen.no/Europaveg/e39stordos/fjordkryssing-bjornafjorden>
- [16] Z. Cheng et al. "Wave load effect analysis of a floating bridge in a fjord considering inhomogeneous wave conditions". (accessed 22.05.2021)
<https://www.sciencedirect.com/science/article/abs/pii/S0141029617335095>

- [17] S. Vegvesen. "Design Basis Bjørnafjorden Side- and end anchored floating bridge". (accessed 22.05.2021)
https://www.vegvesen.no/Europaveg/e39stordos/fjordkryssing-bjornafjorden/rapportar/attachment/3038827?ts=1746d60a3a0&fast_title=Bj%C3%B8rnafjorden+design+basis+rev.pdf
- [18] S. Vegvesen. "Trafikkdata". (accessed 22.05.2021)
<https://www.vegvesen.no/trafikkdata/start/utforsk?datatype=averageDailyYearVolume&display=chart&from=2021-04-06&trpids=10990V804785>
- [19] S. Vegvesen. "Veg- og gateutforming". (accessed 22.05.2021)
<https://www.vegvesen.no/attachment/61414>
- [20] Jagg Xaxx. "Types of Marine Growth". (accessed 22.05.2021)
<https://sciencing.com/info-7750175-types-marine-growth.html>
- [21] S. Vegvesen. "Bruprosjektering Prosjektering av bruer, ferjekaier og andre bærende konstruksjoner". (accessed 22.05.2021)
<https://www.vegvesen.no/attachment/865860/binary/1030718>
- [22] Geological Survey of Norway. "Earthquakes". (accessed 22.05.2021)
<https://www.ngu.no/en/topic/earthquakes>
- [23] Standard Norge. "NS-EN 1998 Eurokode 8: Prosjektering av konstruksjoner for seismisk påvirkning". (accessed 22.05.2021)
<https://www.standard.no/fagomrader/bygg-anlegg-og-eiendom/eurokoder1/eurokode-8/>
- [24] The constructor. "12 Types of Loads Considered for Design of Bridge Structures." (accessed 22.05.2021)
<https://theconstructor.org/structures/bridge-design-loads/21478/>
- [25] J. Dai, B.K. Lim, K.K. Ang, Response of a floating curved pontoon bridge subjected to tide induced water surface variation: an analytical approach, Proceedings of the 10th International Research Conference of KDU, Ratmalana, Sri Lanka, 3-4 August 2017 (accessed 22.05.2021)
- [26] Asif Habibullah. "SAP2000 general purpose civil-engineering software" (accessed 22.05.2021)
<https://wiki.csiamerica.com/display/sap2000/Home>
- [27] Craig Warren. "MATLAB for Engineers: Development of an Online, Interactive, Self-study Course". (accessed 22.05.2021)
<https://www.tandfonline.com/doi/full/10.11120/ened.2014.00026>
- [28] Hui Wang, Qing-Hua Qin "Chapter 2 - Mechanics of solids and structures". (accessed 22.05.2021)
<https://www.sciencedirect.com/science/article/pii/B9780128182833000026>
- [29] J. Dai, K.K. Ang, Steady-state response of a curved beam on a viscously damped foundation subjected to a sequence of moving loads, Journal of Rail and Rapid Transit 229 (2015) 375-394.
- [30] Radu Crahmaliuc. "75 Years of the Finite Element Method (FEM)". (accessed 22.05.2021)
<https://www.simscale.com/blog/2015/11/75-years-of-the-finite-element-method-fem/>
- [31] Trevor English. "What Is Finite Element Analysis and How Does It Work?". (accessed 22.05.2021)
<https://interestingengineering.com/what-is-finite-element-analysis-and-how-does-it-work>
- [32] Jeff Gardiner. "Finite Element Analysis Convergence and Mesh Independence". (accessed 21.05.2021)
<https://www.xceed-eng.com/finite-element-analysis-convergence-and-mesh-independence/>

- [33] Norwegian national mapping service. (accessed 21.05.2021)
<https://www.kartverket.no/til-sjos/se-havniva/resultat?id=9000002>
- [34] W. Gregory Hess et al. "Construction of the world's longest floating bridge". (accessed 21.05.2021)
<https://www.structuremag.org/wp-content/uploads/2016/09/F-FloatingBridge-Oct16-1.pdf>
- [35] Norwegian national mapping service. (accessed 21.05.2021)
<https://www.kartverket.no/til-sjos/se-havniva/resultat?id=9000002>
- [36] Norwegian national mapping service. (accessed 21.05.2021)
<https://www.kartverket.no/til-sjos/se-havniva/resultat?id=9000002>
- [37] W. Contributor "Storm Vivian". (accessed 21.05.2021)
https://en.wikipedia.org/wiki/Storm_Vivian
- [38] S. Vegvesen. "A floating bridge is the chosen concept for crossing Bjørnafjorden". (accessed 21.05.2021)
<https://www.vegvesen.no/en/roads/Roads+and+bridges/Road+projects/e39coastalhighwayroute/new+s/a-floating-bridge-is-the-chosen-concept-for-crossing-bjornafjorden?.it&>
- [39] S. Vegvesen. "Sparer kroner og klima ved å bygge Bjørnafjord-bru i stål". (accessed 21.05.2021)
<https://www.vegvesen.no/Europaveg/e39stordos/nyhetsarkiv/sparer-kroner-og-klima-ved-a-bygge-bjornafjord-bru-i-stal>
- [40] S. Vegvesen. "Straight bridge - navigation channel in south". (accessed 21.05.2021)
https://www.vegvesen.no/_attachment/1605065/binary/1145263?fast_title=Bj%C3%B8rnafjorden+Si+deforankret+flytebru+-+oppsummering+av+analyser.pdf
- [41] S. Vegvesen. "Curved bridge - navigation channel in south". (accessed 21.05.2021)
https://www.vegvesen.no/_attachment/1605060/binary/1145259?fast_title=Bj%C3%B8rnafjorden+En+deforankret+flytebun+-+Oppsummering+av+analyser.pdf
- [42] Z. Cheng et al. Fig 2 (accessed 21.05.2021)
https://www.sciencedirect.com/science/article/pii/S0951833917304094?casa_token=1VLoJslC_iAAAAA:duDWEaowiNKbjN7y9qsPVZ7hHD0-5CSWUvJZar3XXq0-AXEAvOHS0tlxYvJZ_-mOqgslx4Szo
- [43] S. Vegvesen. "Fjordkryssing - Bjørnafjorden". (accessed 21.05.2021)
<https://www.vegvesen.no/Europaveg/e39stordos/fjordkryssing-bjornafjorden>
- [44] S. Vegvesen. "The Bjørnafjorden crossing". (accessed 21.05.2021)
https://www.vegvesen.no/_attachment/2849626/binary/1349802?fast_title=Bj%C3%B8rnafjord+crossing+updates.pdf
- [45] Multiconsult. "Norwegian Public Roads Administration recommends pontoon bridge over Bjørnafjorden". (accessed 21.05.2021)
<https://www.multiconsultgroup.com/norwegian-public-roads-administration-recommends-pontoon-bridge-bjornafjorden/>
- [46] National Ocean Service. "Where is the highest tide?" (accessed 21.05.2021)
<https://oceanservice.noaa.gov/facts/highesttide.html>

